THE ANCIENT ORIGIN OF NF-κB/IκB AND THIOREDOXIN AND THEIR ROLES IN IMMUNE RESPONSE

WANG XIAOWEI
(Master of Science)

A THESIS SUBMITTED

FOR THE DEGREE OF DOCTOR OF PHILOSOPHY

DEPARTMENT OF BIOLOGICAL SCIENCES

NATIONAL UNIVERSITY OF SINGAPORE

2006

Acknowledgements

I would like to express my deepest gratitude to Prof. Ding and Prof. Ho for giving me the opportunity to work on this project. They have provided excellent guidance and support throughout my years in the lab. From them, I have learnt many invaluable skills that are essential for my future career.

I would like to thank especially Dr. Andrew Tan and Dr. Liou Yih-Cherng for giving me countless advices and suggestions for my Ph. D study. I would also like to thank Prof. Sheu Fwu-Shan, Dr. Lu Jinhua for their help in DLR experiments and Prof. Wasserman, Prof. Dan Hultmark for providing antibodies.

I also would like to express my gratefulness to my current and previous lab mates: Li Peng, Naxin, Baozhen, Zehua, Patricia, Li Yue, Belinda, Siou Ting, Wang Jing, Lihui, Zhu Yong, Weidong, Alvin, Xiaolei, Sun Miao, Nicole, Hanh, Derrick and Sandra. Without them, I would not have such an enjoyable time in the lab.

Many thanks also go to Suhba for her help and Shashi, Qingsong and Michelle who have helped me with my analysis of the mass spectrometry data.

I would also like to thank the National University of Singapore for the Research Scholarship award and A*STAR BMRC grant for financial support.

Most importantly, I would like to thank my family for their love, understanding and encouragement, which make the lonely time studying overseas bearable.

THANK YOU!

Table of Contents

Summary

The NF-κB signaling pathway performs a pivotal role in the acute-phase of microbial infection, by activating immune-related gene expression. The NF-κB transcription factors are evolutionarily conserved from *Drosophila* to humans. Unexpectedly, the canonical NF-κB signaling pathway is not functional in the immune system of *C. elegans*. Therefore, the ancient origin of NF-κB signaling pathway is still unknown. This project focused on tracing the ancient origin of the NF-κB signaling pathway, characterization of its functions in innate immune response and regulation of its activity by thioredoxin. To this end, the horseshoe crab was examined as this species boasts >500 million years of evolutionary success.

This thesis reports the discovery and characterization of a primitive and functional NF-κB/IκB cascade in the immune defense of a "living fossil", the horseshoe crab, *Carcinoscorpius rotundicauda*. The ancient NF-κB/IκB homologues, CrNFκB, CrRelish and CrIκB, share numerous signature motifs with their vertebrate orthologues. CrNFκB recognizes both horseshoe crab and mammalian κB response elements. CrIκB interacts with CrNFκB and inhibits its nuclear translocation and DNA-binding activity. We further show that Gram-negative bacteria infection causes rapid degradation of CrIκB and nuclear translocation of CrNFκB. Infection also leads to an increase in the κB-binding activity and up-regulation of immune-related gene expression, like inducible nitric oxide synthase and Factor C, an LPS-activated serine protease. Altogether, our study shows that, although absent in *C. elegans*, the NF-κB/IκB signaling cascade

remained well-conserved from horseshoe crab to human playing an archaic but fundamental role in regulating the expression of critical immune defense molecules.

In connection with the NF-κB mediated immune signaling, we discovered a novel 16 kDa thioredoxin (TRX) from the horseshoe crab, designated Cr-TRX1. TRX is a small ubiquitous protein-disulfide reductase, hitherto known to be conserved from prokaryotes to human. This novel 16 kDa TRX is larger than the known classical 12 kDa counterpart and contains an atypical WCPPC catalytic motif. Although Cr-TRX1 contains three Cys, only the two in its active motif are exposed and redox sensitive. Cr-TRX1 possesses the classical thiodisulfide reductase activity, as indicated by the insulin reduction assay and thioredoxin reductase assay. Additionally, Cr-TRX1 protected DNA from reactive oxygen species-mediated nicking. Over-expression of Cr-TRX1 regulated the expression of NF-κB-dependent genes by enhancing NF-κB DNA-binding activity, suggesting possible roles of the Cr-TRX1 in modulating NF-κB signaling pathway. *In vivo,* the antioxidant downregulated the expression of NF-κB controlled genes, such as IκB and inducible nitric oxide synthase, which further supports our suggestion that oxidative stress is a regulator of NF-κB signaling pathway, a phenomenon which has been entrenched for several hundred million years. Furthermore, we demonstrated that the 16 kDa TRXs are evolutionarily conserved from *C. elegans* to human. Interestingly, thioredoxin-like 6, a human homologue of Cr-TRX1, could enhance the NF-κB DNA-binding activity as well, suggesting that the NF-κB regulatory ability of the 16 kDa TRXs is well conserved through evolution. (470 words)

List of Tables

List of Figures

Chapter 4

List of Abbreviations

AA	Amino acid
ABTS	2,2'-azino-bis[3-ethylbenzthiazoline-6-sulfonic acid
A_{340}	Absorbance at 340 nm
ATP	Adenosine triphosphate
bp	Base pair
BSA	Bovine serum albumin
CALF	*Carcinoscropius rotundicauda* anti-LPS factor
CAT	Chloramphenicol acetyltransferase
CFU	Colony-forming unit
cDNA	Complementary deoxyribonucleic acid
CrC3	*Carcinoscropius rotundicauda* complement 3
CrFC	*Carcinoscropius rotundicauda* Factor C
CrIκB	*Carcinoscropius rotundicauda* IκB
CriNOS	*Carcinoscropius rotundicauda* inducible nitric oxide synthase
CrNFκB	*Carcinoscropius rotundicauda* NF-κB
CrRelish	*Carcinoscropius rotundicauda* Relish
Cr-TRX1	*Carcinoscropius rotundicauda* TRX1 (16 kDa)
CsCl	Cesium chloride
DAP	Diaminopimelic acid
DAPI	4',6-diamidino-2-phenylindole, dihydrochloride
ATP	2'-deoxyadenosine 5'-triphosphate
DIG	Digoxigenin
DLR	Dual-luciferase reporter
DMEM	Dulbecco's modified Eagle's medium
DMSO	Dimethyl sulfoxide
DNA	Deoxyribonucleic acid
DTT	Dithiothreitol
EDTA	Ethylenediaminetetraacetic acid
ELISA	Enzyme linked immuosorbant assay
EMSA	Electrophoretic mobility shift assay
EST	Express sequence tag

FBS	Fetal bovine serum
Fig	Figure
fmol	Femtomole
G	Guanine
β-Gal	β–galactosidase
GR	Glutathione reductase
GSH	Glutathione
GST	Glutathione S-transferase
h	Hour
hpi	Hour post infection
IAM	Iodoacetamide
IKK	Inhibitory κB kinase
IL	Interleukin
iNOS	Inducible nitric oxide synthase
IPTG	Isopropyl-β-D-thiogalactoside
kb	Kilobase
kDa	Kilodalton
LB	Luria Bertani
LPS	Lipopolysaccharide
LTA	Lipoteichoic acid
LUC	luciferase
M	Molar
MFO	Mixed function oxidation
mg	Milligram
min	Minute
ml	Millilitre
mM	Millimolar
MALDI-TOF	Matrix-assisted laser desorption ionization-Time of flight
mRNA	Messenger ribonucleic acid
NEB	New England Biolabs
NF-κB	Nuclear factor-κB
ng	Nanogram
NIK	NF-κB inducing kinase

NLS	Nuclear localization signal
nM	Nanomolar
OD	Optical density
ORF	Open reading frame
PAGE	Polyacrylamide gel electrophoresis
PAMP	Pathogen associated molecular pattern
PBS	Phosphate buffered saline
PCR	Polymerase chain reaction
PDTC	Pyrrolidine dithiocarbamate
PEST	Proline-, glutamic acid-, serine- and threonine-rich
PGRP	Petidoglycan recognition proteins
PLB	Passive lysis buffer
PNK	Polynucleotide kinase
PPR	Pattern recognition receptor
RACE	Rapid amplification of cDNA ends
RdCVF	Rod-derived cone viability factor
RHD	Rel homology domain
RNA	Ribonucleic acid
RNase	Ribonuclease
ROS	Reactive oxygen species
rpm	Revolutions per minute
RT-PCR	Reverse transcriptase-polymerase chain reaction
S2	*Drosophila melanogaster* Schneider line-2 cells
SDS	Sodium dodecyl sulphate
s	Second
T	Thymine
TD	Transactivation domain
TIR	Toll and interlukin receptor
TLR	Toll-like receptor
TNFα	Tumor necrosis factor α
TRX	Thioredoxin
TRXR	Thioredoxin reductase
TRX6	Thioredoxin-like 6 (Human 24 kDa TRX)
TSA	Tryptone soy agar

U	Unit
UTR	Untranslated region
UV	Ultraviolet
V	Volt
v/v	Volume : volume ratio
w/v	Weight : volume ratio

List of Primers

Name	Sequence (5' to 3')	Purpose
Primers for cloning CrNFκB, CrIκB and CrRelish		
CrNFκB forward primer:	TTTCGCTAYRARTGCGARGG	Degenerate forward primer for cloning CrNFκB
CrNFκB reverse primer:	TCCTTIGTWACRCAWGAIACMAC	Degenerate reverse primer for cloning CrNFκB
CrIκB forward primer:	GAYGGIGACWCRIYIITSCACYTRGC	Degenerate forward primer for cloning CrIκB and CrRelish
CrIκB reverse primer:	CAGGMMAIRTGIARIGSIGTRTIDCC	Degenerate reverse primer for cloning CrIκB and CrRelish
CrNFκB primers for expression in bateria and insect cell		
CrNFκB-pAc-F:	GGTACCATGGACACATCTGTTTCTC	Forward primer for cloning full length and RHD of CrNFκB into pAc5.1 vector
CrNFκB-FL-pAc-R:	GGGCCCTGTCGATTCATTTGTCCT	Reverse primer for cloning full length CrNFκB into pAc5.1
CrNFκB-RHD-pAc-R:	GGGCCCAGTTCTTGTTGCTTGCTT	Reverse primer for for cloning RHD of CrNFκB into pAc5.1
CrNFκB-pET-RHD-F:	AGCATATGGACACATCTGTTTCTCAT	Forward primer for cloning RHD of CrNFκB into pET15b
CrNFκB-pET-RHD-R:	GGGATCCAATAGTTCTTGTTGCTTGCTT	Reverse primer for cloning RHD of CrNFκB into pET15b
CrIκB primers for expression in bateria and insect cell		
CrIκB-cMyc-pAc-F:	GGTACCATGGGAAAATCAAAAGAATT	Forward primer for cloning full length CrIκB into pAc5.1
CrIκB-cMyc-pAc-R:	ACCGGTCAGATCTTCCTCTGAGATGAG CTTCTGCTCCACTGCTCTAACTTCATCT CC	Reverse primer for for cloning full length CrIκB with c-Myc tag at C-terminus into pAc5.1
CrIκB-GST-F:	TGTGGATCCATGAGAAAATCAAAA GAA	Forward primer for cloning full length CrIκB into pGEX-4T-1
CrIκB-GST-R:	AGAGAATTCTTACACTGCTCTAACT TC	Reverse primer for cloning full length CrIκB into pGEX-4T-1
Cr-TRX1 primers for expression in bateria and mammalian cell		
Cr-TRX1-pAc-FLAG-F:	GGTACCATGGAATTTATCCAAGG	Forward primer for cloning full length Cr-TRX1 into pcDNA3.1

Cr-TRX1-pAc-FLAG-R:	ACCGGTTTTGTCGTCATCGTCCTTA TAGTCTCTTGCCCAGTTCTGGAA-3'	Reverse primer for cloning full length Cr-TRX1 with FLAG tag into pcDNA3.1
Cr-TRX1-pGEX-F	GGAGGATCCATGGAATTTATCCAAGG	Forward primer for cloning full length Cr-TRX1 into pGEX-4T-1
Cr-TRX1-pGEX-R	ATTCTCGAGTTATCTTGCCCAGTTCTG	Reverse primer for cloning full length Cr-TRX1 into pGEX-4T-1
CrTRX-DM-F:	CAGTGCCCACTGGGCTCCCCCAGCTCG AGGGTTCACC	Forward primer for mutagenesis of Cys to Ala
CrTRX-DM-R:	GGTGAACCCTCGAGCTGGGGGAGCCC AGTGGGCACTG	Reverse primer for mutagenesis of Cys to Ala

The underlined nucleotides encode the restriction sites. All primers were reconsituted in water to 100 μM stock and stored at -20 °C. The coding for degenerate bases are as follows: R=A/G, Y=C/T, M=A/C, K=G/T, S=C/G, W=A/T, B=C/G/T, D=A/G/T, H=A/C/T, V=A/C/G, N=A/C/G/T, I=inosine.

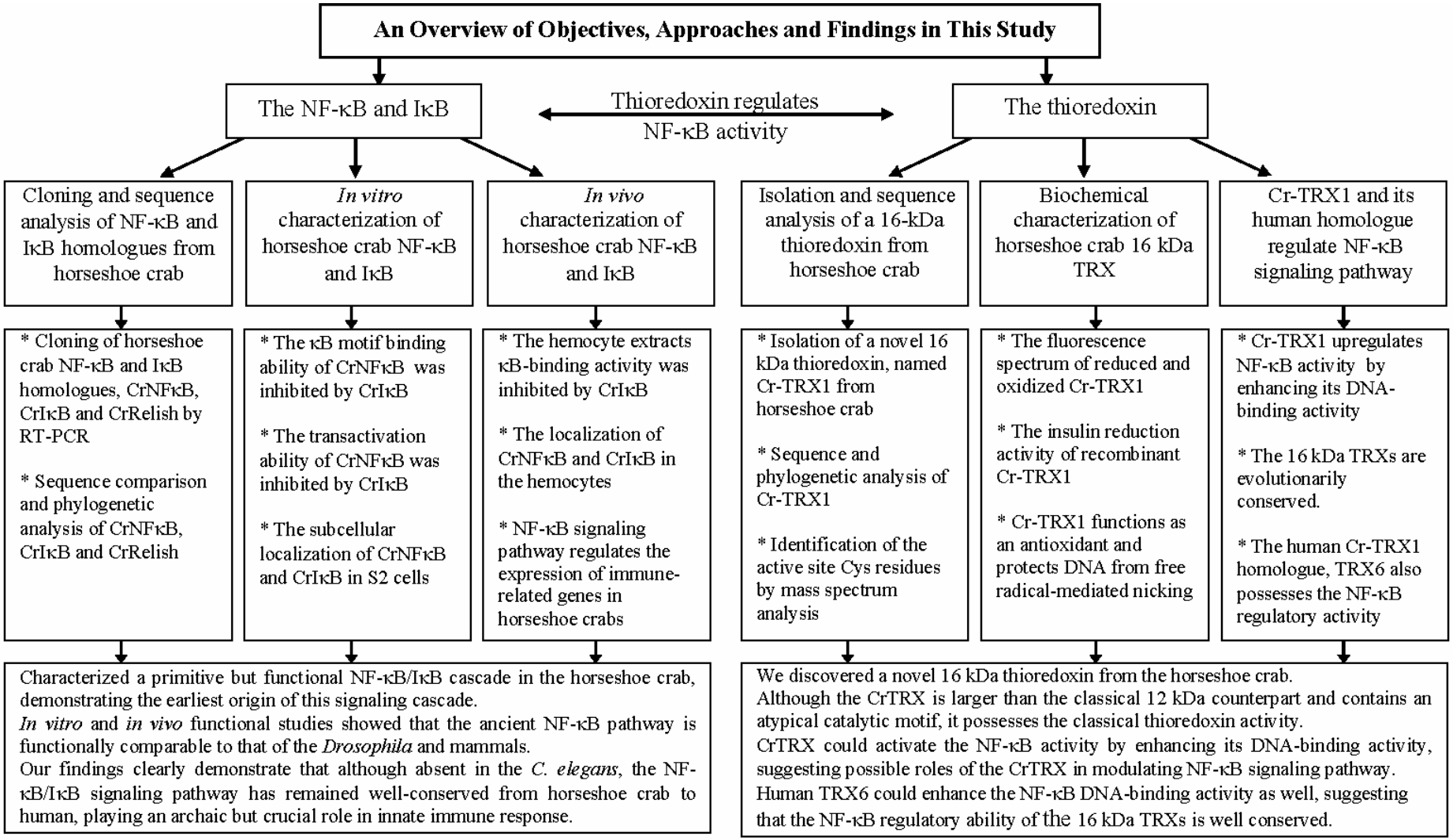
An Overview of Objectives, Approaches and Findings in This Study
The NF-κB and IκB
Thioredoxin regulates NF-κB activity
The thioredoxin
Cloning and sequence analysis of NF-κB and IκB homologues from horseshoe crab
In vitro characterization of horseshoe crab NF-κB and IκB
In vivo characterization of horseshoe crab NF-κB and IκB
Isolation and sequence analysis of a 16-kDa thioredoxin from horseshoe crab
Biochemical characterization of horseshoe crab 16 kDa TRX
Cr-TRX1 and its human homologue regulate NF-κB signaling pathway
* Cloning of horseshoe crab NF-κB and IκB homologues, CrNFκB, CrIκB and CrRelish by RT-PCR
* Sequence comparison and phylogenetic analysis of CrNFκB, CrIκB and CrRelish
* The κB motif binding ability of CrNFκB was inhibited by CrIκB
* The transactivation ability of CrNFκB was inhibited by CrIκB
* The subcellular localization of CrNFκB and CrIκB in S2 cells
* The hemocyte extracts κB-binding activity was inhibited by CrIκB
* The localization of CrNFκB and CrIκB in the hemocytes
* NF-κB signaling pathway regulates the expression of immune-related genes in horseshoe crabs
* Isolation of a novel 16 kDa thioredoxin, named Cr-TRX1 from horseshoe crab
* Sequence and phylogenetic analysis of Cr-TRX1
* Identification of the active site Cys residues by mass spectrum analysis
* The fluorescence spectrum of reduced and oxidized Cr-TRX1
* The insulin reduction activity of recombinant Cr-TRX1
* Cr-TRX1 functions as an antioxidant and protects DNA from free radical-mediated nicking
* Cr-TRX1 upregulates NF-κB activity by enhancing its DNA-binding activity
* The 16 kDa TRXs are evolutionarily conserved.
* The human Cr-TRX1 homologue, TRX6 also possesses the NF-κB regulatory activity
Characterized a primitive but functional NF-κB/IκB cascade in the horseshoe crab, demonstrating the earliest origin of this signaling cascade.
In vitro and in vivo functional studies showed that the ancient NF-κB pathway is functionally comparable to that of the Drosophila and mammals.
Our findings clearly demonstrate that although absent in the C. elegans, the NF-κB/IκB signaling pathway has remained well-conserved from horseshoe crab to human, playing an archaic but crucial role in innate immune response.
We discovered a novel 16 kDa thioredoxin from the horseshoe crab.
Although the CrTRX is larger than the classical 12 kDa counterpart and contains an atypical catalytic motif, it possesses the classical thioredoxin activity.
CrTRX could activate the NF-κB activity by enhancing its DNA-binding activity, suggesting possible roles of the CrTRX in modulating NF-κB signaling pathway.
Human TRX6 could enhance the NF-κB DNA-binding activity as well, suggesting that the NF-κB regulatory ability of the 16 kDa TRXs is well conserved.

CHAPTER 1: INTRODUCTION

1.1 The innate immune system

1.1.1 The innate and adaptive immunity

The immune response is the body's natural defense mechanism that protects us from foreign invaders, such as viruses and bacteria. The vertebrate immune system uses two types of defense mechanisms to combat pathogens –the innate immunity and the adaptive immunity (Medzhitov and Janeway, 2000). Adaptive immunity is mediated by T and B cells by generating antigen-specific antibody through DNA rearrangement, and responding specifically to pathogens. The cornerstone of vertebrate adaptive immunity is the possibility to "remember" previous infections through generating long living memory cells and thereby mount a faster and stronger immune reaction the next time the individual encounters the same pathogen. However, the adaptive immunity is far too slow to take care of invading microorganisms by its own. The sequence of events from the adaptation to the antigens, the maturation of B lymphocytes and thence the production of such a repertoire of antibodies takes several days to be established after an infection (Janeway and Medzhitov, 2002). On the other hand, innate immunity is the immediate front line defense that also shapes the ensuing adaptive immunity. Without the presence of the innate immune system, the adaptive immunity would not even have a chance to initiate its defense, before the host organism is dead.

The innate immune system is phylogenetically the oldest immune system and is present in all higher eukaryotic organisms. Although by the late nineteenth and early

twentieth century, important advances had been made in the study of innate immunity in invertebrates; such as the finding that insects have macrophage-like cells and produce a variety of antimicrobial substances (Kurz and Ewbank, 2003), it was only comparatively recent that the attention of the scientific community turned towards innate immunity. This was partially, a result of the realization that even in the vertebrates, the innate immune mechanisms are extremely important –they can often successfully block infections at an early stage, and if not, they can influence the subsequent adaptive immune response (Medzhitov and Janeway, 1998). In contrast to the adaptive immune system, the innate immune system is functional at birth and includes the first line of defense against foreign agents. Innate immunity is mediated by a repertoire of recognition molecules and responds non-specifically to a broad-spectrum of invaders (Janeway and Medzhitov, 2002). Upon the recognition of invading pathogens by the receptors, the innate immune system rapidly mounts various responses including phagocytosis, synthesis of antimicrobial peptides, production of reactive oxygen species, and activation of the alternative complement pathway to contain the proliferation of infective pathogens until the adaptive immune response is ready to execute effective defense actions (Akira and Takeda, 2004).

1.1.2 Recognition of pathogens by pattern recognition receptors

The first step in innate immune responses is the recognition of microbial components by the germ-line encoded receptors, called pattern recognition receptors, PRRs (Medzhitov and Janeway, 2000). In contrast to the amazing diversity of the T- and B-cell receptors of adaptive immunity, which are generated by somatic recombination

and hypermutation events, the repertoire of PRRs is much more restricted due to the limited number of genes encoded in the genome of every organism. To overcome this limitation, rather than detect every possible antigen, the PRRs have evolved to recognize invariant molecular motifs common for the large groups of microorganisms. These pathogen-specific molecular motifs are called pathogen-associated molecular patterns (PAMPs). Furthermore, most PRRs have evolved into multiple isoforms, which interact in variable combinations during an infection to form formidable pathogen recognition assemblies (Ng *et al*, 2004; Zhu *et al*, 2005). This feature not only allows the detection of a wide variety of microorganisms by a restricted repertoire of PRRs but also ensures that the innate immune system mounts the most appropriate responses at the critical time of infection. Examples of PAMPs are lipopolysaccharide (LPS) of the Gram-negative bacteria, lipoteichoic acid of Gram-positive bacteria; zymosan, mannan and β-glucan of fungi (Aderem and Ulevitch, 2000). On recognition, those receptors activate signaling cascades that regulate the transcription of target genes encoding regulator and effector molecules. One outcome of the recognition, which is probably common to all animals, is the induction of genes encoding antimicrobial peptides that act by damaging the microbial cell membranes (Lehrer and Ganz, 1999; Li *et al*, 2004).

1.1.3 The innate immunity of invertebrates

As the first line of defense against infectious microorganisms, innate immunity is an evolutionarily ancient mechanism in many aspects. Due to the lack of adaptive immunity, the invertebrates have developed a potent innate immune system. Indeed, the findings over the last decade have demonstrated that the study of innate immunity in

invertebrates can aid our understanding of how mammals defend themselves against infection (Kurz and Ewbank, 2003). The invertebrate innate immunity is mainly composed of three parts: (i) cellular response, namely phagocytosis of invading microorganisms by blood cells, (ii) proteolytic cascades leading to localized blood clotting, melanin formation, and opsonization, and (iii) transient expression of potent antimicrobial peptides (Hoffmann *et al*, 1999). Other important components include nitric oxide synthase, clotting reaction and serine protease inhibitors (Little *et al*, 2005).

Among all the mechanisms, the strong and rapid induction of antimicrobial peptides in *Drosophila* is most well-studied and serves as a model system for the analysis of innate immunity (Imler and Bulet, 2005). At least seven distinct antimicrobial peptides have been isolated in *Drosophila*. Among them, drosomycin is potently antifungal, whereas the others (cecropins, diptericin, drosocin, attacin, defensin, and metchniknowin) act primarily on bacteria (Lemaitre *et al*, 1996). The production of antimicrobial peptides is slightly delayed and usually occurs within a few hours after entry of the pathogen. Obviously, the recognition of the foreign particles has to take place in order to transfer the message to the cells that synthesize the appropriate immune effectors. Recognition of the invading pathogen in *Drosophila* is believed to occur through the Toll receptor on the membrane and transmitted to the downstream signaling pathways. Several signaling pathways have been reported to control the innate immune response in *Drosophila* such as JAK/STAT, NF-κB and JNK signaling pathways (Agaisse and Perrimon, 2004; Boutros *et al*, 2002). Within the scope of this thesis, the following sections will focus on the significance of NF-κB-mediated signaling pathway to the host defense against infections.

1.2 The NF-κB signaling pathway

1.2.1 Introduction to the NF-κB signaling pathway

The NF-κB signaling pathway is one of the most important pathways in innate immunity because it controls the expression of numerous immune-related genes including antimicrobial peptides, cytokines and enzymes for the production of reactive oxygen and nitrogen species (ROS, RNS) (Dixit and Mak, 2002; Ghosh *et al*, 1998). NF-κB transcription factors are the central components of the NF-κB signaling pathway as all of the signals will be conveyed to various isoforms of the NF-κB transcription factors. Different stimuli cause the formation of different hetero- or homo- dimers of NF-κB proteins which control the specificity and duration of the immune response (Hayden and Ghosh, 2004). Up to now, five NF-κB transcription factors have been found in mammals: RelA (p65), RelB, c-Rel, NF-κB1 (p105/p50) and NF-κB2 (p100/p52) (Figure 1.1). A common feature of the NF-κB proteins is that all of them contain a Rel-homology domain (RHD) which is located towards the N-terminus of the protein. The RHD is involved in the dimerization, DNA-binding and interaction with the inhibitory IκB (inhibitor of NF-κB) proteins. The difference is that RelA, RelB and c-Rel have an activation domain in their C-terminal which is absent in NF-κB1 and NF-κB2 (Figure 1.1). On the contrary, NF-κB1 and NF-κB2 contain a C-terminal inhibitory IκB-like domain which are later processed to produce the DNA-binding subunits, p50 and p52, respectively (Gilmore, 1999).

The NF-κB members dimerize to form homo- or hetero-dimers, which are associated with specific responses to different stimuli and they induce differential effects on transcription. The balance between different NF-κB homo- and hetero-dimers will determine which dimers are bound to specific κB sites and thereby regulate the level of transcriptional activity (May and Ghosh, 1997). In addition, these proteins are expressed in a cell- and tissue-specific manner providing an additional level of regulation. For example, NF-κB1 (p50) and p65 are ubiquitously expressed, and the p65/p50 heterodimers constitute the most common inducible NF-κB binding activity. In contrast, NF-κB2, RelB, and c-Rel are expressed specifically in lymphoid cells and tissues (Caamano and Hunter, 2002).

In unstimulated cells, NF-κB dimers are retained in the cytoplasm in an inactive form, because of their association with members of another family of proteins called IκB. The IκB family of proteins includes IκBα, IκBβ, IκBγ, IκBε, Bcl-3, and the carboxyl-terminal regions of NF-κB1 (p105) and NF-κB2 (p100) (Figure 1.1). The IκB proteins are characterized by the presence of five to seven ankyrin repeats that assemble into cylinders that bind the dimerization domain of NF-κB dimers (Hatada *et al*, 1992). The IκB proteins bind with different affinities and specificities to NF-κB dimers. Activation of the NF-κB proteins requires phosphorylation and subsequent degradation of the IκB inhibitors, thus allowing the translocation of NF-κB into the nucleus for the transcriptional activation of genes harbouring κB response elements. Therefore, not only are there different NF-κB dimers in a specific cell type, but the large number of

combinations between IκB and NF-κB dimers illustrates the sophistication of the system (Caamano and Hunter, 2002).

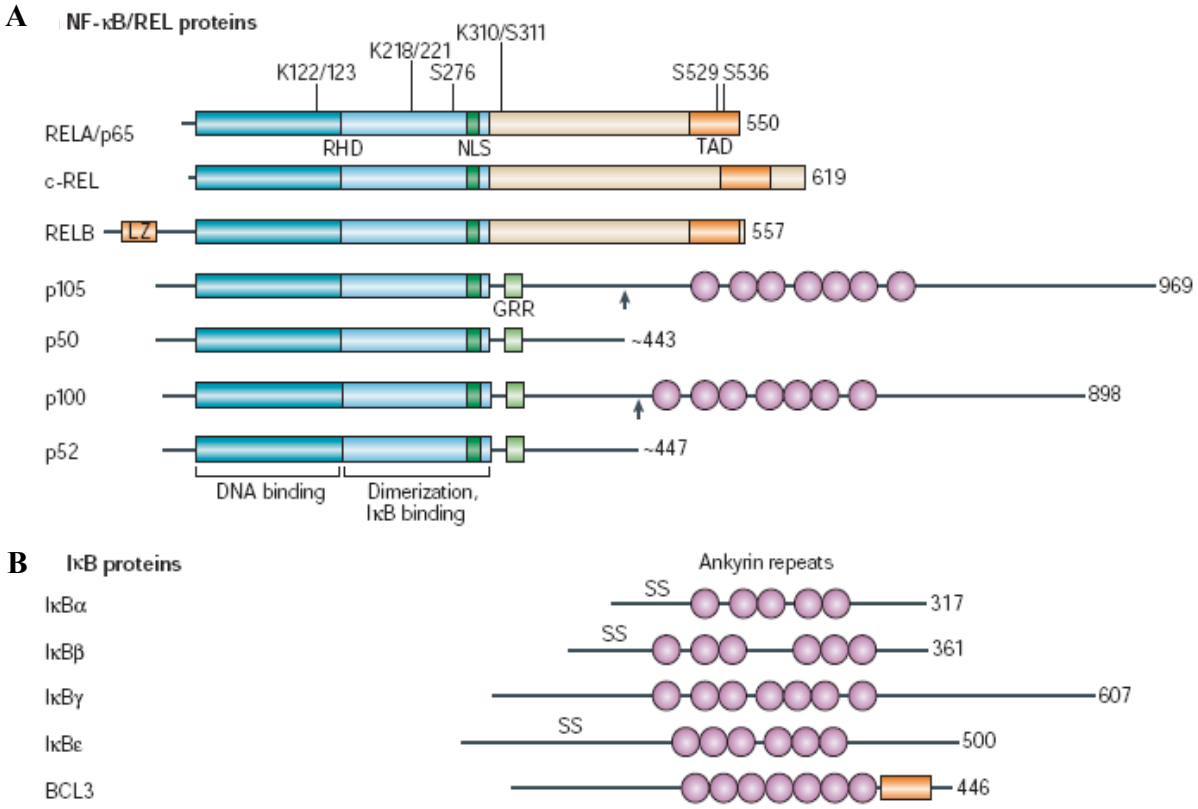

Figure 1.1: The family of mammalian NF-κB and IκB proteins. (A) Schematic representation of the seven mammalian NF-κB proteins — RelA/p65, c-Rel, RelB, p105, p50, p100 and p52. The N-terminal portion of the RHD is responsible for DNA-binding. The C-terminal portion of the RHD mediates dimerization with other NF-κB family members and binds to the IκB proteins. The p105 and p100 proteins also contain ankyrin repeats (circles), as well as glycine-rich regions (GRRs). The GRRs are important for processing of p100 to p52. Phosphorylation of p65 at S276, S311, S529 and/or S536 is required for optimal NF-κB transcriptional activity. Acetylation of p65 at K122, K123, K218, K221 and K310 regulates distinct functions of NF-κB, including DNA binding, IκBα association and p65-mediated transactivation. **(B)** The family of IκB proteins. The IκB family protein includes IκBα, IκBβ, IκBγ, IκBε and BCL3. A hallmark of these IκB proteins is an ankyrin-repeat domain, which mediates the assembly with NF-κB proteins. When bound by IκBα, the nuclear localization signal (NLS) of p65 is masked, and p65 cannot localize to the nucleus or bind to DNA. Phosphorylation of two serine residues (SS) at the amino-terminal region of IκBα triggers polyubiquitylation and proteasome-mediated degradation of IκBα. Adapted from Chen and Greene (2004).

In mammals, two major signaling pathways (the classical and alternative pathways) lead to the translocation and activation of NF-κB dimers (Bonizzi and Karin, 2004). In the classical pathway, NF-κB family proteins are sequestered in the cytoplasm by their natural inhibitor, IκB proteins. Bacterial factors such as lipopolysaccharides (LPS) and peptidoglycans can be recognized by the Toll-like receptor (TLR) on the cell membrane. TLRs are evolutionarily conserved PRRs that recognize conserved PAMPs present on the surface of various microbes. Up to now, 11 mammalian TLRs have been described and different TLRs can recognize different PAMPs including LPS, peptidoglycan, DNA, RNA and flagellin. After recognition, the TLR will convey signals stimulated by these factors, through the adapter proteins such as MyD88 and TRAF6 to the IκB kinase (IKK) complex (Hayden and Ghosh, 2004).

The IKK complex comprises IKKα and IKKβ catalytic subunits and IKKγ regulatory subunits. In the classical NF-κB pathway, the IKKβ will phosphorylate the IκBs (Ghosh *et al*, 1998). The phosphorylated IκB proteins are then degraded by the proteasome via the ubiquitin pathway (Figure 1.2). The degradation of IκB unmasks the nuclear localization signal (NLS) of the NF-κB protein, leading to its nuclear translocation. In the nucleus, NF-κB transcription factor binds to the promoter of various genes with the consensus κB sequence, 5'–GGGRNNYYCC–3', and upregulate the expression of these target genes (Bonizzi and Karin, 2004). The activation and nuclear translocation of classical NF-κB dimers (mostly p50-p65) activate the expression of genes encoding chemokines, cytokines and adhesion molecules. These molecules are important components of the innate immune response to invading pathogens and are required for the ability of inflammatory cells to migrate into areas where NF-κB is being

activated (Bonizzi and Karin, 2004). The activated NF-κB pathway can then be downregulated through multiple mechanisms, such as the synthesis of IκBα proteins.

Recently, a new pathway for NF-κB activation that is strictly dependent on IKKα but not IKKβ and IKKγ was described (Figure 1.2) (Senftleben *et al*, 2001). The alternative pathway is activated by LTβ (lymphotoxin), BAFF (B-cell activating factor) and CD40L (CD40 ligand) and leads to the phosphorylation and processing of p100, generating the p52/RelB heterodimers. It has been shown that the NF-κB inducing kinase (NIK) is responsible for directly phosphorylating and activating IKKα; however events that occur upstream of NIK are still unclear.

Because LTβ, BAFF and CD40L also activate the classical pathway, it would appear that intracellular signaling domains of these receptors possess additional sequence motifs that allow their coupling to NIK and activation of the alternative pathway (Hayden and Ghosh, 2004). Many findings strongly support that the alternative pathway plays a central role in the expression of genes involved in the development and maintenance of secondary lymphoid organs (Bonizzi and Karin, 2004). Based on evolutionary considerations, the original function of the NF-κB signaling pathway was the activation of innate immune responses. Indeed, the function of IKK and NF-κB in the fruit fly is in the activation of innate immune responses. Thus, it has been proposed that the function of the alternative NF-κB pathway in adaptive immunity and lymphoid organ development is probably a more recent adaptation (Bonizzi and Karin, 2004).

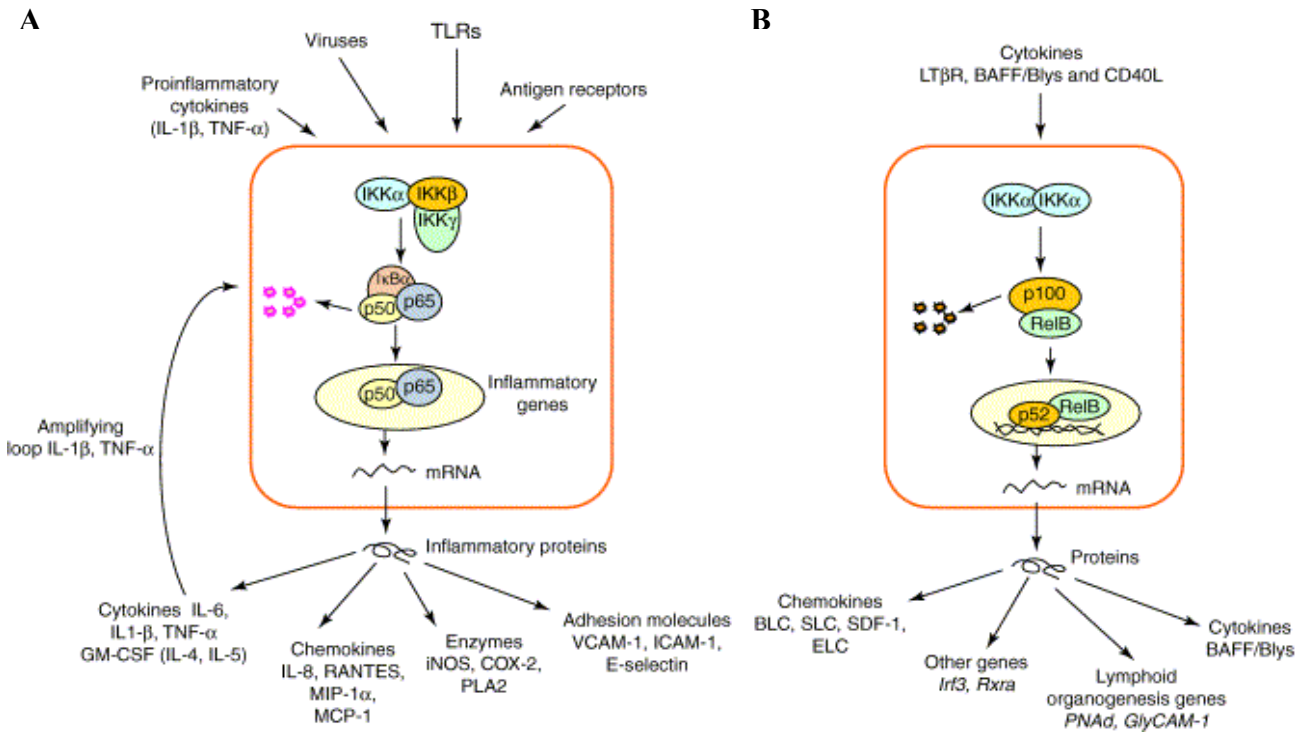

Figure 1.2: Classical and alternative NF-κB signaling pathway. (A) The classical NF–κB pathway is activated by a variety of inflammatory signals, resulting in coordinate expression of multiple inflammatory and innate immune genes. The proinflammatory cytokines IL-1β and TNF-α activate NF-κB, and their expression is induced in response to NF-κB activation, thus forming an amplifying feed forward loop. **(B)** The alternative pathway for NF-κB results in nuclear translocation of p52–RelB dimmers, which is strictly dependent on IKKα homodimers and is activated by LTβR, BAFF and CD40L by NIK. Many data strongly suggest that the alternative pathway plays a central role in the expression of genes involved in development and maintenance of secondary lymphoid organs. Abbreviations: BAFF, B-cell-activating factor belonging to the TNF family; BLC, B-lymphocyte chemoattractant; CD40L, CD40 ligand; COX-2, cyclooxygenase 2; ELC, Epstein–Barr virus-induced molecule 1 ligand CC chemokine; GM-CSF, granulocyte–macrophage- colony-stimulating factor; ICAM-1, intercellular adhesion molecule 1; IKK, IκB kinase; IL-1β, interleukin-1β; iNOS, inducible nitric oxide synthase; LT, lymphotoxin; MCP-1, monocyte chemotactic protein-1; MIP-1α, macrophage inflammatory protein-1α; NIK, NF–κB-inducing kinase; PLA2, phospholipase 2; SDF-1, stromal cell-derived factor-1α; SLC, secondary lymphoid tissue chemokine; TLRs, Toll-like receptors; VCAM-1, vascular cell adhesion molecule-1. Adapted from Bonizzi and Karin (2004).

1.2.2 NF-κB signaling pathway in *Drosophila*

The NF-κB signaling pathway is conserved in many different species, underscoring its pivotal role in immune response. Studies on *Drosophila* NF-κB signaling pathway have had a major impact on this field, leading to the key discoveries on the fundamental concepts on how organisms effectively fight pathogens (Hoffmann, 2003). In *Drosophila,* three NF-κB homologues have been described -Dorsal, Dif, and Relish (Figure 1.3). Of these three NF-κB proteins, Dif is the predominant transactivator in the antifungal and anti-Gram-positive bacterial defense in adults. Dorsal can substitute for Dif in the larvae (Baeuerle and Baltimore, 1996; Rutschmann *et al*, 2000). Both Dorsal and Dif can be activated by a transmembrane protein called Toll, which is a homologue of human TLR. Two main groups of microorganisms (Gram-positive bacteria and fungi) can induce the Toll pathway. Among Gram-positive bacteria, *Micrococcus luteus* is a very strong inducer of this pathway. In contrast to what has been proposed for the TLRs in mammals, *Drosophila* Toll is not a *bona fide* pattern recognition receptor for microbial substances, but binds instead to the cleaved form of its endogenous ligand, Spätzle (Schneider *et al*, 1994). The recognition of Gram-positive bacteria requires PGRP-SA, which initiates an extracellular signaling cascade (Royet *et al*, 2005). Recently, Wang *et al* (2006a) found that gram-negative binding protein 1 (GNBP1) is essential for for sensing of pepitoglycan (PG) by PGRP-SA and the interaction between these proteins and PG is essential for downstream signaling. Downstream of the extracellular signaling events is the cleavage of Spätzle, which then binds to and activates the Toll receptor (Belvin and Anderson, 1996).

Most of the intracellular signaling components of the Toll pathway are related to factors of the human IL-1 and Toll-like receptor pathways (Hoffmann and Reichhart, 2002). Upon activation, Toll binds to the intracellular adapter protein, MyD88, which is a homologue of the adapter protein MyD88 in mammals. Then the signal is transmitted to Pelle (a homologue of mammalian IRAK) which leads to the phosphorylation of Cactus (Figure 1.3) (Hoffmann *et al*, 1999). Cactus is a homologue of the mammalian IκB protein, which keeps transcription factors of Dorsal and Dif at the resting stage, preventing them from entering the nucleus (Geisler *et al*, 1992). The phosphorylation of Cactus is believed to be mediated by an unknown serine protease, which leads to its degradation. Like IκB, the ubiquitin/proteasome pathway is required for signal-dependent Cactus degradation. Mutants in *slimb*, the *Drosophila* β-TrCP homolog, exhibit defects in dorsoventral patterning (Spencer *et al*, 1999). Like the mammalian NF-κB proteins, after the inhibitor Cactus is degraded, Dif and Dorsal are released and translocated into the nucleus (Figure 1.3). Thus, it appears that the mechanisms involved in the activation of the *Drosophila* Dorsal and Dif proteins during antifungal immunity are highly similar to those required for the activation of NF-κB in mammals.

The most specific target gene of the Toll pathway is *Drosomycin*, which have antifungal activity (Silverman and Maniatis, 2001). The Toll/Dif pathway also partially activates the expression of *Cecropins* and *Attacins* and seems to be indispensable for some Gram-positive bacterial infections. However many insect antibacterial genes, including *cecropin, defensin* and *diptericin* are not regulated by Dorsal or Dif. It suggests that an additional NF-κB transcription factor is involved in responding to microbial infection in *Drosophila.* Indeed, the third NF-κB protein known as Relish was described

in 1996, which is the homolog of the mammalian p105 and p100 proteins (Dushay *et al*, 1996).

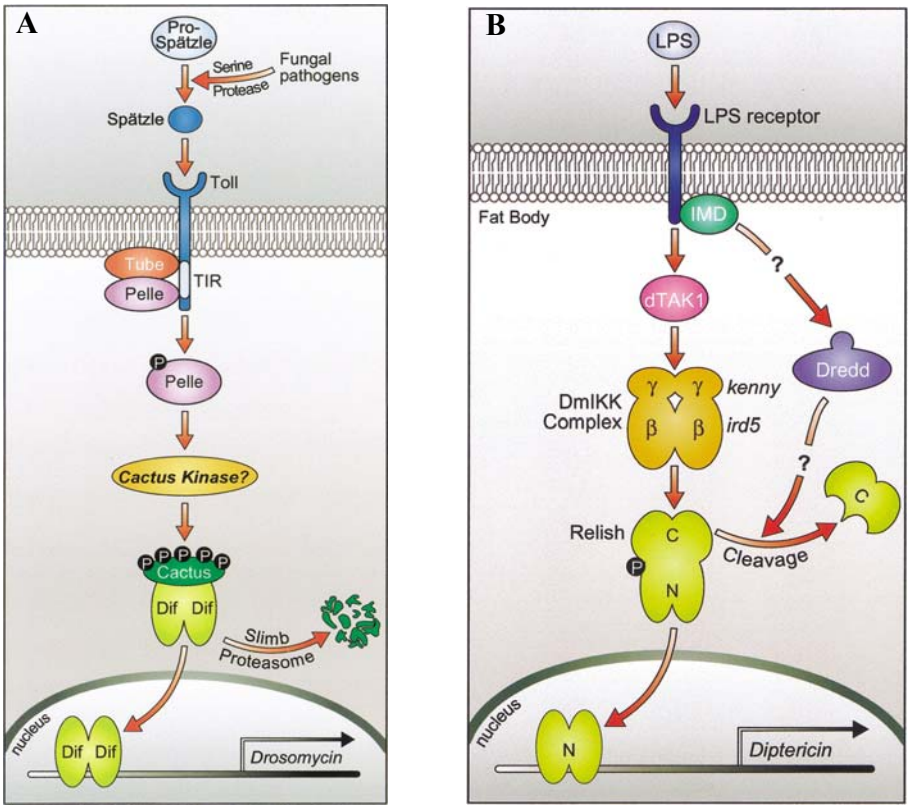

Figure 1.3: The *Drosophila* NF-κB signaling pathway. (A) Toll/anti-fungal signaling pathway. The pattern recognition receptors that recognize fungal pathogens are believed to activate a serine protease cascade, culminating in the cleavage of the Toll ligand Spätzle. Ligand binding to Toll leads to the recruitment of two proteins, the adaptor Tube and the kinase Pelle. Recruitment of Pelle is thought to cause its activation and disassociation from Toll. Activated Pelle may then activate, directly or indirectly, a Cactus kinase that is responsible for signaling the proteasome-mediated degradation of Cactus. Currently, the biochemical steps between Pelle and Cactus degradation remain undetermined, and the Cactus kinase has not yet been identified. **(B)** The antibacterial signaling pathway. In this model, the signaling pathway is activated by LPS through unidentified receptor(s) and leads to Relish cleavage. Downstream of the receptors, this signaling pathway bifurcates. One part leads to activation of the *Drosophila* IKK complex, which then phosphorylates Relish. The other part functions through the caspase Dredd and leads to the cleavage of phosphorylated Relish. At present it is not known whether Dredd acts directly or indirectly to cleave Relish. The Imd protein may function in one or both of these pathways. N: Amino-terminal domain; C: carboxy-terminal domain. Adapted from Silverman and Maniatis (2001).

Compared to Dorsal and Dif, Relish contains both the transcription factor and the inhibitor in one protein (see Figure 1.1A). Like mammalian p105 and p100, the Relish contains the N-terminal Rel-homology domain and the C-terminal IκB-like domain (Dushay *et al*, 1996). This Relish pathway shares similarity with the human TNF pathway, however there is no TNF receptor homolog found in *Drosophila*. Subsequently, it was shown that the putative transmembrane protein PGRP-LC is the receptor of the Relish pathway (Choe *et al*, 2002). Intracellular activation of the Relish pathway commences with recruitment of Imd, a death domain protein sharing similarities with the mammalian TNF-α receptor interacting protein, RIP, although the mechanism of how PGRP-LC signals to Imd is still unknown.

In unstimulated cells the Relish C-terminal IκB module sequesters its own N-terminal NF-κB module in the cytoplasm. Upon activation of the antibacterial signaling pathway, Relish is proteolytically cleaved and the N-terminal NF-κB module translocates into the nucleus (Figure 1.3B), while the stable C-terminus remains in the cytoplasm. The activation of Relish requires the *Drosophila* IKKγ homolog, Kenny, for which Relish is the substrate (Silverman *et al*, 2000). Genetic studies with mutant flies for the Relish gene revealed that the Relish pathway has influence on all antimicrobial peptides. The *Diptericin* gene stands solely under the regulation of Relish, while all the other genes are also partially influenced by Dif (Hedengren *et al*, 1999). It suggests that different members of the NF-κB family are activated to regulate distinct sets of antimicrobial genes in response to different pathogens.

1.2.3 Evolution and conservation of NF-κB signaling pathway

An intriguing parallel to the human NF-κB signaling pathway also exists in other insects and vertebrates such as mosquito, beetle and zebrafish. The second NF-κB homologue in invertebrates was cloned from *Anopheles gambiae*, a species of mosquito (Barillas-Mury *et al*, 1996). Gambif, which is the mosquito orthologue of Dorsal, has been characterized and shown to translocate to the nucleus following bacterial infection. In 2002, a Relish-like NF-κB protein was described in *Aedes aegypti*, another species of mosquito (Shin *et al*, 2002). The *A. aegypti* Relish gene has three alternatively spliced transcripts encoding three different proteins: full length Relish, IκB-type, which lacks the Rel homology domain (RHD) and the Rel-type in which the carboxy-terminal ankyrin repeats are missing. The involvement of *A. aegypti* Relish in the regulation of immune response to bacterial challenge has been shown using transgenic mosquitoes (Shin *et al*, 2003). Although no orthologue of Dif has been found in the mosquito genome, the identification of the mosquito orthologue of MyD88, Tube and Pelle indicates that the Toll pathway in the mosquito is at least partially conserved (Christophides *et al*, 2002). The absence of a Dif orthologue in the mosquito genome suggests that Dorsal may play a functional role in the mosquito Toll-mediated innate immune responses. Indeed, Shin *et al.* (2005) found that AaREL1, the mosquito homologue of *Drosophila* Dorsal, is a key regulator of the Toll antifungal immune pathway in *A. aegypti* female mosquitoes.

The evolutionary conservation of NF-κB transcription factors was further demonstrated by the cloning and characterization of NF-κB proteins in zebrafish, beetles and mollusk in 2004 (Correa *et al*, 2004; Montagnani *et al*, 2004; Sagisaka *et al*, 2004). The evolutionary conservation of the NF-κB transcription factors, from *Drosophila* to

humans, probably suggests that the NF-κB signaling pathways of *Drosophila* and humans have evolved from a common ancestral family of building blocks (Hoffmann and Reichhart, 2002).

1.2.4 TLR/NF-κB signaling pathway in *C. elegans*

Unexpectedly, the NF-κB signaling pathway seems not to be conserved in the *C. elegans*. Although sequence comparisons show the worm possesses homologues of certain components of the NF-κB pathway (Figure 1.4), the genetic studies showed that these functional homologues (Toll, Traf, Cactus) in *C. elegans* are not involved in resistance to pathogen infection (Pujol *et al*, 2001). Most strikingly, there is no obvious NF-κB homologue in the genome of the *C. elegans* (Figure 1.4) (Pujol *et al*, 2001). These observations suggest that the classical NF-κB signaling pathway is not functional in the immune system of *C. elegans* (Kim and Ausubel, 2005). Those findings indicate that the NF-κB signaling pathway should have originated in a species between *C. elegans* and *Drosophila* in the evolutionary chain. However, the origin of the NF-κB signaling pathway remains unknown. Furthermore, whether the similarities between *Drosophila* and human NF-κB signaling pathway have resulted from convergent evolution or reflected common ancestral pathways is still a conundrum. As Hoffmann and Reichhart (2002) have suggested, more information on the NF-κB-signaling pathway in species more ancient than the *Drosophila* will shed light on this mystery.

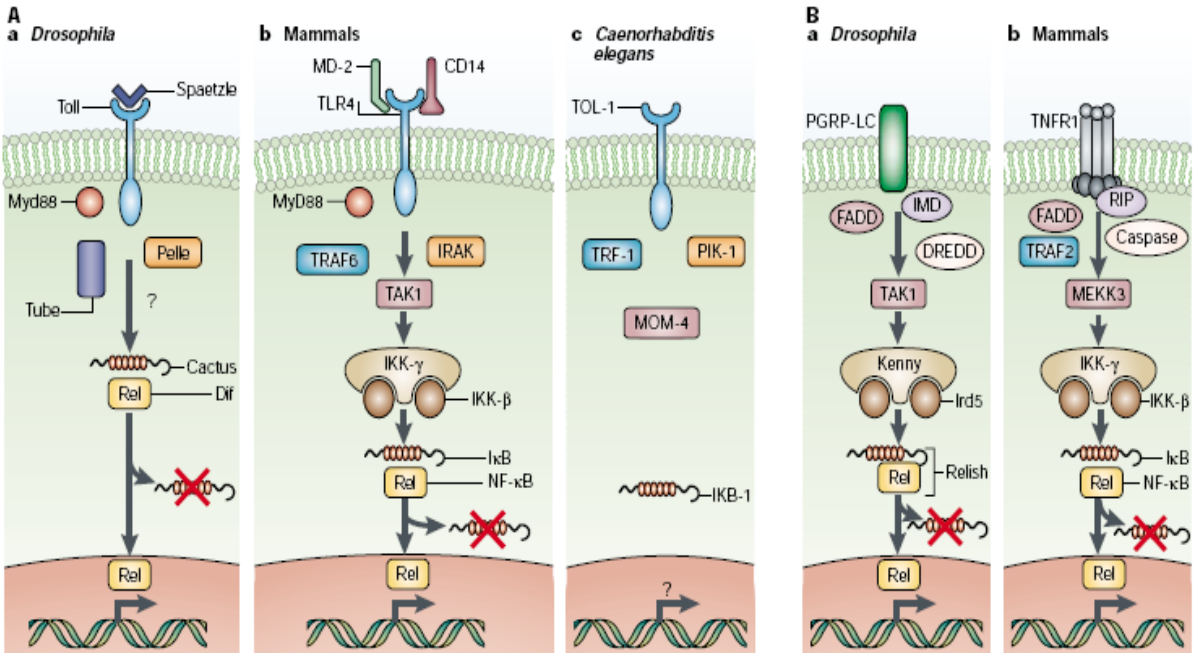

Figure 1.4: The NF-κB signaling pathways in human, *Drosophila* and *C. elegans*. (A) A simplified Toll signaling pathway in *Drosophila* (a) compared to the mammalian TLR4 pathway (b). Homologues of some, but not all, of these proteins can be found in *C. elegans* (c). **(B)** A simplified Imd signaling pathway in *Drosophila* (a) compared to the mammalian tumor necrosis factor (TNF) pathway (b). Activation of the *Drosophila* Toll and Imd pathways leads to the nuclear import of Relish-type transcription factors. Crosses indicate the degradation of Cactus/IκB. CD, cluster of differentiation; Dif, Dorsal-related immunity factor; DREDD, death-related cell death abnormality-3 (*ced-3*)/Nedd2-like; FADD, Fas-associated death domain protein; Ird, immune response deficient; Imd, immune deficiency; IRAK, interleukin 1 receptor associated kinase; IRD, immune response deficient; MEKK, mitogen-activated protein kinase kinase; MOM, more of MS; NF, nuclear factor; PIK, Pelle/IRAK homologue; RIP, receptor interacting protein; TAK, TGFβ activated kinase; TOL, Toll homologue; TRAF, TNF receptor associated factor; TRF, TRAF homologue. Adapted from Kurz and Ewbank (2003).

1.2.5 Some clues on the possible existence of NF-κB signaling pathway in the horseshoe crab

The horseshoe crab, commonly referred to as *Limulus* is one of the most ancient arthropods, which has survived unchanged for almost ~550 million years (Størmer, 1952). It has evolved a formidable host defense system (Iwanaga, 2002). Therefore, it will be interesting to examine if horseshoe crab harbors an NF-κB signaling pathway, as it will be helpful in the understanding of the origin and evolution of this crucial innate immune signaling pathway. Recently, Inamori *et al* (2004) reported the presence of TLR in the horseshoe crab. However the existence of TLR does not necessarily suggest the presence of NF-κB proteins as was observed in the *C. elegans* (Kim and Ausubel, 2005). Thus, the question of whether the horseshoe crab possesses functional NF-κB homologue remains uncertain. Recently, in our laboratory, it has been found that the Factor C (the LPS-activated serine protease that triggers the coagulation cascade in immune defense) promoter contains several functional κB motifs, suggesting the possible existence of NF-κB transcription factor in this ancient animal (Wang *et al*, 2003). Besides this clue, there is no direct evidence to demonstrate the presence of NF-κB transcription factor in the horseshoe crab. Thus, the issue of whether the ancient origin of the NF-κB signaling cascade can be traced back to this "living fossil" remains a mystery. Therefore, we decided to investigate if the NF-κB signaling pathway also existed in the horseshoe crab and the function of the ancient NF-κB signaling pathway in innate immunity in this archaic arthropod species. The cloning of NF-κB transcription factors from horseshoe crab will provide critical insights into the evolution of the NF-κB transcription factor.

This will clarify the viewpoint that the NF-κB signaling cascade originated from a common ancestral family of building blocks and was already present in the *Urbilateria* (Hoffmann and Reichhart, 2002).

1.3 Thioredoxins and their roles in regulating immune response

1.3.1 Reactive oxygen species (ROS) and antioxidant system

It is well known that ROS plays important roles in immune defense by directly killing the pathogen, or as a signaling molecule (Flohe *et al*, 1997; Nakano *et al*, 2006; Segal, 2005; Swain *et al*, 2002). Although the ROS response is designed to restrict any damage to the smallest possible region where the pathogen is located, some of the ROS inevitably leak into the surrounding areas where they have the capacity to inflict tissue damage at sites of inflammation (Swain *et al*, 2002). Thus, it is essential that the host defense responses of these cells are finely tuned to result in the appropriate level of oxidative response to any given situation. To protect themselves against ROS toxicity, the hosts have developed different antioxidant systems. Amongst these are low molecular weight antioxidant molecules, such as ascorbic acid, uric acid and glutathione (GSH) as well as antioxidant enzymes such as superoxide dismutase (SOD), catalase, glutathione peroxidase (GPX), glutathione reductase (GR) and the thioredoxin (TRX) system (Nakano *et al*, 2006). Figure 1.5 illustrates the mechanisms for the generation of ROS in the mitochondria and their elimination by cellular antioxidants. Within the scope of this thesis, the following sections will focus on the significance of thioredoxin in

regulating the redox status to ensure accurate self-nonself recognition, and antimicrobial combat without inflicting damage to the host.

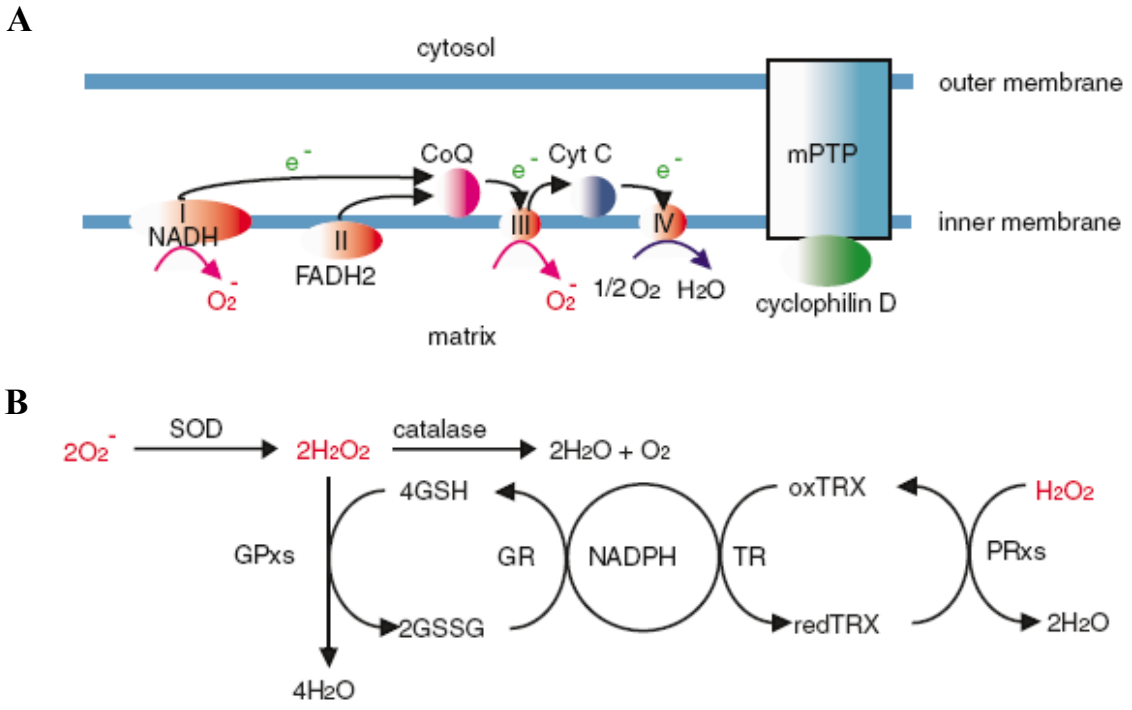

Figure 1.5: Generation of ROS in the mitochondria and their elimination by cellular antioxidants. (A) The mitochondrial respiratory chain consists of four multimeric complexes (complexes I–IV), coenzyme Q (CoQ), and cytochorome c (Cyt C). Electrons (e^-) are transferred from the reducing equivalent (NADH-$FADH_2$) to molecular oxygen through the mitochondrial respiratory chain, finally generating water at complex IV. During the electron transfer, reactive oxygen species (ROS) are generated at complexes I and III. The mitochondrial permeability transition pore (mPTP) is regulated by cyclophilin D. Opening of this pore results in massive loss of ions and metabolites from the matrix. **(B)** O^-_2 is converted into H_2O_2 by superoxide dismutases (SODs). H_2O_2 is then eliminated by catalase, glutathione peroxidases (GPXs), and peroxiredoxins (PRXs). During elimination of H_2O_2, reduced glutathione (GSH) is converted to disulfide form (GSSG) by GPXs, and then GSSG is recycled to GSH by glutathione reductase (GR). However, PRXs also catalyze H_2O_2 into H_2O by using reduced thioredoxin (TRX). Oxidized TRX is then recycled back to reduced TRX by thioredoxin reductase (TR). NADPH is essential for both recycling reactions. Adapted from Nakano *et al* (2006).

1.3.2 Thioredoxin superfamily

Thioredoxin (TRX), which functions as a general protein-disulfide reductase, is commonly known to be a small ubiquitous protein of 12 kDa. It is evolutionarily conserved from prokaryotes to eukaryotes, plants, and animals (Holmgren, 1985). The redox activity of TRX has been reported to reside in a conserved active site, Cys-Gly-Pro-Cys (CGPC), in which the two Cys residues undergo reversible oxidation, converting its dithiol group to a disulfide bond (Powis and Montfort, 2001). The three-dimensional structure of TRX is conserved throughout evolution and consists of four or five central β-sheets externally surrounded by three or four α-helices (Figure 1.6). The active site is located in a protrusion of the protein between the β2-strand and the α2-helix. Both the conserved active site sequence and the three-dimensional structure of TRX are the hallmarks of this superfamily (Martin, 1995).

TRX is maintained in its active reduced form by the thioredoxin reductase (TR), a selenocysteine-containing protein that uses the reducing power of NADPH (Powis and Montfort, 2001). TRXs have been implicated in a number of mammalian cell functions: (a) outside the cell in cell growth stimulation and chemotaxis, (b) in the cytoplasm as an antioxidant and a cofactor, and (c) in the nucleus in regulation of transcription factor activity. TRX is also upregulated in response to a wide variety of oxidative stresses, including viral infections and ultraviolet irradiation (Nakamura *et al*, 1997). Furthermore, abnormal expression of TRX has been correlated with a number of pathophysiological conditions such as cancer, Alzheimer's and Parkinson's diseases,

suggesting that the activation-regulation of TRX plays an important role in human diseases (Hirota *et al*, 2002).

Thioredoxin functions in a variety of cellular processes that can be generalized into two major roles. Firstly, the TRX functions as an electron carrier to catalyze the biosysthesis of antioxidant enzymes such as ribonucleotide reductases, methonine sulfoxide reductase and the peroxiredoxins. Secondly, they act as antioxidants to protect cytosolic proteins from inactivation via oxidant-mediated disulfides (Arner and Holmgren, 2000).

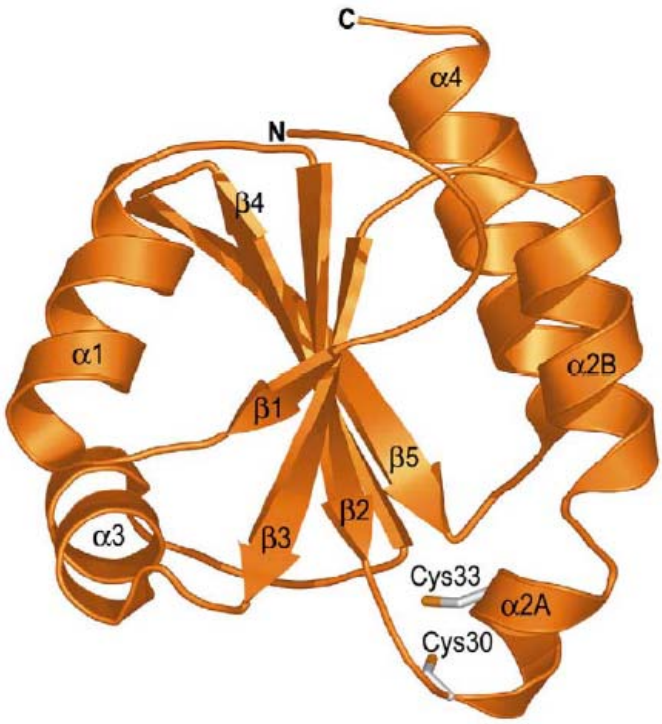

Figure 1.6: The three-dimensional structure of TRX. Schematic drawing of the *T. brucei* TRX with central pleated five β sheets surrounded by four α helices. The redox active disulfide (Cys^{30} & Cys^{33}) is located in a small cleft between the main body of the molecule and a protrusion in the protein at the N-terminus of the α2A helix. Adapted from Friemann *et al* (2003).

So far, several kinds of TRX with different catalytic sites have been characterized in various organisms (see Figure 3.44). The first characterized human TRX (TRX1) is a 12 kDa protein with a catalytic sequence of CGPC. Although the 12 kDa bacterial TRX only contains the two cysteine residues at its catalytic site, the human 12 kDa TRX contains three other cysteine residues. The C-terminal Cys^{73} is involved in dimerization, and may convey unique biological properties to mammalian TRX (Holmgren, 1985). A second slightly larger TRX (TRX2) is a 166-amino acid protein with a molecular weight of 18 kDa, containing a conserved TRX catalytic site. It has been identified in the mitochondria of pig's heart (Spyrou *et al*, 1997). The 60-amino acid N-terminal extension of TRX-2 exhibits characteristics consistent with a mitochondrial translocation signal, and mitochondrial localization of TRX-2 was confirmed by Western blotting (Miranda-Vizuete *et al*, 2000). A 32 kDa thioredoxin-like cytosolic protein was first cloned from a human testis cDNA library (Lee *et al*, 1998). The 289 amino acid protein has an N-terminal TRX domain of 105 amino acids, a conserved TRX active site (CGPC), and a high degree of homology to human TRX. It is ubiquitously expressed in human testis. In 1997, a type of TRX called nucleoredoxin (NRX) with a WCPPC catalytic site was cloned from mice. Interestingly, this 435-amino acid protein is localized to the nucleus (Kurooka *et al*, 1997). Recently, a family of 16 kDa TRX has been identified from the Nematodes and protozoa of the family Trypanosomatidae with an active site of WCPPC (Kunchithapautham *et al*, 2003). Despite notable differences in the molecular mass and amino acid sequence of the catalytic site, those forms of TRXs appear to be functionally similar to the classical 12 kDa TRXs. Therefore, it appears that there is

considerable flexibility in the two residues between the conserved Cys residues in the active site, and that the different catalytic sequences might confer diverse enzymatic activity and substrate specificity (Kunchithapautham *et al*, 2003). This observation supports the versatility of the TRX molecule and reflects its prowess in anti-oxidative protection of the host.

1.3.3 The influence of TRX in NF-κB signaling pathway

In resting cells, TRX does not have a specific localization signal; and is hence expressed in the cytoplasm. However, under pathophysiological stress, TRX shows various intracellular localizations. It was observed that in HeLa cells, TRX translocates from the cytoplasm into the nucleus after exposure to phorbol 12-myristate 13-acetate, PMA (Hirota *et al*, 1999). In human retinal pigment epithelial cells, TRX was detected in the mitochondria after H_2O_2 treatment. From the varied subcellular localizations of TRXs, it may be suggested that TRXs play essential roles in many cellular processes (Hirota *et al*, 2002). Indeed, several functions have been assigned to TRX, mostly related to its redox activity, including the regulation of transcription factor DNA-binding activity, antioxidant defense, modulation of apoptosis, and the immune response (Hirota *et al*, 2002; Powis and Montfort, 2001). Furthermore, TRX has been shown to selectively activate the DNA-binding activity of a number of transcription factors, including NF-κB, AP-1, p53, estrogen receptor and glucocorticoid receptor (Hirota *et al*, 2002). This thesis will focus on the roles of TRX in the NF-κB signaling pathway.

The binding of NF-κB to DNA requires the NF-κB to be fully reduced especially the Cys^{62} of the NF-κB p50 subunit. If the Cys^{62} of one subunit is linked in a disulfide bridge with the Cys^{62} of the other subunit, the DNA can no longer gain access to the binding surface of the p50 homodimer (Powis and Montfort, 2001). In the nucleus, the human 12 kDa TRX1 enhances the DNA-binding of NF-κB by directly reducing the cysteine groups in the DNA-binding motif of NF-κB (Figure 1.7) (Flohe *et al*, 1997). It has been shown that TRX1 is 500 times more effective in enhancing NF-κB DNA-binding ability than 2-mercaptoethanol or DTT, conventionally used in EMSA (Electrophoretic mobility shift assay) techniques to demonstrate DNA-binding (Hayashi *et al*, 1993). However, other studies have found that transient transfection of TRX1 also inhibits NF-κB activation upon PMA stimulation (Schenk *et al*, 1994). From the study of Hirota *et al.* (1999), it has been suggested that TRX plays dual and opposing roles in the regulation of NF-κB in the nucleus and cytoplasm. In the cytoplasm, TRX interferes with the signals to IκB kinases, and blocks the degradation of IκB, thus maintaining the inactivity of NF-κB as a complex; but in the nucleus, it was observed that TRX enhances NF-κB transcriptional activities by augmenting its DNA-binding ability. The authors proposed that this two-step TRX-dependent opposing regulation of the NF-κB complex might be a novel activation mechanism of redox-sensitive transcription factors. However, the dual roles of TRX in the regulation of NF-κB underlying the accompanying redox processes have to be viewed as events separate in time, or space, or both (Flohe *et al*, 1997).

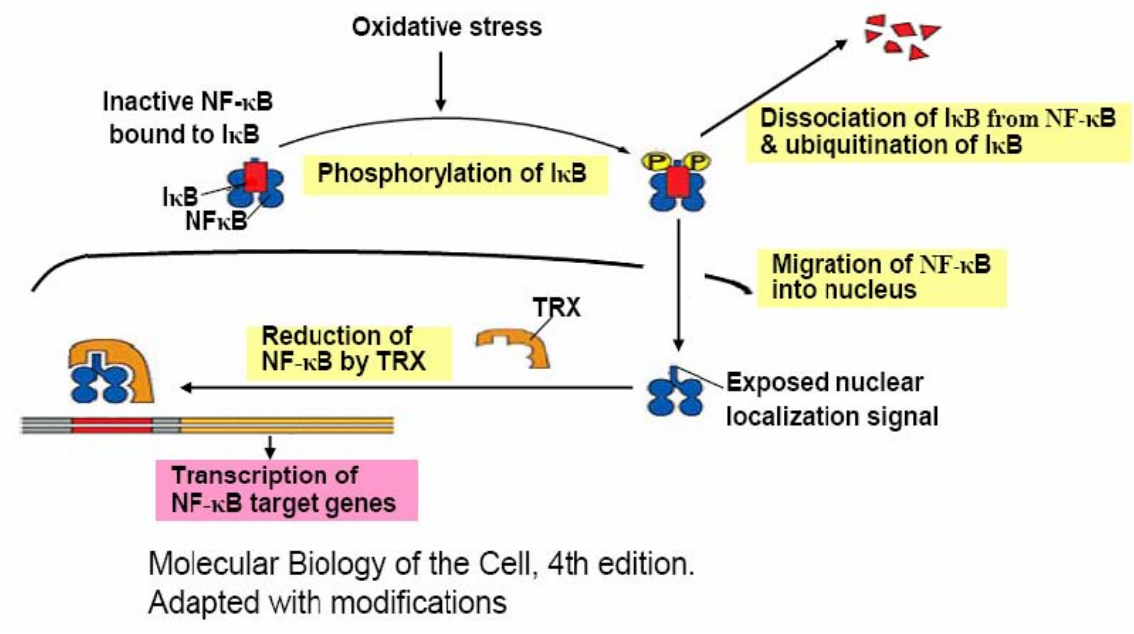

Figure 1.7: Activation of NF-κB signaling pathway involves TRX. Oxidative stress causes activation signals to phosphorylate IκB, which results in the dissociation of IκB from NF-κB and ubiquitination of IκB. Activated NF-κB translocates into the nucleus, and TRX enhances NF-κB DNA binding, resulting in the transcription of NF-κB dependent genes. Adapted with modification from Alberts *et al* (2002).

1.3.4 The thioredoxin family in arthropods

It has been shown that the defense mechanisms against oxidative damage in insects have diverged from both higher and lower organisms. In insects, which lack a genuine glutathione reductase, TRXs fuel the glutathione system with reducing equivalents (Kanzok *et al*, 2001). The crucial role of the thioredoxin system *in vivo* is supported by the fact that *Drosophila* TRX reductase (TRXR) null mutations are lethal in

the larval stage and that reduced TRXR activity severely affects the life span of the insects. Thus, characterizing TRXs from these organisms contributes to our understanding of redox control in glutathione reductase-free systems and provides information on novel targets for insect control (Wahl *et al*, 2005). So far, two TRX proteins from *Drosophila melanogaster* and one TRX from *Anopheles gambiae* have been biochemically characterized (Bauer *et al*, 2002). However, no report is available on the TRX system in other arthropod species besides insects. Furthermore, in invertebrates, the functions of TRX in regulating transcription factors are still unknown.

Previously, we utilized subtractive cDNA hybridization to identify genes that are important for immune defense in horseshoe crab (*C. rotundicauda*) (Ding *et al*, 2005). The subtracted cDNAs were subsequently cloned into plasmids and screened for differential expression. Using this approach, we identified one cDNA clone that was differentially expressed in the hepatopancreas (equivalent to liver in mammals) upon *P. aeruginosa* challenge. Sequence analysis revealed that this gene encodes a protein possessing the characteristic organization of TRX proteins, henceforth referred to as *C. rotundicauda* TRX (Cr-TRX1). In order to understand the functions of TRX in the arthropod anti-oxidant system and NF-κB signaling pathway, we decided to examine the biochemical characteristics of the Cr-TRX1 and investigate its roles in regulating the NF-κB signaling pathway.

1.4 The horseshoe crab as model for innate immunity study

1.4.1 Horseshoe crab is a "living fossil"

The horseshoe crab belongs to the order *Xiphosura* that has more than 500 million years of evolutionary success. Because its basic body design remains virtually unchanged for millions of years, the horseshoe crab is often called the "living fossil" (Størmer, 1952). Today, there are four species of horseshoe crabs in different habitats around the world: *Limulus polyphemus* in the East coast of USA; *Tachypleus tridentatus* in China and Japan and *Tachypleus gigas* and *Carcinoscorpius rotundicauda* in South Asia. The species of interest in this project is *Carcinoscropius rotundicauda*, which thrive in 30 % seawater condition, in brackish mangrove swamps that teem with very high counts of pathogenic microbes.

1.4.2 Advantages of using horseshoe crab for innate immunity research

Several obvious reasons have made invertebrates good models for the study of innate immunity. First, the invertebrates lack adaptive immunity and rely solely on the innate immune system for protection against pathogen infection. Therefore, the influence from the adaptive immune system to the innate immune responses is totally absent. Secondly, due to the evolutionary conservation of innate immune-related molecules, knowledge of the innate immunity in the invertebrates is very useful for the understanding of molecular mechanisms underlying the innate immune responses in the vertebrates (Little *et al*, 2005). Particularly, those molecules which have counterpart

homologs in humans will be an important translational significance to understanding the immune system in humans.

Over the last two decades, a wide variety of invertebrates have been used as experimental models for the studies of the innate immunity, such as the *C. elegans*, freshwater crayfish, ascidians, Pacific oysters, horseshoe crab and insects including *Drosophila melanogaster* (fruit fly), *Bombyx mori* (silkworm), *Manduca sexta* (tobacco hornworm), *Anopheles gambiae* (mosquito) (Iwanaga and Lee, 2005). Amongst these species, the *Drosophila* and *C. elegans* are the animal models of choice due to the availability of genome sequences that allows the high throughput genomic and proteomic analysis and ease of genetic manipulation (Royet, 2004). Indeed, studies in these organisms have greatly contributed to the understanding of innate immunity, especially the discovery of Toll/NF-κB signaling pathway in *Drosophila*. However, there are some drawbacks with the model organism, *Drosophila*. These include such impracticalities such as the low volume of hemolymph obtainable from each individual and the fragile nature of the experimental subject. In contrast, the horseshoe crab is a good model for innate immune study since it has much larger volume of blood and bigger tissues compared with most of the other invertebrate models, allowing convenient physiological and molecular manipulations. In addition, this organism harbors a very sophisticated innate immune system that has enabled it to survive for more that 500 million years. Furthermore, it has been shown that the horseshoe crab possesses some critical components in innate immune response, for example, the complements which are evolutionarily conserved in the human but absent in *Drosophila* (Zhu *et al*, 2005).

1.4.3 Horseshoe crab possesses a powerful innate immune system

The burrowing habits of the horseshoe crabs cause them to encounter large numbers of challenging microorganisms. The horseshoe crab has developed a powerful innate immune system to combat the pathogenic microorganisms, especially Gram-negative bacteria. Indeed, it has been demonstrated that the horseshoe crab, *C. rotundicauda*, survived an infection of 2×10^7 CFU of *P. aeruginosa* / kg of body weight (Ng *et al*, 2004), a dose that was shown to be lethal to mice (Stieritz and Holder, 1975). The immune response was so fast and efficient that the majority of the bacterial inoculum was cleared from the plasma after three hours of infection and the rest was completely eradicated within 72 hours (Ng *et al*, 2004).

The horseshoe crab relies completely on innate immunity, employing a unique array of efficient host defense system. The hemolymph of the horseshoe crab contains soluble defense molecules and large members of granular hemocytes (amoebocytes), which undergo degranulation upon contact with Gram-negative bacteria. Ninety nine % of the circulating hemocytes are granular being filled with two types of granules (Figure 1.8): large (L)- and small (S)- granules (Iwanaga *et al*, 1998). In *Tachypleus tridentatus* (the Japanese species), the L-granule selectively stores more than 20 defense molecules with molecular masses mainly between 8 and 123 kDa, such as clotting factors (Factor C, B and G), a clottable protein coagulogen, proteinase inhibitors, lectins and antimicrobial peptides (Iwanaga, 2002). In contrast, the S-granule contain at least 6 proteins with molecular masses of less than 30 kDa, and large amounts of hairpin-like tachyplesin peptides, tachystatins, tachycitins and big defensins (Table 1.1), all of which show

antimicrobial activities against Gram-negative and Gram-positive bacteria, and fungi (Iwanaga, 2002). The hemocytes are extremely sensitive to LPS and respond to its presence by degranulation, so releasing large numbers of defense molecules that work in concert to defend the host from the invading microbes.

The presence of such a broad spectrum of immune responsive molecules suggests that the molecular mechanisms of innate immune responses in the horseshoe crab are very complex. However, how the sophisticated immune system is regulated is largely unknown and the cellular signaling pathways that are critical for controlling innate immunity in the horseshoe crab remain to be uncovered and exploited. Since the horseshoe crab contains many innate immune molecules which are well conserved in humans, an understanding on the molecular mechanism of actions of these functional homologues would be very beneficial towards the understanding of the functions of their counterparts in the humans for meaningful translational research on human immune response.

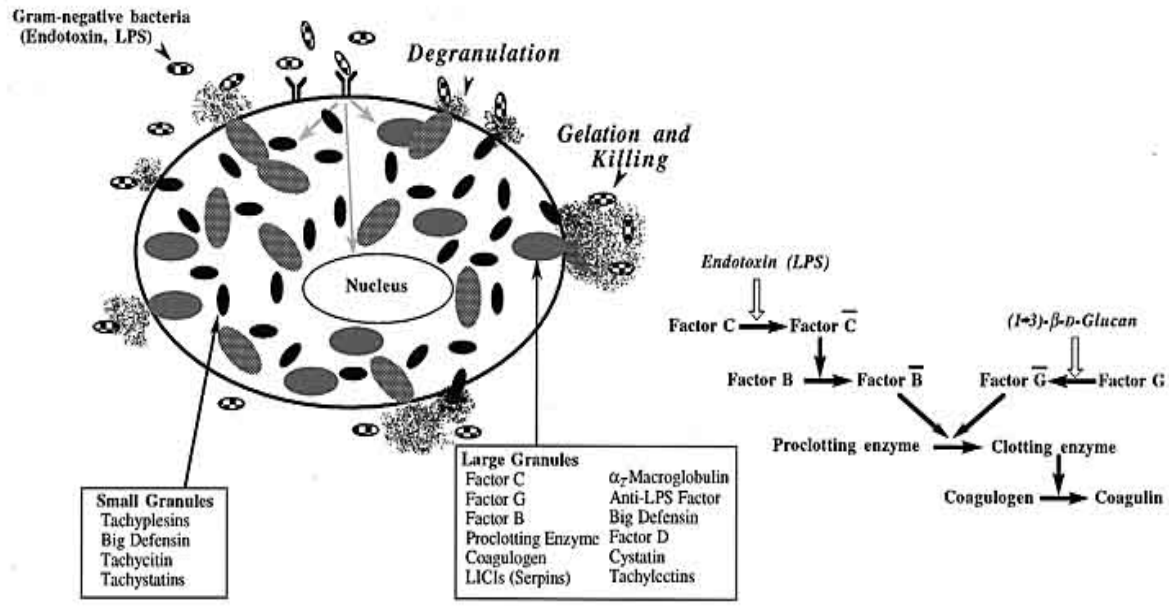

Figure 1.8: Defense systems in horseshoe crab hemocytes. The hemocytes detect LPS on Gram-negative bacteria and initiates exocytosis of the large and small granules. The clotting factors thus released are activated by LPS or (1, 3)-β-D-glucan on the pathogens, which result in hemolymph coagulation. Thus, the pathogens are cell-agglutinated by various lectins and subsequently killed by antibacterial substances. The large granules also contain protease inhibitors, such as serpins, α2-macroglobulin, and cystatin, and an azurocidin-like pseudoserine protease with antibacterial activity, named factor D. The figure was adapted from Iwanaga and Kawabata (1998).

Table 1.1: Defense molecules found in the horseshoe crab

Proteins and peptides	Mass (kDa)	Function/specificity	Localization
Coagulation factors			
Factor C	123	Serine protease	L-granule
Factor B	64	Serine protease	L-granule
Factor G	110	Serine protease	L-granule
Proclotting enzyme	54	Serine protease	L-granule
Coagulogen	20	Gelation	L-granule
Protease inhibitors			
LICI-1	48	Serpin/factor C	L-granule
LICI-2	42	Serpin/clotting enzyme	L-granule
LICI-3	53	Serpin/factor G	L-granule
Trypsin inhibitor	6.8	Kunitz-type	ND
LTI	16	New type	ND
LEBP-PI	12	New type	L-granule
Limulus cystatin	12.6	Cystatin family 2	L-granule
α_2-Macroglobulin	180	Complement	Plasma & L-granul
Chymotrypsin inhibitor	10	ND	Plasma
Antimicrobial substances			
Anti-LPS factor	12	GNB	L-granule
Tachyplesins	2.3	GNB, GPB, FN	S-granule
Polyphemusins	2.3	GNB, GPB, FN	S-granule
Big defensin	8.6	GNB, GPB, FN	L & S-granule
Tachycitin	8.3	GNB, GPB, FN	S-granule
Tachystatins	6.5	GNB, GPB, FN	S-granule
Factor D	42	GNB	L-granule
Lectins			
Tachylectin-1	27	LPS (KDO), LTA	L-granule
Tachylectin-2	27	GlcNAc, LTA	L-granule
Tachylectin-3	15	LPS (O-antigen)	L-granule
Tachylectin-4	470	LPS (O-antigen), LTA	ND
Tachylectin-5	380-440	*N*-acetyl group	Plasma
Limunectin	54	PC	L-granule
18K-LAF	18	Hemocyte aggregation	L-granule
Limulin	300	HLA/PC, PE, SA, KDO	Plasma
LCRP	300	PC, PE	Plasma
TCRP-1	300	PE	Plasma
TCRP-2	330	HLA/PE, SA	Plasma
TCRP-3	340	HLA/SA, KDO	Plasma
Polyphemin	ND	LTA, GlcNAc	Plasma
TTA	ND	SA, GlcNAc, GalNAc	Plasma
Liphemin	400-500	SA	Hemolymph
Carcinoscorpin	420	SA, KDO	Hemolymph
GBP	40	Gal	Hemolymph
PAP	40	Protein A	Hemolymph
$(1 \rightarrow 3)\beta$-D-glucan binding protein	168	Pachyman, cardlan	Hemocyte
Others			
Transglutaminase (TGase)	86	Cross-linking	Cytosol
8.6 kDa protein	8.6	TGase substrate	L-granule
Pro-rich proteins (Proxins)	80	TGase substrate	L-granule
Limulus kexin	70	Precursor processing	ND
Hemocyanin	3600	O_2 transporter (PO activity)	Plasma
Toll-like receptor (tToll)	110	ND	Hemocyte
L1	11	Unknown	L-granule
L4	11	Unknown	L-granule

LICI, *Limulus* intracellular coagulation inhibitor; LTI, *Limulus* trypsin inhibitor; LEBP-PI, *Limulus* endotoxin-binding protein-protease inhibitor; FN, fungus; LAF, *Limulus* 18-kDa agglutination-aggregation factor; KDO, 2-keto-3-deoxyoctonic acid; PC, phosphorylcholine; PE, phosphorylethanolamine; SA, sialic acid; TTA, *Tachypleus tridentatus* agglutinin; LCRP, *Limulus* C-reactive protein; HLA, hemolytic activity; LTA, lipoteichoic acid; GBP, galactose-binding protein; PAP, protein A binding protein; PO, phenoloxidase; ND, not determined. Adapted from Iwanaga and Lee (2005).

1.4.4 Homology between the two serine protease cascades in horseshoe crab and *Drosophila*

Serine protease cascades are indispensable in various fundamental biological processes in both the invertebrates and vertebrates. They play major roles in signal transduction in development, immunity, and hemostasis.

In *Drosophila*, a well-established serine protease cascade is thought to be upstream of the Toll/NF-κB signaling pathway. This serine protease cascade includes four different members of the serine protease family (Figure 1.9), Nudel, Gastrulation defective (Gd), Snake and Easter (Smith and DeLotto, 1992). The proteolytically processed product of this cascade---Spätzle, in its active form, is thought to be recognized by the Toll receptor (Figure 1.9). Toll receptor triggers signal transduction through Tube and Pelle, and ultimately leads to the nuclear translocation of the Dorsal transcription factor and promotes ventral and lateral development of the embryo (Belvin and Anderson, 1996).

In the horseshoe crab, two serine protease pathways that involve either an LPS-mediated or a (1-3)-β-D-glucan-mediated coagulation reaction have been well-established. Three serine protease zymogens: Factor C, Factor B and proclotting enzyme are involved in the coagulation cascade triggered by LPS (Ding *et al*, 1993). In this cascade, Factor C responds to LPS, and is autocatalytically activated to its active form; this in turn transforms Factor B to its active form (Figure 1.9). The activated Factor B converts the proclotting enzyme to clotting enzyme, which converts coagulogen to an insoluble coagulin gel (Ding *et al*, 2004).

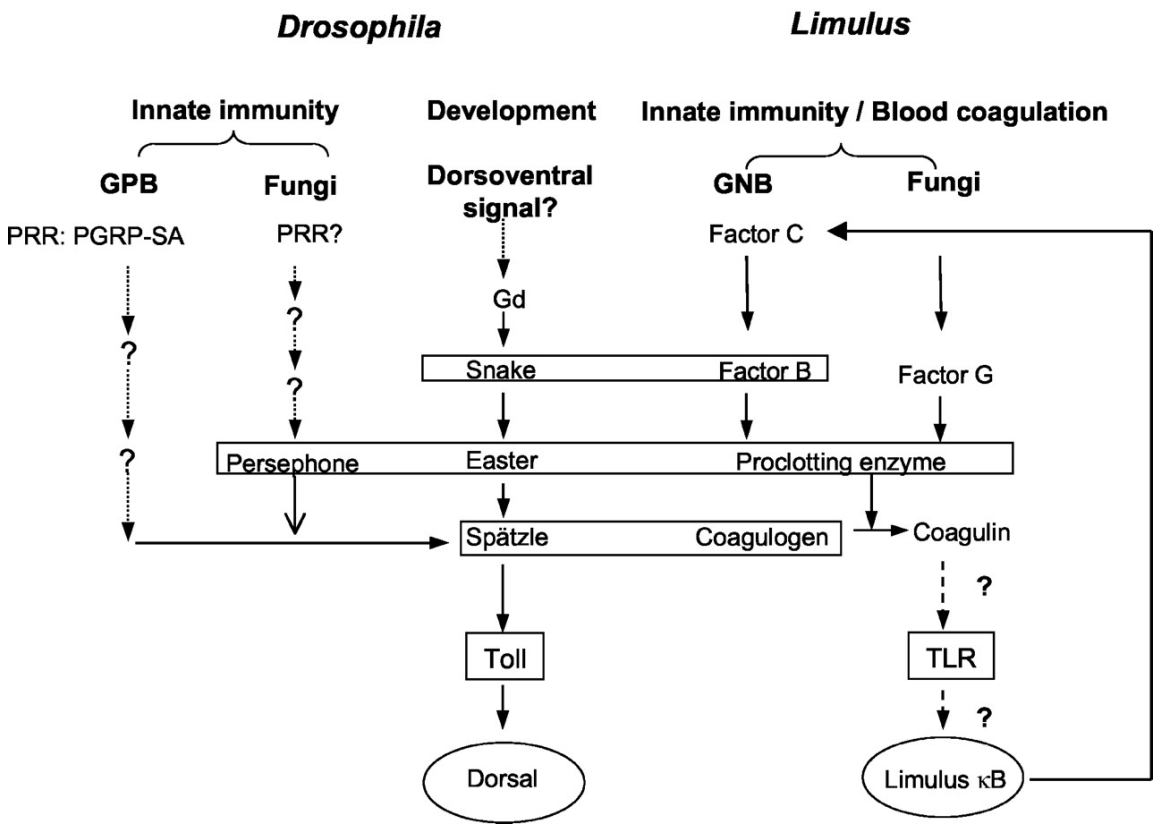

Figure 1.9: Serine protease cascades in the *Drosophila* and horseshoe crab (*Limulus*). On the *left* are the serine protease cascades in dorsoventral determination, immune response against Gram-positive bacteria and fungal infection in *Drosophila. Dotted arrows* with "?" indicate unidentified components in the cascades. On the *right* are the serine protease cascades in *limulus* blood coagulation and innate immunity, which are activated by Gram-negative bacteria and fungi, respectively. Factor G is the upstream serine protease in the alternate blood coagulation pathway that is triggered by β-1, 3-glucan. *Discontinuous arrows* annotate the putative signaling pathway. Homologues in all the cascades are *boxed. Gd*, gastrulation defective. Adapted from Wang *et al*. (2003).

A striking similarity between the horseshoe crab blood clotting serine protease cascade and the *Drosophila* dorsoventral-determination serine protease cascade has long been noticed (Gay and Keith, 1992). The horseshoe crab clotting enzyme and the

Drosophila serine protease, Snake and Easter, show significant sequence homology. Therefore, they have been considered as members of a distinct subfamily of serine proteases (Ding *et al*, 2004; Smith and DeLotto, 1992). Horseshoe crab Factor B also exhibits a similar primary structure and the disulfide linkage to the clotting enzyme and Easter. Furthermore, persephone, a serine protease involved in signal transduction of anti-fungal immune responses, is deduced to contain structural domains homologous to those in Easter, Snake in *Drosophila* and proclotting enzymes in horseshoe crab (Ding *et al*, 2005). Spätzle, the ligand for Toll, also shares homology with the horseshoe crab coagulogen (Osaki and Kawabata, 2004). The proposed similarity amongst these serine proteases in each cascade (Factor B, Proclotting enzyme and Coagulogen versus Snake, Easter and Spätzle) strongly suggests a common ancestry of the two serine protease pathways in the *Drosophila* and horseshoe crab (Figure 1.9).

Interestingly, a Toll-like receptor has recently been reported in the Japanese horseshoe crabs (Inamori *et al*, 2004) and a *C. rotundicauda* TLR cDNA clone has also been isolated from a hepatopancreas cDNA library in our laboratory (Loh *et al*). Although the ligand of the horseshoe crab TLRs remains to be determined, the structural homology between coagulogen and Spätzle has raised speculations that the processed coagulogen might be the candidate ligand for horseshoe crab TLR (Figure 1.9) (Osaki and Kawabata, 2004; Wang *et al*, 2003). Therefore, it is reasonable to postulate that the horseshoe crab blood coagulation cascade probably transduces an extracellular signal into the hemocytes during the innate immune response initiated by LPS. The bacterial infection signaled by the serine protease cascades ultimately results in the activation of the NF-κB transcription factors as illustrated in Figure 1.9 (Ding *et al*, 2004; Wang *et al*,

2003). Similar to its counterparts in *Drosophil*a, the putative horseshoe crab NF-κB transcription factors also transactivate other antimicrobial effector genes to defend against microbial infection.

1.5 Objectives and experimental approaches

1.5.1 Objectives of this project

The main objective of this research was twofold: (1) to trace the ancient origin of the NF-κB signaling pathway in the horseshoe crab and investigate the function of the ancient NF-κB/IκB signaling cascade in innate immunity; (2) to define the biochemical characteristics of the novel 16 kDa TRX and examine its roles in regulating the NF-κB signaling pathway.

1.5.2 Experimental strategies

First, degenerate PCR, using primers that were designed based on the sequence analysis of RHDs and ankyrin repeats was used to isolate the horseshoe crab (*C. rotundicauda*) NF-κB and IκB homologues. Then, the following main experiments were carried out to study the functions of NF-κB signaling pathway in the immune defense of horseshoe crab. (1) Electrophoretic mobility shift assay (EMSA) was used to examine the DNA-binding activity of recombinant horseshoe crab NF-κB. (2) The interaction between the horseshoe crab NF-κB and IκB proteins was examined by *in vitro* pull-down and immunoprecipitation assays. (3) Transient co-transfection studies in *Drosophila* S2 cells with the κB-reporter were utilized to investigate if the horseshoe crab NF-κB can

regulate gene transcription. Then the inhibitory effects of horseshoe crab IκB on NF-κB transactivation activity were determined by co-transfection. (4) The subcellular localization of horseshoe crab NF-κB and IκB in transfected cells and horseshoe crab hemocytes was investigated by method of immunocytochemistry. (5) The functions of the horseshoe crab NF-κB signaling pathway on the expression of immune-related gene were examined by RT-PCR, with or without NF-κB specific inhibitors.

To investigate the functions of horseshoe crab TRX, first the recombinant protein was expressed. After that, a series of mass spectrometric methods was used to determine the active motif of the horseshoe crab TRX. To understand the biochemical characteristics of the 16 kDa Cr-TRX1, an array of enzymatic assays were carried out, such as insulin reduction assay, thioredoxin reductase assay and DNA-nicking assay. The relationship between Cr-TRX1 and NF-κB signaling pathway was then examined in a mammalian cell line, HeLa, by overexpression using the gel shift assay and κB-reporter assay. Finally, using bioinformatics methods, we identified the human homologue of Cr-TRX1 and examined its NF-κB regulatory ability by EMSA.

CHAPTER 2: MATERIALS AND METHODS

2.1 Organisms and Materials

2.1.1 Organisms

The horseshoe crab, *C. rotundicauda*, was collected from mangrove swamps at the northeastern part of Singapore and cleaned off mud and barnacles. The specimens were acclimated overnight in 30% (v/v) sea water/fresh water before being used for experiments.

Drosophila Schneider S2 cells were maintained at 25 °C in *Drosophila* SFM^{TM}, Serum-Free Medium, (Invitrogen, Carlsbad, CA) supplemented with 20 mM L-Glutamine and 5% fetal bovine serum (FBS). HeLa cells are routinely grown in complete medium consisting of Dulbecco's modified Eagle's medium, DMEM (Invitrogen) supplemented with 10 % FBS and 1 % penicillin/streptomycin at 37 ºC in a humidified atmosphere of 5 % CO_2 and 95 % air. Bacteria strains used for infection experiments was *Pseudomonas aeruginosa* ATCC 27853. *Escherichia coli* BL21 (DE3) was used for recombinant protein expression.

2.1.2 Biochemicals, enzymes and antibodies

Glutathione Sepharose 4B, protein A Sepharose, redivue [γ-p^{32}] ATP, thrombin and hybond-N^{+} nylon membrane were products of GH Healthcare. Advantage 2 DNA polymerase and X-α-gal was from BD Biosciences, Clontech. Complete cocktail

protease inhibitors were from Roche. SuperSignal® West Pico Chemiluminescent Substrate was from Pierce. Phenylmethylsufonylfluoride (PMSF), bovine serum albumin (BSA) fraction V, the recombinant TRX (thioredoxin), rat liver TRXR (TRX reductase) and NADPH were from Sigma. Super RX X-ray film was from Fuji. Common chemicals of molecular biology grade were from Sigma and Merck. The NF-κB inhibitors MG-132 and helenalin were from Calbiochem. All restriction enzymes were from New England Biolabs, Roche or Fermentas.

Mouse monoclonal anti-V5, anti-c-Myc, anti-c-Myc-HRP and anti-pEGFP antibody were from Invitrogen. Mouse monoclonal antibody to FLAG (M2) and rabbit antibody to actin were obtained from Sigma. Polyclonal antibodies to NF-κB p50 and IκB were from eBiosciences. Anti-CrNFκB and anti-CrIκB antibodies were raised in rabbits against Keyhole Limpet Hemocyanin (KLH)-conjugated peptides (CrNFκB: LPVNRDPEGLSRKR; CrIκB: VSSHSHHSPQKEYK), by BioGenes (Germany). The antibodies were affinity-purified using specific peptide as ligand. All antibodies were tested for specificity by Western blot using recombinant CrNFκB and CrIκB as controls.

2.2 cDNA cloning of targeted molecules

In order to clone the NF-κB gene from the horseshoe crab, we first prepared the mRNA from naïve and Gram-negative bacteria challenged horseshoe crab tissues. Those mRNA were then used for RT-PCR to clone the targeted molecules and gene expression analysis.

2.2.1 Infection of horseshoe crab and RNA extraction

2.2.1.1 Preparation of *P. aeruginosa* for infection

A single clone of *P. aeruginosa* was inoculated into 5 ml of Tryptone soy broth (Oxoid) and cultured overnight at 37 °C with shaking at 230 rpm. Bacteria was collected by centrifugation at 5,000 × *g* for 10 min at 4 °C, washed with 10 ml of saline (0.9 % NaCl) and resuspended to the original culture volume in saline. An aliquot of 100 µl of this *Pseudomonas* suspension was serially diluted for bacterial enumeration and the rest was stored at 4 ^{o}C as stock culture for infection of the horseshoe crabs.

2.2.1.2 Challenging horseshoe crabs with bacteria and collection of tissues

Prior to infection, the dorsal hinge of the horseshoe crab leading to the cardiac chamber was swabbed with 70 % ethanol. A sub-lethal dose of 1.2×10^7 colony-forming unit (CFU) of *P. aeruginosa*/ kg body weight was injected intracardially to challenge the horseshoe crab (Ng *et al*, 2004). Sample collection was performed at indicated hours post infection (hpi). Uninfected (naïve) or infected horseshoe crabs were bled for the collection of the hemocytes. The animals were bled by cardiac puncture using an 18 G needle (Becton-Dickinson). The hemolymph was collected in pre-chilled pyrogen free tubes (Falcon). The hemolymph was diluted with the same volume of 3 % pyrogen-free NaCl. The mixture was immediately pelleted by centrifugation at 150 × g for 5 min at 4 ^{o}C. The supernatant was discarded and the hemocytes were snap-frozen in liquid nitrogen before storage at -80 ^{o}C. Hepatopancreas was excised under RNase-free condition and immediately frozen in liquid nitrogen and stored at - 80 ^{o}C until use.

2.2.1.3 RNA purification

RNA is extremely sensitive to RNase contamination. In order to maintain the RNase free condition, water and solutions were treated overnight with 0.1 % of diethylpyrocarbonate (DEPC, Sigma) at 37 °C and autoclaved for 2 h to remove residual DEPC. Plastic-wares were soaked overnight in 3 % hydrogen peroxide, rinsed thoroughly with DEPC treated water and autoclaved for 2 h. Metal and glass apparatus were baked at 200 ^{o}C for 4 h.

Tissues were homogenized in Trizol reagent (Invitrogen) on ice with an Ultra-Turrax T25 homogenizer (IKA-labotechnik). The total RNA was extracted according to the manufacturer's instructions with slight modifications. Briefly, homogenized samples were left at room temperature for 5 min. Chloroform (1/5 volume of the homogenate) was then added and the mixture was shaken vigorously for 15 s, and incubated at room temperature for 2 min. Next, the mixture was centrifuged 1,000 × g for 15 min at 4 ^{o}C and the top colorless aqueous phase, which contained RNA, was transferred to a fresh tube. RNA was precipitated by incubation with isopropanol for 10 min and the RNA precipitate was collected by centrifugation. The RNA pellet was washed twice with 75 % ethanol and the air-dried RNA pellet was stored at – 70 ^{o}C.

The RNA pellet was dissolved in DEPC treated water by incubation at 60 ^{o}C for 10 min. The concentration of the isolated RNA was determined by OD reading at 260 nm. The ratio of OD_{260nm} and OD_{280nm} of ≥ 1.8 was the acceptable purity of RNA for subsequent experiments.

2.2.2 Cloning of CrNFκB, CrIκB and CrRelish

To obtain a cDNA fragment of targets, cDNA was first synthesized with SuperScript^{TM} RT-PCR System (Invitrogen) using oligo-dT primers according to the manufacturer' instructions. Briefly, a mixture of 1 μl of 0.5 μg/μl oligo-(dT), 1 μl of 10 mM dNTP and 3 μg of total RNA was made to a final volume of 10 μl with DEPC-treated water. The RNA was incubated at 65 °C for 5 min and then placed on ice. A reaction mixture containing 2 μl of 10 × RT buffer, 2 μl of 0.1 M dithiothreitol (DTT) stock, 4 μl of 25 mM $MgCl_2$, 1 μl of RNaseOUT and 1 μl of Reverse Transcriptase enzyme was prepared in a final volume of 10 μl and added to the denatured RNA sample. The 20 μl sample was then incubated for 50 min at 42 °C for cDNA synthesis. The reaction was terminated at 70 °C for 15 min and 1 μl of RNase H was added and incubated for 20 min at 37 °C to remove the RNA. The synthesized cDNA was then frozen at -20 °C for later use.

Homologues of NF-κB (CrNFκB) and IκB (CrIκB) from *C. rotundicauda* were obtained by RT-PCR using degenerate primers designed from the conserved region of insect and mammalian NF-κB and IκB proteins. The primers used were: CrNFκB forward primer, 5′-TTTCGCTAYRARTGCGARGG-3′; CrNFκB reverse primer, 5′-TCCTTIGTWACRCAWGAIACMAC-3′; CrIκB forward primer, 5′-GAYGGIGACWCRIYIITSCACYTRGC-3′; CrIκB reverse primer, 5′-CAGGMMAIRTGIARIGSIGTRTIDCC-3′. The PCR products were electrophoresed on 1-1.2 % agarose gels. The correctly sized bands were excised and isolated from the gel

using QIAquick gel extraction kit (Qiagen) and cloned into pGEM-T Easy vector (Promega) for sequencing.

2.2.3 Cloning of PCR products and sequencing

For ligation into pGEMT-Easy vector (Promega), purified cDNA was incubated overnight at 4 °C with pGEM®-T Easy vector and T4 DNA ligase in the Rapid Ligation Buffer. The next day, the ligation product was transformed into competent cells, *E. coli* Top 10. For transformation, 5 µl of the ligated product was added to 80 µl of competent bacteria, and the mixture was incubated in ice for 30 min. This was followed by a 90 s 'heat shock' treatment at 42°C and rapid cooling in ice for 2 min. The cells were then incubated in 900 µl of LB broth for 1 h at 37°C with shaking at 150 rpm. The transformed bacteria cells was resuspended with fresh LB and plated on selective LB-ampicillin plates. The plates were incubated overnight at 37°C.

Transformed bacteria were isolated and cultured for purification of recombinant DNA for sequence verification. The Wizard® *Plus* SV Minipreps DNA Purification System (Promega) was used to purify plasmid DNA for sequencing. The sequencing reaction was performed in a 20 µl volume, using 2 µl of BigDye Terminator V3.1 (Applied Biosystems), 100-250 ng of DNA template, 3 µl of 5 × buffer and 100 nM primer. The sequencing reaction was then subjected to 1 min of incubation at 95 °C, followed by 40 cycles of 95 °C for 10 s, 50 °C for 10 s and 60 °C for 4 min. At the end of the reaction, the extension products were precipitated with 70 % ethanol with sodium acetate (pH 4.6) to remove excess dye terminators. The DNA was pelleted by centrifugation at 14,000 × g for 30 min. The pellet was rinsed twice with 70 % ethanol

and air-dried. The precipitated DNA was redissolved in HiDye formamide (Applied Biosystems) before loading in the capillary sequencer for sequencing (ABI 3100, Applied Biosystems).

2.2.4 Isolation of full length cDNA by RACE PCR

The 3′ and 5′ ends of CrNFκB, CrIκB and CrRelish were obtained using BD SMART™ RACE cDNA amplification kit (Clontech). The first strand cDNA for 5′ and 3′-RACE PCR were generated with 3.0 μg of total RNA from naïve hemocytes according to the instructions in the manual. The reaction mixture was then diluted in 50 μl of water and stored at – 20 ^{o}C until use.

RACE PCR was performed with the gene-specific primers and the universal primer mix (UPM), which was the mixture of the long (5'-CTAATACGACTCACTATAGGGCAAGCAGTGGTATCAACGCAGAGT-3') and the short (5'-CTAATACGACTCACTATAGGGC-3') oligonucleotides. Typically, the RACE PCR reactions were set up with 2.5 μl of first strand cDNA, 1 μl of 10 mM gene specific primer, 5 μl of 10 × UPM (0.4 mM of long and 2.0 mM of short oligonucleotide), 0.2 mM dNTP mix, and 1 μl of 50 × BD Advantage 2 Polymerase Mix in 1 × Advantage 2 PCR Buffer. Standard PCR program was performed with one cycle at 95 °C for 3 min, followed by 28 - 35 cycles of denaturing at 95 °C for 30 s, annealing at 68 °C for 30 s, extension at 72 °C for 3 min, and termination with one cycle at 72 °C for 8 min. In some cases, touchdown PCR that is performed by cycles of decreasing annealing temperature and nested PCR were used for the amplification of the 3′ or 5′ end. After agarose gel analysis, the correctly sized bands were excised and isolated from the gel using QIAquick

gel extraction kit (Qiagen). The purified band was cloned into pGEMT-Easy vectors and then sequenced using primers that bind to the vectors at the regions flanking the insert.

2.2.5 Phylogenetic analysis of target molecules

To investigate the evolutionary relationship of CrNFκB, CrIκB, CrRelish, Cr-TRX-1 and their homologues, multiple sequence alignments were performed to compare the degree of sequence homology between them. The amino acid sequences of their homologues were obtained from the NCBI database. Sequence alignment was performed using Clustal X (version 1.83) or DNAMAN with the default parameters. Based on the alignments, unrooted phylogenetic trees were constructed using neighbor-joining method. Bootstrap tests at 1000 replicates were carried out to examine the validity of the branching topologies.

2.2.6 Transcriptional analysis during *Pseudomonas* infection

First strand cDNAs of various tissues were synthesized using SuperScript™ First-Strand Synthesis System (Invitrogen). For each sample, 20 μl reaction mixture was set up with 3 μg of total RNA, 0.5 mM dNTP mix, 500 ng of oligo-$(dT)_{12-18}$ primers, 5 mM of $MgCl_2$, 10 mM DTT, 40 Units of RNaseOUT™ recombinant RNase inhibitor and 50 units of SuperScript™ II reverse transcriptase in 1 × RT buffer. Reverse transcription reaction was carried out for 50 min at 42 ^{o}C and terminated by incubation at 70 ^{o}C for 15 min. Next, RNA was removed by incubation of the reaction mixture with 2 Units of RNase H at 37 ^{o}C for 20 min. First strand cDNA was stored at - 20 ^{o}C until use. Changes in the transcription level of CrNFκB, CrIκB and Cr-TRX1 were studied by

semi-quantitative RT-PCR. Horseshoe crab Actin-11 was used as an internal normalization standard to eliminate sample-to-sample variations in the initial cDNA concentrations. PCR was performed under the following conditions: initial denaturation at 95 ^{o}C for 3 min, followed by 25 - 35 cycles of denaturation at 95 ^{o}C for 30 s, annealing at 56 ^{o}C for 30 s, and extension at 72 ^{o}C for 1 min. PCR products were resolved on 1.2 % agarose gel, stained with ethidium bromide and the gel image was acquired and analyzed by Image Master VDS version 2.0 software (Pharmacia Biotech).

2.3 Functional characterization of CrNFκB and CrIκB

2.3.1 Construction of expression vectors

For bacterial recombinant protein expression, a cDNA fragment encoding the N-terminal half of the CrNFκB including RHD (amino acids: 1-353), was subcloned into the *Nde*I and *BamH*I sites of the pET15b expression vector (Novagen). The full length CrIκB was subcloned into the *BamH*I and *Xho*I sites of expression vector pGEX-4T-1 (GE Healthcare).

For insect expression plasmids, *Drosophila* expression vector, pAc5.1/V5-HisA (Invitrogen), was used for expression of full-length and truncated CrNFκB proteins (CrNFκB-RHD and CrNFκB-ΔNLS). All fusion proteins are tagged with His and V5. Except for CrNFκB-ΔNLS, the other 2 constructs contained the nuclear localization signal (NLS) (see Figure 2.1 & Figure 3.12). All the primers were designed according to the CrNFκB sequence with the additional digestion site sequences. Figure 2.1 illustrated the cloning strategies of full-length and truncated CrNFκB. The full-length CrIκB with a

c-Myc epitope was similarly cloned into the *Kpn*I and *Age*I sites of pAc5.1/V5-HisA. The primers used for cloning CrIκB with a c-Myc tag at the C-terminus are listed below. The underlined nucleotides encode the c-Myc tag. Forward primer: 5'-GGTACCATGGGAAAATCAAAAGAATT-3'; Reverse primer: 5' ACCGGTCAGATC TTCCTCTGAGATGAGCTTCTGCTCCACTGCTCTAACTTCATCTCC-3'.

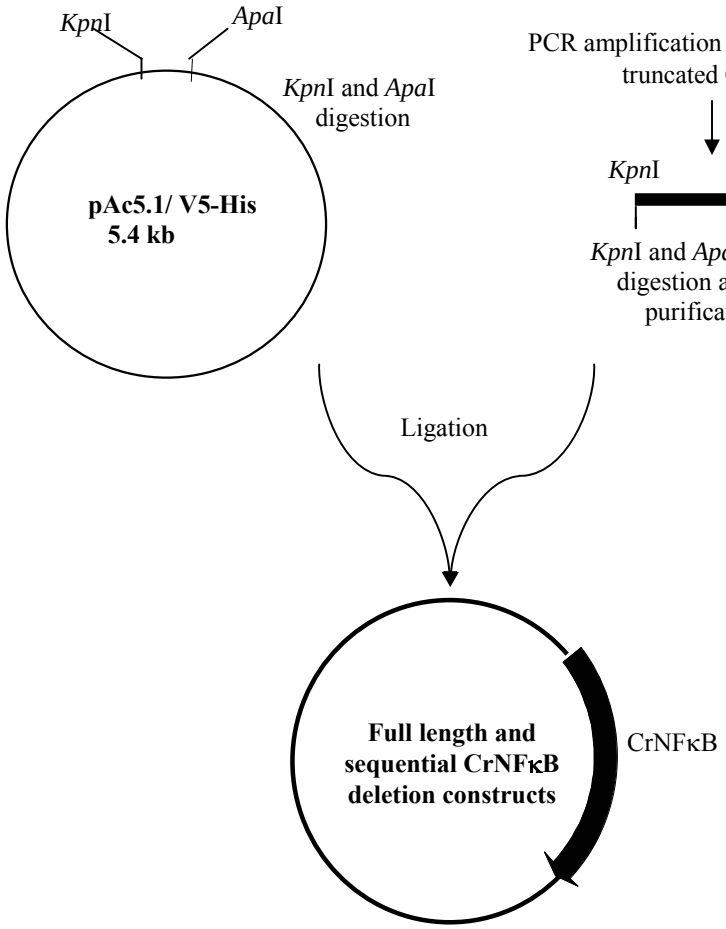

Figure 2.1: The cloning strategy of the full-length and truncated CrNFκB into the pAc5.1 expression vector. After PCR reaction, the fragment was doubled digested by *Kpn*I and *Apa*I and gel purified. The purified fragment was subsequently cloned into the *Kpn*I and *Apa*I sites of the pAc5.1 expression vector. The full length CrIκB with the c-Myc tag was similarly cloned into the pAc5.1 vector.

2.3.2 SDS-PAGE & Western Blot

SDS-PAGE was carried out in vertical gel composed of 10 % - 15 % running gel and 5 % stacking gel using the Mini-Protean II system (Biorad). Prior to electrophoresis, samples were reduced with SDS-PAGE gel loading buffer (125 mM Tris-HCl, pH 6.8, 10 % glycerol, 2 % β-mercaptoethanol, 0.1 % bromophenol blue and 2 % SDS) and boiled for 5 min to denature the proteins. Electrophoresis was performed in Tris-glycine buffer (25 mM Tris, pH 8.3, 250 mM glycine, and 0.1 % SDS). Precision Plus Protein Standards (prestained protein ladder, GibcoBRL, USA) was electrophoresed alongside the sample for molecular weight determination.

In Western blot, the electrophoretic transfer was performed in the Mini Trans-Blot Electrophoretic Transfer Cell (Biorad). The transfer of proteins was carried out at a constant current of 220 mA for 2 h at 4 °C. After transfer, the membrane was incubated for 2 h at room temperature with 20 ml of blocking buffer containing 5 % (w/v) skim milk in PBST (PBS containing 0.1 % of Tween-20, v/v). After incubation, the membrane was rinsed 3 times with 20 ml of PBST. The blot was then incubated overnight at 4 ºC with primary antibody at indicated dilution in PBST containing 3 % BSA. Subsequently, the membrane was washed four times with 20 ml of PBST to remove unbound antibody. Secondary antibody in PBST containing 3 % BSA was then added to the membrane and incubated for 2 h with gentle shaking. The antigen-antibody complexes were then immunoblotted by incubating the blot with Supersignal® West Pico (Pierce) chemiluminescent substrate. The film was subsequently developed in an automated developer.

2.3.3 Pull-down assay for protein-protein interaction analysis

The GST-CrIκB recombinant protein was expressed in *E. coli* strain BL21. After 4-6 h induction with 0.1 mM IPTG at 30 °C, the bacterial culture was pelleted at 6,000 × g for 5 min and resuspended in PBS. The cell lysate was prepared by sonicating on ice at 28 amplitude microns, for 6 × 10 s each with intervals of 30 s chilling in ice and centrifuged at 12,000 × g. The bacterial lysate containing the recombinant GST-CrIκB was immobilized onto Glutathione-Sepharose 4B beads (GE Healthcare). The preparation of His-tagged CrNFκB will be described under Section 2.3.5.1. For protein-protein interaction assays, one μg of GST-CrIκB fusion protein was bound to 25 μl of Glutathione Sepharose 4B beads in phosphate-buffered saline (PBS). The beads were washed 5 times with 0.5 ml of ice-cold PBS after incubating with bacterial lysate expressing recombinant CrNFκB-RHD. Bound proteins were eluted with 30 μl of SDS-PAGE sample buffer, resolved by SDS-PAGE, and detected with anti-GST and anti-His antibodies.

2.3.4 Immunoprecipitation assay

For immunoprecipitation assays, *Drosophila* S2 cells were transfected with several combinations of 500 ng CrNFκB-V5 and 500 ng IκB-c-Myc using CellFectin kit (Invitrogen). After 48 h of transfection, the cells were disrupted by lysis buffer (50 mM Tris, pH 8.0, 150 mM NaCl, 0.2 % Nonidet P40, protease inhibitor cocktail (Roche) and 10 μM MG-132. The cell lysate was centrifuged at 12,000 × g for 10 min at 4 ºC to remove particulate matter. The supernatant was transferred to a fresh tube and pretreated

with Protein A Sepharose (GE Healthcare) at 4 ^{o}C for 1 h. After centrifugation at 12,000 × g for 20 s, the supernatant was precipitated with 2 μg of anti-V5 antibody and 2 μg rabbit anti-mouse bridge antibody at 4 ^{o}C overnight. Then the immunocomplex was precipitated by adding the Protein A Sepharose beads and incubated at 4 ^{o}C for 1 h. The immunoprecipitates were then washed three times with lysis buffer and analyzed by Western blot.

2.3.5 Electrophoretic gel mobility-shift assay (EMSA)

The electrophoretic mobility shift assay (EMSA) was used to study DNA-protein interactions. This technique is based on the fact that DNA-protein complexes migrate slower than non-bound DNA in a native polyacrylamide gel, resulting in a "shift" in migration of the DNA.

2.3.5.1 Preparation of recombinant CrNFκB from bacteria and whole hemocyte lysate for EMSA

To obtain the His-tagged CrNFκB recombinant protein extract, the recombinant plasmid was transformed into *E. coli* BL21 and cultured at room temperature with shaking at 230 rpm until the OD_{600} reaches 0.8. The culture was then induced with 0.02 mM IPTG and for another 8 h. The bacteria was harvested by centrifugation at 5,000 × g for 5 min, washed with PBS and then pelleted again. The cells were resuspended in binding buffer (50 mM NaCl, 2 mM $MgCl_2$, 2 mM DTT, 1 mM EDTA, 10 % glycerol and 10 mM HEPES, pH 7.8) and sonicated for 6 times on ice at 28 amplitudes for 10 s each time. After centrifugation at 9,000 × g for 1 h at 4 °C, the supernatant was collected

into a fresh tube. The freshly prepared supernatant of the lysate was immediately used in EMSA.

Horseshoe crab hemocytes were collected according to Section 2.2.1.2. Hemocytes were washed with PBS and homogenized in binding buffer (50 mM NaCl, 2 mM $MgCl_2$, 2 mM DTT, 1 mM EDTA, 10 % glycerol and 10 mM HEPES, pH 7.8). Whole hemocyte extracts were centrifuged at 4 °C for 10 min at 13,000 × *g*, and the resulting supernatants were used for subsequent EMSA.

2.3.5.2 Extraction of nuclear proteins from hemocytes

Nuclear extracts were prepared according to the procedures described previously (Lin *et al*, 2004; Wang *et al*, 2003) with modifications. Briefly, the horseshoe crab hemocytes were collected by centrifugation for 10 min at 150 × g. Cell pellets were resuspended in ice cold PBS to remove the plasma and collected again by centrifugation. All the remaining steps were carried out at 4 ^{o}C. Washed cells were resuspended in two packed cell volumes of lysis buffer (10 mM HEPES pH 7.9, 1.5 mM $MgCl_2$, 10 mM KCl, 0.5 mM DTT and 0.2 mM PMSF). After 10 min, cells were homogenized with 20 strokes of a loose fitting Dounce homogenizer (Wheaton, USA). Nuclei were collected by centrifugation for 10 min at 3,000 × g, and resuspended in 5 volumes of lysis buffer. Proteins were extracted from washed nuclei by high salt buffer (20 mM HEPES pH 7.9, 25 % (v/v) glycerol, 420 mM KCl. 0.2 mM EDTA, 0.5 mM PMSF, 0.5 mM DTT and 1.5 mM $MgCl_2$). After centrifugation, the extracts was dialysised against buffer (20 mM HEPES, pH 7.8, 25 mM NaCl, 25 mM KCl, 0.1 mM EDTA, 0.5 mM DTT, 0.5 mM PMSF, 20 % glycerol and 0.05 % Nonidet-P40). The supernants and nuclear extracts were quickly frozen and stored at – 70 ^{o}C for subsequent use by EMSA.

2.3.5.3 [γ–^{32}P] ATP labeling of the oligonucleotides

The sequences of the commercially synthesized oligonucleotides for EMSA are listed in Table 3.2 (page 85). Before labeling, the single-stranded oligonucleotides were annealed in the annealing buffer (10 mM Tris-HCl pH 7.9, 2 mM $MgCl_2$, 50 mM NaCl and 1 mM EDTA) with corresponding DNA strands at 85 ^{o}C for 15 min. After incubation, the reaction was cooled down slowly to 25 ^{o}C and incubated for another 30 min. Subsequently, the annealed double-stranded oligonucleotides were end-labeled with fresh [γ–^{32}P] ATP with T4 polynucleotide kinase (NEB). The ^{32}P labeled probes were subsequently purified using the Qiagen Nucletide Removal Kit (Qiagen). The radioactivity and labeling efficiency of the labelled probes were measured by dry Cerenkov count.

2.3.5.4 Electrophoretic gel mobility-shift assay (EMSA)

EMSA was performed using the recombinant CrNFκB protein, whole hemocyte lysate or nuclear extract of hemocytes. The reactions were set up in the presence of 1×10^5 cpm/pmol ^{32P}-labeled oligonucleotide and 2 μg of poly (dI-dC) at 25 °C for 30 min in binding buffer (50 mM NaCl, 2 mM $MgCl_2$, 2 mM DTT, 1 mM EDTA, 10 % glycerol and 10 mM HEPES, pH 7.8) before electrophoresis on a 4 % native PAGE gel (acrylamide:bisacrylamide ratio of 79:1). In competition assays, 10×, 100× cold probes (see Table 3.2) or indicated amounts of recombinant CrIκB were used in each reaction and incubated for 30 min before adding the ^{32}P-probe. For supershift assays, hemocyte extracts were incubated with the respective antibody for 30 min on ice before adding the

probe. After 2-3 h of electrophoresis at 120 V-130 V at 25 ^{o}C, the gel was fixed in 7 % acetic acid for 5 min. Next, the gel was transferred to a Whatman paper with a comparable size to the gel and covered with a saran wrap to be dried in the gel drier (Biorad, model 583) for 1.5-2 h. The dried gel was subsequently exposed to an X-ray film (Biomax, Kodak). After autoradiography, the film was developed in an automated X-ray developer (Kodak).

2.3.6 Cell culture and transfection

Because of the lack of direct cell lines derived from the horseshoe crab, and the relative evolutionary closeness of horseshoe crabs to insects, *Drosophila* S2 cell line was used in our transfection studies (Wang *et al*, 2003). The *Drosophila* Schneider S2 cells were maintained at 25 °C in *Drosophila* SFM^{TM} supplemented with 20 mM L-glutamine and 5 % FBS. Twelve hours prior to transfection, cells were seeded in a 6-well plate at 1.2×10^{6} cells/well. When the cells had attached to the well surface and had reached 60-80 % confluency, transfections were conducted with 2 μg of DNA using CellFectin (Invitrogen) according to the manufacturer's recommendation. After 6 h incubation of the cells with the transfection medium, the cells were renewed with 2 ml fresh medium. At 36 - 48 h post-transfection, the cell were harvested and lysed. In this study, the κB reporter was horseshoe crab Factor C promoter (p186) CAT reporter (CrFC-CAT) whose activity correlates with the activity of NF-κB (Wang *et al*, 2003). pACH110 containing the β-galactosidase gene fused with the *Drosophila* actin promoter, was used as internal control (Wang *et al*, 2003). Plasmids used for transfection were isolated using CsCl/ethidium bromide gradient ultracentrifugation described by Sambrook *et al* (1988).

2.3.7 CAT and β-Gal ELISA assay

CAT and β-Gal activities were measured in the cell extracts using the CAT and β-Gal ELISA kits (Roche). Following lysis of the transfected cells, 200 μl of the cell extracts, which contain the CAT enzyme and the β-Gal enzyme, were added to the wells of the microtiter plate modules (MTP modules), and incubated at 37 °C for 2 h. After rinsing with the wash buffer, a digoxigenin-labeled antibody to CAT (anti-CAT-DIG) or to β-Gal (anti-β-Gal-DIG) was added and incubated at 37 °C for 1 h. The excess antibody was removed by rinsing with the wash buffer. Next, an antibody to digoxigenin conjugated to peroxidase was added. This was incubated at 37°C for 1 h, followed by rinsing to remove excess antibody. Finally, the peroxidase substrate ABTS® was added. The peroxidase enzyme catalyzes the cleavage of the substrate yielding a colored product. The absorbance of the sample was determined at 405 nm using an ELISA reader (Molecular Divices, Spectra MAX 340) and is directly correlated to the level of CAT present in the cell extract.

2.3.8 Immunofluorescence

To determine the subcellular localization of CrNFκB and CrIκB, immunofluorescence experiments were performed. In these experiments, the S2 cells were transfected with plasmids expressing either CrNFκB-V5 or CrIκB-c-Myc fusion proteins. After 24 h, cells were transferred to an 8-well chamber slide (NUNC) and allowed to attach for 2 h. The cells were fixed for 15 min in 4 % paraformaldehyde and

permeabilized by 0.1 % Triton X−100/PBS for 2 min at room temperature. The permeabilization reagent was removed and the cover slip was rinsed thrice with PBS for 5 min each time. They were then incubated with mouse monoclonal antibody against V5 or c-Myc (1:500 dilutions, Invitrogen) overnight at room temperature. After washing with PBS, the cells were incubated with Alex594 rabbit anti-mouse IgG antibody (1:500 dilutions, Molecular Probes) for 2 h at room temperature. These cells were counterstained with DAPI (1 μg/ml) for 1 min and rinsed thrice with PBS prior to fluorescence microscopy analysis (Olympus, BX60).

To examine the subcellular localization of CrNFκB and CrIκB in horseshoe crab hemocytes, the hemocytes from naïve horseshoe crab or 30 min-challenged with *P. aeruginosa* (1.2×10^7 colony forming units/kg) were collected into 3 % saline at 42 °C. The diluted hemocytes were spread on pyrogen free cover slip for cell attachment. After 5 min, the cells were fixed in 2 % paraformaldehyde, blocked with 5 % goat pre-immune serum (Sigma) in PBS for 1 h and incubated for 2 h with anti-CrNFκB or anti-CrIκB antibody (1:500 dilutions). After washing with PBS, cells were incubated with Alex594 goat anti-rabbit IgG antibody (1:500 dilutions, Molecular Probes) which has been pre-absorbed to paraformaldehyde-fixed hemocytes in 5 % goat pre-immune serum for 1 h. The secondary antibody was then completely removed and the cover slip was rinsed thrice with PBS for 5 min each time. The cover slips were carefully blotted dry using Kimwipes, and a drop of Prolong® Gold antifade reagent with DAPI (Molecular Probes) was added onto the center of the cover slip. The cover slip was carefully placed onto a glass slide. Cells were then observed under the confocol microscope (Zeiss). The procedures for immunocytochemistry are summarized in Figure 2.2.

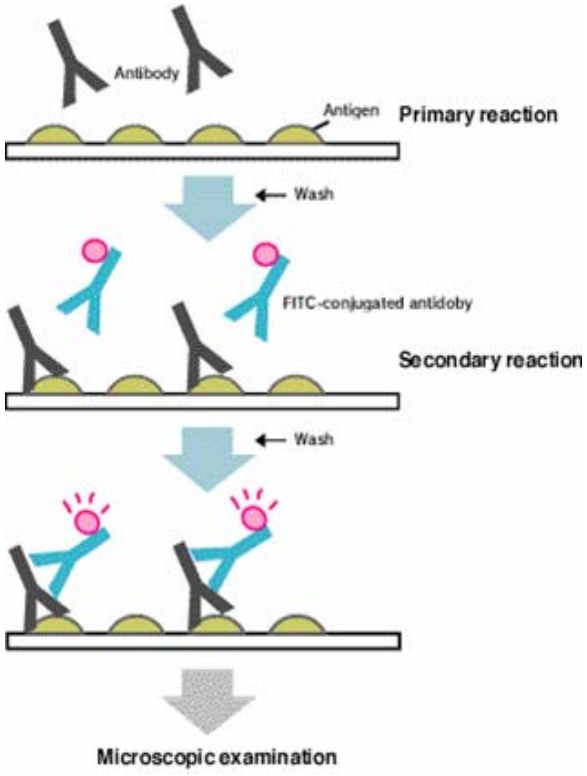

Figure 2.2: A schematic diagram of immunocytochemistry. Indirect cell stainining method is used. Cell was fixed onto a glass slide, permeabilized 0.1 % Triton X-100 and tagged with rabbit or mouse antibody against the target protein of interest. A secondary fluorophore-coupled antibody is directed against the rabbit or mouse antibodies, and cells were observed directly under fluorescence microscope for location of antigen. This figure is adapted from: http://www.mbl.co.jp/e/diagnostics/product/method.html#IIF.

2.3.9 Inhibitor treatments and reverse-transcription PCR

NF-κB inhibitors were obtained from Calbiochem. Helenalin and MG-132 were dissolved in dimethylsulfoxide (DMSO) at stock concentrations of 10 mM and 25 mM respectively. Five hundred microliters/kg (body weight) of DMSO or inhibitor drug solution were given intracardially. One hour later, the horseshoe crabs were injected with

P. aeruginosa at 1.2×10^7 colony forming units/kg of horseshoe crab body weight (Ng *et al*, 2004). The hemocytes were collected at indicated time points. Total RNA was prepared by the Trizol technique according to previous description. RT-PCR was performed by using the Invitrogen RT-PCR kit with 3 μg of total RNA and oligo dT. Semi-quantitative RT-PCR was performed with a rapid heating to 95 °C for 3 min followed by 19–25 cycles of 56 °C for 30 s, 72 °C for 1 min, and 95 °C for 30 s. PCR products were resolved on 1.2 % agarose gel, stained with ethidium bromide and the gel image was acquired and analyzed by Image Master VDS version 2.0 software (Pharmacia Biotech). The mRNA expression was normalized according to the expression level of horseshoe crab actin-11 gene. The primers used for RT-PCR experiments are listed as follows: Actin, primer 1 (5′-CGAGGGTACAGTTTCACCAC-3′) and primer 2 (5′-TCCTTTTGCATTCTATCAGC-3′); CrNFκB, primer 1 (5′-AAATGGTGCCAACAAATCCTAC-3′) and primer 2 (5′ACAACAACTACTGCTGAGCCTTT-3′); CrIκB, primer 1 (5′-CAACAGTGGACATGAGGGATCGCCAT-3′) and primer 2 (5′-GTCAACATCACTTTCTGGAGGTCTTC-3′); CrFC, primer 1 (5′-AATAGGTCAGTGGCCGTGG-3′) and primer 2 (5′-TGCTGGCTGCAACAACAG-3′); CriNOS, primer 1 (5′-CCATCAGTTAAAATCAACGCTGCAT-3′) and primer 2 (5′-CTTGAACATACTTCTTTGGGTTTAGG-3′); Transglutaminase, primer 1 (5′-TGGGCAGTTTAAAGACTCGG-3′) and primer 2 (5′-TCATGAGCTGGCACGAAGT-3′).

2.4 Functional characterization of Cr-TRX1

2.4.1 Construction of plasmids

In order to study the enzymatic function of horseshoe crab TRX homologue (henceforth referred to as *C. rotundicauda* TRX, Cr-TRX1), we expressed the full length Cr-TRX1 in bacteria. For bacterial expression, the full length Cr-TRX1 was cloned into the *Bam*HI-*Xho*I sites of the pGEX-4T-1 expression vector (GE Healthcare). Figure 2.3 illustrated the cloning strategies of the full-length Cr-TRX1. TRX6, the human homologue of Cr-TRX1, was similarly cloned into the pGEX-4T-1 plasmid for bacterial expression.

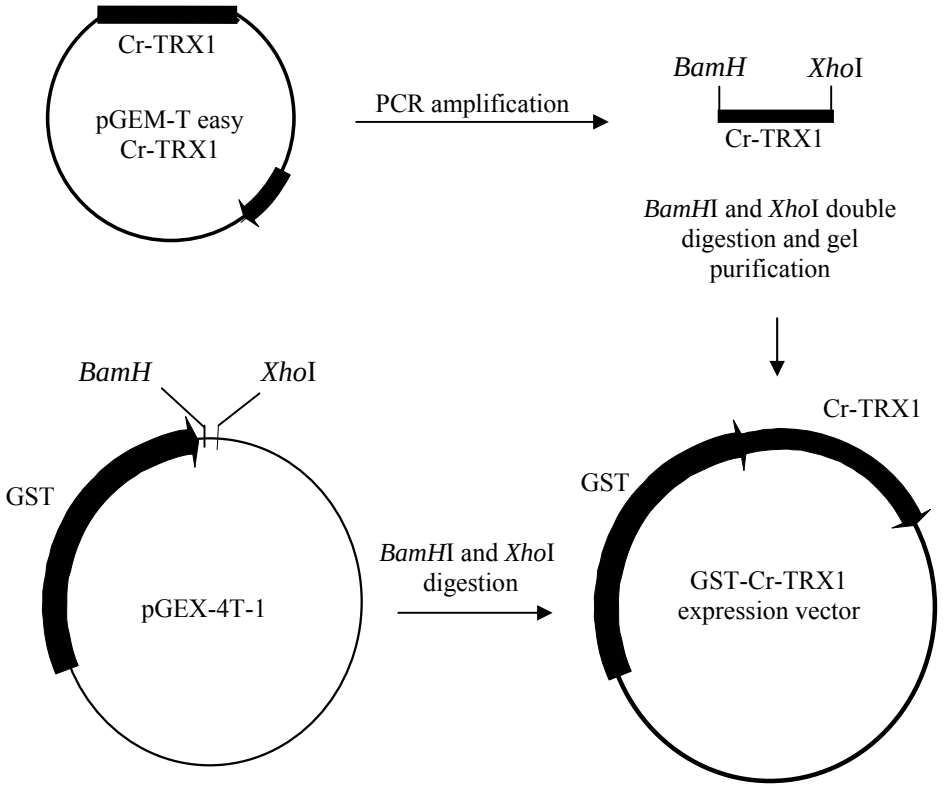

Figure 2.3: The cloning strategy of GST-Cr-TRX1 expression vector. The Cr-TRX1 fragment was PCR-amplified from the pGEM-T easy Cr-TRX1 construct. With the *BamH*I and *Xho*I sites introduced into the primers, the fragment was subcloned into the *BamH*I and *Xho*I sites in the pGEX-4T-1 construct as illustrated above.

For mammalian expression, full-length Cr-TRX1 was cloned into the expression vector pcDNA3.1 (Invitorgen) as follows. We used PCR to amplify the Cr-TRX1 with the following two primers: Primer1: 5'-GGTACCATGGAATTTATCCAAGG-3'; Primer 2: 5'-ACCGGTTTTGTCGTCATCGTCCTTATAGTCTCTTGCCCAGTTCTGG AA-3'. The primer 2 introduced a FLAG tag at the C-terminus of the Cr-TRX1. The amplified Cr-TRX1-FLAG sequence was inserted into pGEM-T vector (Promega). Then, the insert was released by digestion with *Kpn*I and *Age*I and ligated into pcDNA3.1 vector using T4 DNA ligase. For the mutant Cr-TRX1, both of the cysteine residues at the active site were replaced with alanine residues using QuikChange® XL Mutagenesis Kit (Stratagene).

2.4.2 Site-directed mutagenesis of Cr-TRX1

The two cysteine residues in the catalytic site (CXXC) are responsible for the oxido-reductase function of the thioredoxin superfamily. Hence, to investigate the importance of these two residues in catalyzing the redox function of Cr-TRX1, they were converted to alanine residues. Alanine was selected due to its small functional group and non-polarity; hence the effect on protein structure would be minimized without change in polarity of protein. The primers used for the mutagenesis are listed at below:

Cr-TRX1-DM-For: 5'-CAGTGCCCACTGGGCTCCCCCAGCTCGAGGGTTCACC-3'

Cr-TRX1-DM-Rev: 5'-GGTGAACCCTCGAGCTGGGGGAGCCCAGTGGGCACTG-3'. The underlined nucleotides are the ones that are responsible for the amino acid change.

Site-directed mutagenesis of both the cysteine residues at the active site of Cr-TRX1 was performed using QuikChange® XL Site-Directed Mutagenesis Kit (Stratagene) according to the kit manual. Briefly, 10 ng of pcDNA3.1-Cr-TRX1, 5 µl of 10 × reaction buffer, 125 ng each of the primers for mutation, dNTP mixture, QuikSolution and 2.5 U of *Pfu Turbo* DNA polymerase were sequentially added and mixed in a PCR tube. PCR was carried out with initial denaturation at 95 ºC for 1 min, denaturation at 95 ºC for 50 s, annealing at 60 °C for 50 s, and extension at 68 °C for 6 min for 18 cycles, and kept at 68 °C for 7 min. Following the temperature cycling, the product was treated with 10 U *Dpn* I endonuclease, which was used to digest the parental DNA template. The nicked vector DNA incorporating the desired mutations was then transformed into XL10-Gold® ultracompetent cells (Stratagene).

2.4.3 Expression and purification of Cr-TRX1

The pGEX-4T-1 Cr-TRX1 plasmids were transformed into *E. coli* BL21 (DE3) for bacterial expression. The induction and purification of the GST-Cr-TRX1 fusion protein was performed as previously described (Sadek *et al*, 2003). Briefly, after 4-6 h induction with 0.1 mM IPTG at 30°C, the bacterial culture was pelleted at 6,000 × g for 10 min and resuspended in 20 ml PBS. Overexpressing cells were disrupted by sonication on ice at 28 amplitude microns, for 6 × 10 s each with intervals of 30 s and centrifuged at 12,000 × g, and the supernatant was loaded onto a Gutathione-Sepharose 4B column (GE Healthcare). Binding to the matrix was allowed to occur overnight at 4 °C. Thrombin (5 Units/mg of fusion protein) was used to cleave off the Glutathione S-

transferase. The protein concentration was determined by Bradford method (Bradford, 1976) using bovine serum albumin, BSA, fraction V (Sigma) at calibration standard.

2.4.4 Mass spectrometric analysis

In addition to the two conserved Cys residues, the horseshoe crab TRX contains 1 extra Cys residues (Cys^{15}) at the N-terminus (Figure 3.27). Therefore, it was important to identify which Cys residue is redox sensitive in Cr-TRX1. To achieve this, we determined the number and the position of the active Cys residues in horseshoe crab TRX molecule using mass spectrum.

First, the number of active Cys residues in Cr-TRX1 molecule was determined using MALDI-TOF. In this experiment, the reduced Cr-TRX1 was prepared by incubation with 1 mM dithiothreitol (DTT) for 30 min at room temperature. The unreduced controls were treated under identical conditions but in the absence of DTT. The reduced and non-reduced Cr-TRX1 were incubated with 3 mM iodoacetamide (IAM) for 30 min at room temperature for derivatisation (Gommel *et al*, 1997). The samples were diluted 10 times with 0.1 % (v/v) trifluoroacetic acid and mixed with an equal volume of a saturated solution of sinapinic acid in 33 % (v/v) acetonitrile and 0.1 % (v/v) trifluoroacetic acid. An aliquot of 0.5 μl of this mixture was crystallized on a microcrystalline layer and analyzed using ABI Voyager-DE™ STR Biospectrometry™ in the linear model.

To identify the position of active Cys residues, aliquots of the Cr-TRX1 samples were subjected to SDS-PAGE. The Cr-TRX1 bands were recovered and subjected to in-gel digestion analysis according to the methods described by Shevchenko *et al* (1997).

However, the alkylation step was omitted. After overnight in-gel digestion with trypsin, the protein fragments were extracted from the gel with 20 mM ammonium bicarbonate, followed by 5 % formic acid in 50 % aqueous acetonitrile and with 100 % acetonitrile. The extracts were pooled and the solvent was allowed to vaporize in a speed-vacuum before mass spectrometric analysis. The peptide samples were analyzed by the Applied Biosystems 4700 Proteomics Analyzer.

2.4.5 Biochemical characterization of Cr-TRX1

In order to investigate the enzymatic function of Cr-TRX1, we expressed and purified the recombinant full-length Cr-TRX1 in *E. coli*. With this recombinant Cr-TRX1, the following biochemical experiments were performed.

2.4.5.1 Fluorescence spectroscopy analysis

Reduction of oxidized *E. coli* TRX was previously shown to increase tryptophan fluorescence due to the quenching effect of the active site disulfide on the fluorescence of the adjacent tryptophan (Windle *et al*, 2000). The horseshoe crab TRX also contains a Trp residue in the active site motif, WCPPC. Therefore, we examined the fluorescence emission spectra of horseshoe crab TRX before and after reduction. The change of fluorescence emission spectra indicates the status of the disulfide band in the active motif. The fluorescence emission spectra of Cr-TRX1 were determined with a Perkin Elmer LS50B spectrofluorimeter by excitation at 280 nm and emission was recorded from 300 to 400 nm using a light path of 1 cm. The bandwidth of the excitation and emission were 5 nm. All measurements were made in 50 mM Tris-HCl, pH 7.4 containing 1 mM EDTA

and 20 μg/ml TRX at room temperature. Complete reduction of TRX was achieved by the addition of 1 mM DTT (Windle *et al*, 2000). The solvent blanks were run as control spectra.

2.4.5.2 Insulin reduction assay & thioredoxin reductase assay

Enzymatic activity of TRX is usually assayed by their capacity to reduce the disulfide bonds of insulin using DTT as artificial reductant (Kunchithapautham *et al*, 2003). Insulin reduction can be measured spectrophotometrically as an increase in turbidity due to precipitation of the free insulin B chain. To examine the enzymatic antivity of horseshoe crab TRX, the insulin reduction assay was performed using DTT, insulin and recombinant TRX as previously described (Sadek *et al*, 2001). The reduction of insulin was recorded by monitoring the OD_{600}.

Except for DTT, the NADPH and TRX reductase (TRXR) can function as a physiological system to reduce TRX. Therefore, we also examined whether oxidized horseshoe crab TRX is reduced by TRXR in the presence of NADPH by monitoring NADPH oxidation at 340 nm. Thioredoxin reductase assays were conducted at room temperature in phosphate buffered saline (PBS), pH 7.4, containing 2 mM EDTA, 55 μM insulin, 100 μM NADPH and 1 μm Cr-TRX1. The assay was initiated by the addition of 50 nM rat liver TRXR (Reckenfelderbaumer *et al*, 2000).

2.4.5.3 Peroxidase activity assay of Cr-TRX1

Like peroxidase, the human TRX1 has been suggested to act as an antioxidant that directly scavenges H_2O_2 (Hirota *et al*, 2002). The reactive CXXC motif of TRX readily

undergoes oxidation-reduction in the presence of H_2O_2, NADPH and TRXR. In order to examine if the horseshoe crab TRX also possesses the peroxidase activity, we performed the peroxidase activity assay. The peroxidase reactions were performed at room temperature and the absorbance at 340 nm (A_{340}) was monitored. Sample mixtures lacking Cr-TRX1 served as controls. The reaction mixtures contained phosphate buffered saline, pH 7.4, 2 mM EDTA, 100 μM NADPH, 50 nM rat liver TRXR, 2.5 mM H_2O_2, and Cr-TRX1 (Jeong *et al*, 2004b).

2.4.5.4 DNA nicking assay

Thioredoxin is detectable in human plasma up to a concentration of 6 nM and it has been suggested that TRX plays a direct role as an antioxidant (Kunchithapautham *et al*, 2003). A DNA nicking assay was performed to determine whether recombinant horseshoe crab TRX was capable of functioning as an antioxidant protein. pGEM-T easy plasmid DNA (Promega) was used as a substrate for detecting DNA damage mediated by the mixed function oxidase (MFO) system which generates hydroxyl (OH^-) and thiol (RS*) radicals capable of damaging a DNA template (Kunchithapautham *et al*, 2003). The extent of MFO-mediated nicking can be evaluated by assessing the shift in gel mobility of the plasmid as it was converted from the supercoiled to the nicked form. The MFO system consists of 66 μM $FeCl_3$, 3.3 mM DTT and 2 mM EDTA in 25 mM HEPES buffer, pH 7.0. Plasmid DNA (500 ng) was incubated in the MFO system at 37 °C with or without recombinant Cr-TRX1. The recombinant GST and commercial BSA were used as controls. The extent of DNA damage was evaluated on ethidium bromide-stained agarose gels.

2.4.6 Gene reporter assay

To determine if Cr-TRX1 could regulate the NF-κB transactivation activity, we performed the co-transient transfection assay in HeLa cells with the wild type and mutant Cr-TRX1 and κB-reporter. In this project, the κB reporter was p5 × NF-κB-luciferase (Stratagene, La Jolla, CA), whose activity correlates with the expression of NF-κB. pRL-CMV (Promega) was used as an internal control. pcDNA3.1 vector (Invitrogen) was used for the expression of wild type and mutant Cr-TRX1 proteins.

For transient transfection, HeLa cells were maintained at 37 °C in DMEM supplemented with 10 % FBS. Twelve hours prior to transfection, cells at a density of 0.8×10^6 cells/well were seeded in a 6-well plate. Transfection was conducted using Lipofectamine 2000 (Invitrogen), according to the manufacturer's recommendation. Briefly, cells were transfected by incubation with 2 μg of DNA and 5 μl of Lipofectamine 2000 dissolved in 1.5 ml of Dulbecco's modified Eagle's medium (DMEM) alone for 6 h at 37 ºC. The transfection medium was completely removed, replaced with complete growth medium and incubated for another 36-48 h.

Collection of cell lysate was performed using the passive lysis buffer (PLB) from the Dual Luciferase Reporter Assay System (Promega). In brief, the growth medium was removed and the cells in the six-well plate were rinsed twice with 2 ml of ice-cold phosphate buffered saline (PBS). Five hundred μl of 1 × PLB was added to each well and the plate was placed on an orbital shaker with gentle shaking for 15 min at room temperature. The lysate was then transferred into a 1.5 ml tube and centrifuged for 30 s at 14,000 × g at 4 ºC in a refrigerated centrifuge. The cleared lysate was then transferred

to a new 1.5 ml tube. The protein concentration in the soluble cell lysate was quantified by Bradford analysis. To perform gene reporter assays, dual luciferase activities were measured using the Dual-Luciferase Reporter (DLR) Assay System (Promega) at 36 h after transfection according to the manufacturer's manuals. The luminescent signal was measured using TD-20/20 Luminometer (Turner Designs).

2.4.7 Non-radioactive electrophoretic mobility shift assay (EMSA)

In order to examine if Cr-TRX1 could affect the NF-κB DNA-binding activity, we performed the EMSA. In this experiment, the LightShift® Chemiluminescent EMSA Kit (Pierce), based on a non-isotopic method, was used to detect DNA-protein interactions. To perform the EMSA, we first extracted the nuclear extraction and prepared the biotin-labeled DNA probe according to the procedures described below.

2.4.7.1 Preparation of nuclear and cytoplasmic extraction

Nuclear extract was prepared using NE-PER® Nuclear and Cytoplasmic Extraction Reagents (Pierce). In brief, the growth medium was removed and the cells in the six-well plate were rinsed with 2 ml of PBS. An aliquot of 0.5 ml of TryLE™ Express (Invitrogen) was added to each well and incubated for 5 min at 37 °C until all cells have detached. The cell suspension was transferred to a 2 ml centrifuge tube. The nuclear and cytoplasm extracts were prepared according to the manufacturer's recommendation. The nuclear and cytoplamic extracts were immediately stored at - 80 °C. The extracts were thawed just before use in EMSA.

2.4.7.2 3' End biotin labeling

Biotin-labeled double stranded DNA was prepared using the Biotin 3' End DNA Labeling kit (Pierce). The mammalian κB DNA sequence was synthesized in both the forward and reverse orientations. The complementary oligos were first end-labeled separately as follows: 1 × TdT Reaction Buffer, 5 pmol ends of DNA, 0.5 μM biotin-11-UTP and 0.2 U/μl diluted TdT were incubated at 37 ºC for 30 min; and the reaction was stopped by adding 2.5 μl of 0.2 M EDTA. Fifty μl of chloroform/isoamyl alcohol (24:1) was added to extract the TdT. The mixture was then vortexed and centrifuged at 16,000 × g for 2 min to separate the phases. The aqueous phase, containing the biotin-labeled DNA, was removed and saved. The labeled complementary oligos were annealed by adding equal amounts of each and incubating at room temperature for 1 h. The mammalian κB DNA sequence is 5'-AGTTGAGGGGACTTTCCCAGGC-3'. The annealed oligos were stored at -20 ºC.

2.4.7.3 Electrophoretic mobility shift assay (EMSA)

The EMSA was used to study DNA-protein interactions. The LightShift® Chemiluminescent EMSA Kit (Pierce), based on a non-isotopic method, was used to detect DNA-protein interactions. A 4 % native polyacrylamide gel in 0.5 × TBE was prepared. The gel was pre-electrophoresed for 60 min at 100 V. Twenty fmol of biotin end-labeled DNA was incubated with 2 μl of nuclear extract, 1 × Binding Buffer and 50 ng/μl Poly (dI•dC) for 30 min at room temperature, and finally mixed with Loading Buffer via gentle pipetting. Twenty μl samples were loaded and electrophoresed at 100 V until the bromophenol blue dye had migrated approximately 3/4 down the length of the

gel. The Hybond-N^+ (GE Healthcare) membrane was soaked in 0.5 × TBE for 15 min, before transfer. Electrotransfer was carried out at 380 mA for 30 min in 0.5 × TBE cooled to 10 ºC. The membrane was placed on a dry paper towel and cross-linked at 120 mJ/cm^2 using the Spectrolink™ XL-1000 UV Crosslinker (Spectronics Corporation). The membrane was then processed according to the manual of LightShift® Chemiluminescent EMSA Kit (Pierce).

2.4.8 Antioxidant inhibits NF-κB signaling pathway

To determine if oxidative stress could also play a crucial role in mediating immune response in the horseshoe crab, we checked the effect of an antioxidant - pyrrolidine dithiocarbamate, PDTC (Calbiochem) on the expression of immune-related genes. At 50 mM, the antioxidant PDTC was administered intracardially at 500 μl/kg body weight of horseshoe crab. After 1 h, the horseshoe crabs were injected with 1.2 × 10^7-colony forming unit of *P. aeruginosa* / kg body weight. The hemocytes were collected at indicated time points after infection with *P. aeruginosa.* The semi-quantitative RT-PCR was performed according to the descriptions in Section 2.3.9.

CHAPTER 3: RESULTS

3.1 Isolation of *C. rotundicauda* NF-κB and IκB homologues

To address the issue of whether the ancient origin of the NF-κB signaling cascade can be traced back to this "living fossil", we decided to clone the horseshoe crab homologues of NF-κB and IκB. Because the genome of the horseshoe crab is still unknown and the homology of Rel homology domains (RHD) amongst different NF-κB proteins is relatively well-conserved from the vertebrate and insect, we used the degenerate primers that were designed based on the RHDs from various species to isolate the horseshoe crab NF-κB homologue. Similarly, in order to clone the IκB gene from the horseshoe crab, we designed the degenerate primers based on the sequence homology of the ankyrin repeats.

3.1.1 Cloning and characterization of NF-κB p65 homologue, CrNFκB

Using degenerate primers that were designed based on sequence homology of RHDs and *C. rotundicauda* hemocyte cDNA as template, we performed the RT-PCR to isolate the horseshoe crab NF-κB. The RT-PCR amplified a 160 bp product. Sequence analysis of this PCR fragment confirmed that it is a homologue of NF-κB transcription factor. Based on this 160 bp sequence, we designed two gene specific primers and performed the 3′ and 5′ RACE to obtain the full-length horseshoe crab NF-κB. By 3′ and

5′ RACE, the full-length *C. rotundicauda* NF-κB cDNA of 2527 bp was isolated (GenBank accession number: DQ090482). With an open reading frame of 1686 bp, the horseshoe crab NF-κB encodes a protein of 562 amino acids with a predicted molecular weight of 62 kDa (Figure 3.1). Amino acid analysis revealed that *C. rotundicauda* NF-κB possesses the characteristic organization of Rel/NF-κB proteins, thus, it is henceforth referred to as CrNFκB.

The overall sequence identity of CrNFκB with other NF-κB proteins ranged from 16 % to 32 %. In particular, CrNFκB shares homology with insect Dorsal-like proteins with highest sequence similarity to that of the honey bee, *Apis mellifera* dorsal protein (GeneBank accession number: AAP23055). Specifically, the CrNFκB contains an N-terminal Rel homology domain (RHD) of 282 amino acids (residues: 19-301) and a C-terminal transactivation domain, TD (residues: 315-562) (Figure. 3.1). The CrNFκB contains two conserved motifs in the RHD: the DNA binding motif (R-XX-R-X-R-XX-C) and the nuclear localization signal, NLS, which characterizes all NF-κB family of proteins (Figure 3.1). Sequences flanking the RHD show no homology to known proteins and do not contain any recognizable protein motifs. Interestingly, like the molluscan NF-κB homologue Cg-Rel (Montagnani *et al*, 2004), the C-terminal TD of CrNFκB also lacks the polyglutamine, polyalanine or polyasparagine stretches which characterizes the TD of *Drosophila* Dorsal and several insect Dorsal-like proteins (Shin *et al*, 2005).

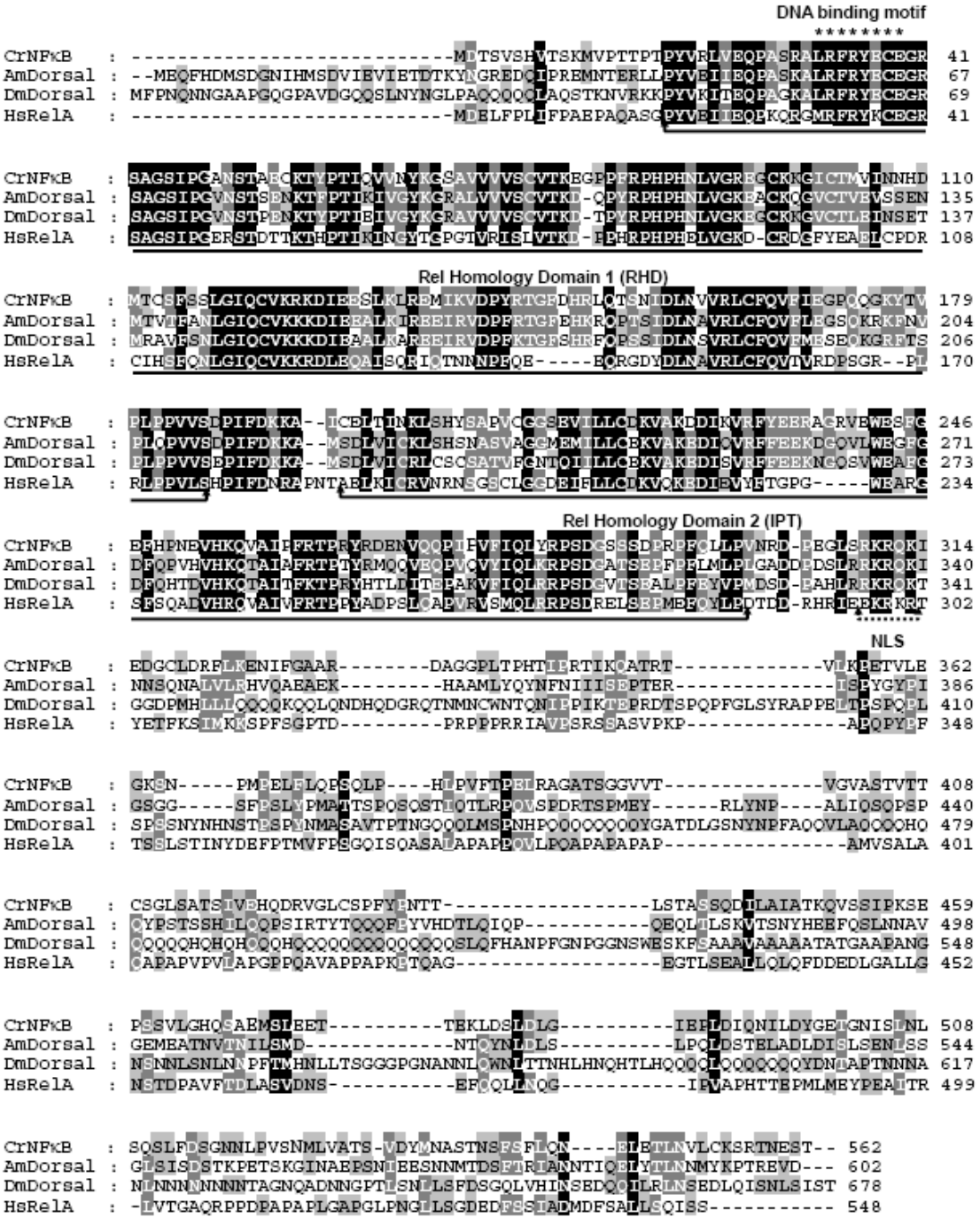

Figure 3.1: Comparison of amino acid sequence of CrNFκB with homologous proteins. *Drosophila* Dorsal (DmDorsal, AAA28479), Honey bee Dorsal (AmDorsal, AAP23055) and human RelA (HsRelA, AAH33522) were used for the comparison. Alignments were done by Clustal X. The RHD (Rel homology domain) is indicated by black lines. The NLS (Nuclear localization signal) is indicated by *. The potential DNA binding motif is indicated by a dotted line. Black and grey shades indicate identity and similarity of the residues, respectively.

The availability of the vertebrate and invertebrate (mostly insect) NF-κB protein sequences in databases allowed us to perform a phylogenetic analysis of the NF-κB family to confirm the relationship between CrNFκB and the other NF-κB transcription factors. The accession numbers of all the NF-κB and IκB proteins used in this study are listed in Table 3.1 (page 78). Based on the multisequence alignment of full-length proteins built with ClustalX, we constructed an unrooted phylogenetic tree.

The NF-κB protein family can be divided into two subfamilies. The class I subfamily includes vertebrate p100, p105 and invertebrate Relish proteins. The class II subfamily includes vertebrate RelA/p65, RelB, c-Rel and invertebrate Dorsal-like proteins (Gilmore, 1999). The difference is that RelA, RelB and c-Rel have an activation domain in their C-terminal which is absent in NF-κB1 and NF-κB2. On the contrary, NF-κB1 and NF-κB2 contains a C-terminal inhibitory IκB-like domain (see Figure 1.1). The phylogenetic analysis demonstrated that CrNFκB clustered amongst Dorsal-like proteins that belong to the invertebrate class II NF-κB (Figure 3.2). This cluster differs from the vertebrate class II NF-κB, which includes RelA, RelB and c-Rel proteins. This result is consistent with the previous sequence analysis where CrNFκB shared most similarities with insect Dorsal-like sequences. The class II NF-κB proteins from the invertebrates and vertebrates are more distant from the class I NF-κB proteins (Figure 3.2), which includes vertebrate p100, p105 and invertebrate Relish-like proteins (Gilmore, 1999).

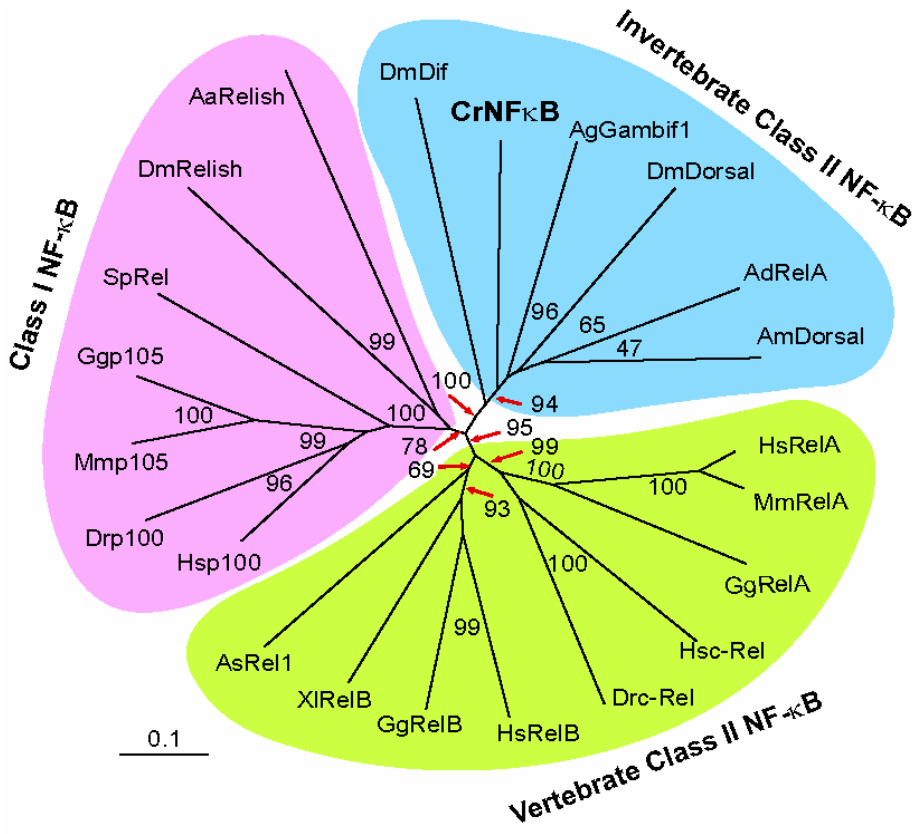

Figure 3.2: Phylogeny of CrNFκB and related NF-κB proteins. Multiple sequence alignments were produced with Clustal X using Gonnet series protein weight matrix. Unrooted phylogenetic tree was constructed using neighbor-joining method based on the alignments. The confidence scores (in %) of a bootstrap test of 1000 replicates are indicated for major branching nodes. The accession numbers of all the proteins used in this study are listed in Table 3.1 (page 78).

3.1.2 Cloning of Cactus and IκB homologue, CrIκB

The *C. rotundicauda* IκB (CrIκB) cDNA was similarly cloned using primers designed from the conserved ankyrin repeat regions of *Drosophila* and mammalian IκB proteins using horseshoe crab hemocyte cDNA as template. Subsequently, the full-length

CrIκB cDNA was obtained by 3′ and 5′ RACE. The full-length CrIκB cDNA (GenBank Accession number: DQ090483) contains 1566 bp encoding a 439 amino acid protein with a predicted molecular weight of 49 kDa. The CrIκB protein (Figure 3.3) contains several features exemplified by IκB members: 5 ankyrin repeats with homology to the mammalian and *Drosophila* IκB counterparts; two serine residues at the N-terminal serine rich region that are critical for its degradation; and the C-terminal PEST (proline-, glutamic acid-, serine- and threonine-rich) domain necessary for phosphorylation and intrinsic stability of the IκB protein (Ernst *et al*, 1995). Furthermore, at the C-terminal PEST domain, several putative casein kinase II phosphorylation sites can be identified which have been shown to be required for PEST-mediated Cactus degradation (Liu *et al*, 1997).

A comparison of full-length amino acid sequences between CrIκB and insect IκB proteins showed that CrIκB has the highest homology to *Drosophila* IκB homologue, Cactus. Using the vertebrate and invertebrate (mostly insect) IκB protein sequences in databases, we performed a phylogenetic analysis of the IκB family. The accession numbers of all the IκB proteins used in this study are listed in Table 3.1. Based on the multisequence alignment, we constructed an unrooted phylogenetic tree. The phylogenetic analysis revealed three main clusters: the invertebrate IκB, vertebrate IκBα, and vertebrate IκBβ and IκBε (Figure 3.4). The horseshoe crab IκB, together with *Drosophila* IκBs, formed a separate cluster that is different from the group of vertebrate IκB proteins. Interestingly, compared with that of the invertebrate IκB proteins, the

genetic distances between the vertebrate IκB clades are rather short. This is in contrast to the large genetic distance between the sequences in the invertebrate IκB clade.

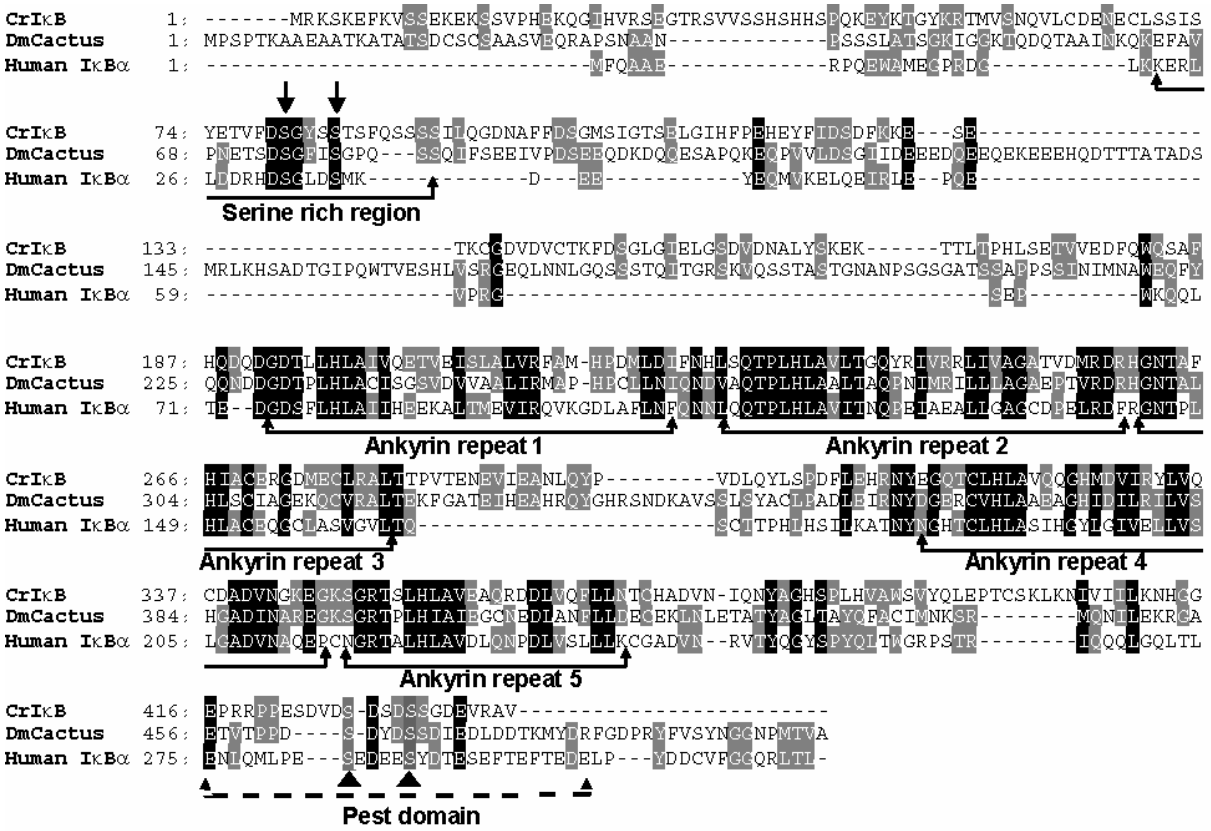

Figure 3.3: Amino acid sequence alignment of CrIκB and homologous proteins. *Drosophila* Cactus (AAA85908) and human IκBα (AAP35754) were aligned with CrIκB using Clustal X. The five ankyrin repeats of CrIκB are underlined in black lines. The N-terminal serine rich region is underlined by a black line. The potential N-terminal phosphorylation sites which have been shown to be critical for IκB degradation in response to extracellular signals are indicated by arrows. The C-terminal PEST domain implicated in regulating the stability of IκB is underlined in dashed line. The serine residues which are potentially phosphorylated by casein kinase II are indicated by triangles.

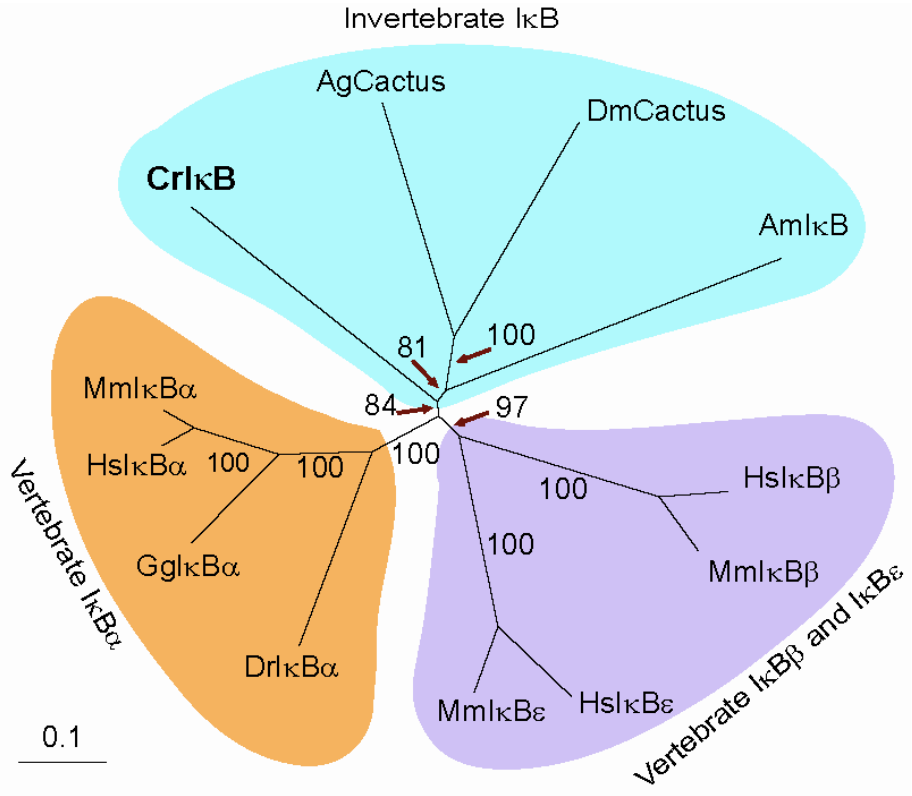

Figure 3.4: Unrooted phylogenetic tree of IκB proteins. The tree was built by the neighbor-joining method based on the alignment of the sequences using Clustal X. The confidence scores (in %) of a bootstrap test of 1000 replicates are indicated for major branching nodes. The accession numbers of all the IκB proteins used in this study are listed in Table 3.1.

Table 3.1: The sequences used for phylogenetic analysis of the NF-κB and IκB proteins

NF-κB proteins			
Code Name	**Name**	**Accession Number**	**Organism**
DmDif	*Drosophila* Dif	A49435	*Drosophila melanogaster*
DmDorsal	*Drosophila* Dorsal	AAA28479	*Drosophila melanogaster*
AmDorsal	Honey bee Dorsal	AAP23055	*Apis mellifera*
AdRelA	Beetle RelA	BAD20728	*Allomyrina dichotoma*
AgGambif1	Mosquito Gambif1	S71889	*Anopheles gambiae*
CrNFκB	Horseshoe crab NF-κB	DQ090482	*Carcinoscorpius rotundicauda*
HsRelA	Human RelA	AAH33522	*Homo sapiens*
MmRelA	Mouse RelA	AAH94053	*Mus musculus*
GgRelA	Chicken RelA	NP_990460	*Gallus gallus*
Hsc-Rel	Human c-Rel	X75042	*Homo sapiens*
Drc-Rel	Zebra fish c-Rel	AAO26402	*Danio rerio*
HsRelB	Human RelB	Q01201	*Homo sapiens*
GgRelB	Chicken RelB	NP_990181	*Gallus gallus*
XlRelB	Frog RelB	S60161	*Xenopus laevis*
AsRel1	Ascidian Rel1	BAB47172	*Halocynthia roretzi*
CrRelish	Horseshoe crab Relish	DQ345784	*Carcinoscorpius rotundicauda*
Ggp105	Chicken p105	Q04861	*Gallus gallus*
Mmp105	Mouse p105	NM_008689	*Mus musculus*
Drp100	Zebra fish p100	NP_001001840	*Danio rerio*
Hsp100	Human p100	AAW56071	*Homo sapiens*
SpRel	Sea urchin NF-κB	NP_999819	*Strongylocentrotus purpuratus*
AaRelish	Mosquito Relish	AAM97895	*Aedes aegypti*
DmRelish	*Drosophila* Relish	AAF20137	*Drosophila melanogaster*
IκB proteins			
Code Name	**Name**	**Accession Number**	**Organism**
CrIκB	Horseshoe crab IκB	DQ090483	*Carcinoscorpius rotundicauda*
AgCactus	Mosquito Cactus	EAA12805	*Anopheles gambiae*
DmCactus	*Drosophila* Cactus	AAA85908	*Drosophila melanogaster*
AmIκB	Honey bee IκB	XP_394485	*Apis mellifera*
HsIκBα	Human IκBα	AAP35754	*Homo sapiens*
MmIκBα	Mouse IκBα	NP_035037	*Mus musculus*
GgIκBα	Chicken IκBα	NP_001001472	*Gallus gallus*
DrIκBα	Zebra fish IκBα	AAH62524	*Danio rerio*
HsIκBβ	Human IκBβ	AAP36616	*Homo sapiens*
MmIκBβ	Mouse IκBβ	Q60778	*Mus musculus*
HsIκBε	Human IκBε	AAC51216	*Homo sapiens*
MmIκBε	Mouse IκBε	AAB97517	*Mus musculus*

3.1.3 Cloning of horseshoe crab NF-κB p100 and Relish homologue, CrRelish

During the process of cloning CrIκB with the degenerate primers designed based on the ankyrin repeats, a 120 bp DNA fragment was serendipitously isolated, which shows moderate homology with mammalian p100. Because the ankyrin repeat region is conserved between the IκB proteins and class I NF-κB, which include vertebrate p100, p105 and invertebrate Relish proteins, we speculated that this 120 bp fragment probably represents the horseshoe crab class I NF-κB homologue. To confirm this possibility, the full-length sequence was cloned by 5′ and 3′ RACE.

Indeed, this clone shows high homology with *Drosophila* Relish and mammalian p100 (Figure 3.5), therefore, it was designated as CrRelish. The full-length CrRelish contains 3405 bp encoding an 1135 amino acids protein. Like the p100, p105 and Relish proteins, it contains an N-terminal RHD with conserved DNA-binding motif and NLS, and a C-terminal IκB-like domain (Figure 3.5). Like *Drosophila* Relish, the CrRelish also contains 6 ankyrin repeats in its C-terminal IκB-like domain. In *Drosophila* Relish, two serine-rich stretches are located at the N-terminal region (S22-S45) and just downstream of the nuclear localization signal (S460-S475). Similarly, in CrRelish, two long serine-rich stretches were found in the N-terminal region and downstream of the nuclear localization signal. Interestingly, similar to mosquito Relish and mammalian p100 and p105 but not *Drosophila* Relish (Shin *et al*, 2002), a death domain is located at the C-terminus of the CrRelish. Another apparent difference between the CrRelish and *Drosophila* Relish is that the length of the linker sequence between the RHD and C-terminal IκB domain in CrRelish is longer than that of the *Drosophila* homologue.

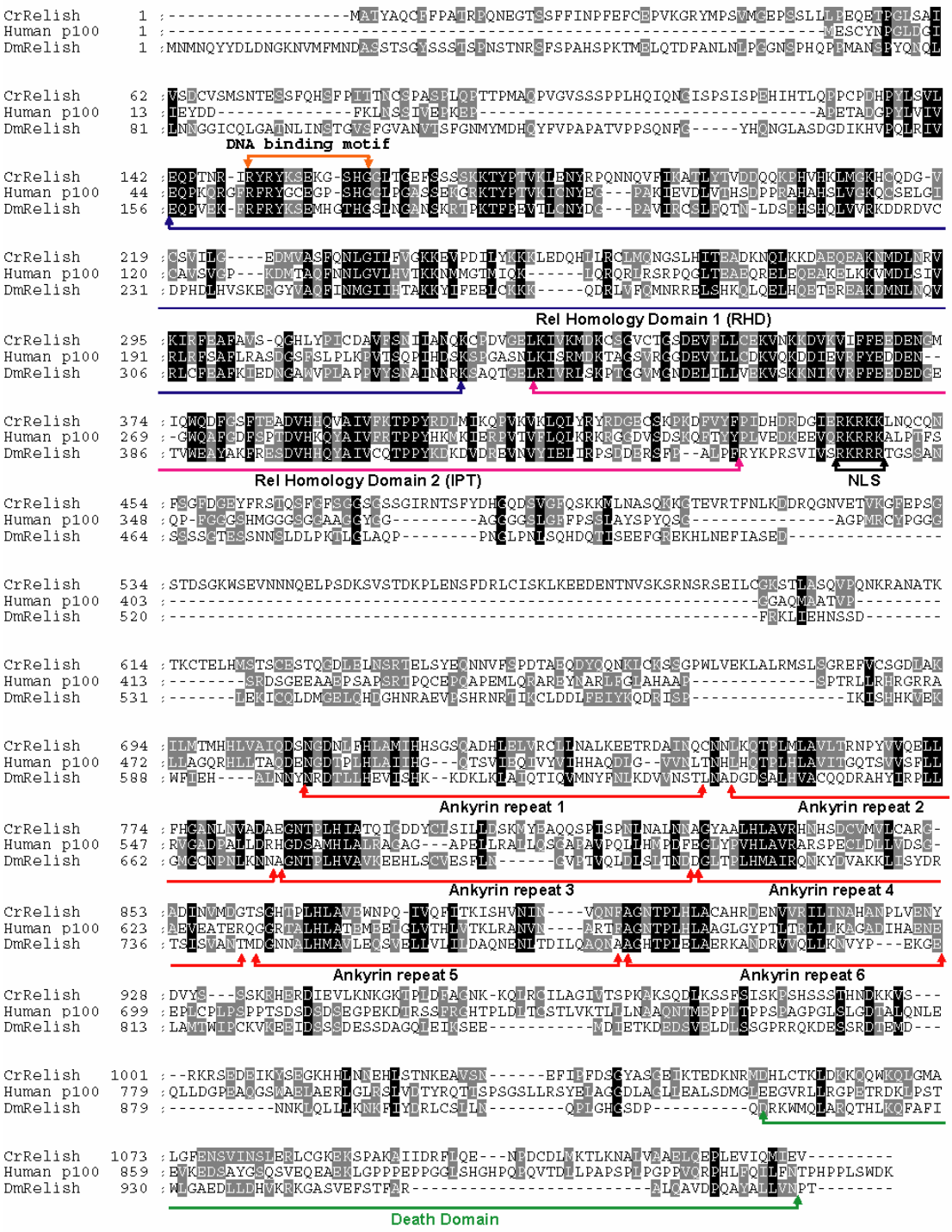

Figure 3.5: Amino acid sequence comparison of CrRelish with homologous proteins. *Drosophila* Relish (NM_206467) and human p100 (NM_002502) were used for the comparison**.** Alignments were done by Clustal X. The potential DNA binding motif is indicated by a yellow line. The Rel homology domain 1 (RHD) is underlined by blues lines and the Rel homology domain 2 (IPT) is marked by purple lines. The NLS (nuclear localization signal) is indicated by a black line. The six ankyrin repeats of CrIκB are underlined in red. The C-terminal death domain is indicated by a green line.

A phylogenetic study demonstrated that both the horseshoe crab and insect Relish proteins were clustered to the same subgroup, distinctive from the invertebrate class II NF-κB family proteins (Figure 3.6). This Relish subgroup could be clustered with p105 and p100, indicating that these Rel/IκB compound proteins might have branched off at an early evolutionary stage from other NF-κB family proteins including the insect NF-κB proteins.

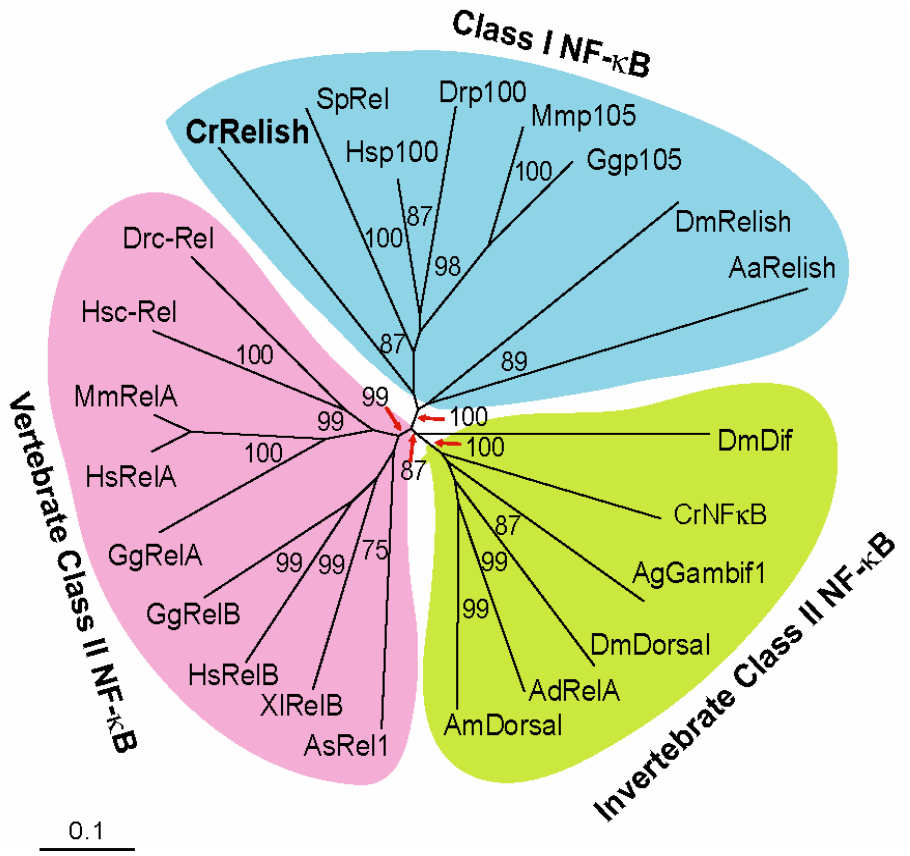

Figure 3.6: Phylogeny of CrRelish and related NF-κB proteins. Multiple sequence alignments were produced with Clustal X using Gonnet series protein weight matrix. Unrooted phylogenetic tree was constructed using neighbor-joining method based on the alignments. The confidence scores (in %) of a bootstrap test of 1000 replicates are indicated for major branching nodes. The accession numbers of all the proteins used in this study are listed in Table 3.1

3.2 CrNFκB binding to κB motif is inhibited by CrIκB

3.2.1 CrNFκB binding to the κB motif

To examine the ability of CrNFκB to recognize the κB motif, recombinant His-tagged RHD of CrNFκB (amino acids: 1-353) was produced. EMSA was performed using the recombinant protein with the *C. rotundicauda* Factor C (CrFC) promoter NF-κB binding site. This CrFC NF-κB response element (-143 to -133) was previously reported to be recognized by the human NF-κB and *Drosophila* Dorsal protein (Wang *et al*, 2003).

The results of EMSA revealed that the RHD of the CrNFκB could interact with the κB response element on CrFC promoter (Figure 3.7). As a negative control, the GST (Glutathione S-transferase) and CrIκB could not bind to the CrFC κB probe. The presence of κB motif is critical to the binding; since mutation of the κB motif (-143 to -141), from GGG to ATT, abolished the binding (Figure 3.7; lane 8). The interaction is specific as the binding was markedly reduced by excess cold competitor oligonucleotides (Figure 3.7; lane 2-3), whereas the addition of mutant competitor did not affect the binding (Figure 3.7; lane 6-7). The identity of the two small bands below the NF-κB-DNA complexes is still unknown at present. However, when the mutant probe was used for EMSA (lane 8), the intensity of the two lower bands decreased significantly. This suggests that they are probably the CrNFκB-DNA complexes as well. Furthermore, because only the N-terminal CrNFκB was used for the EMSA experiments, this result indicates that the C-terminal TD of CrNFκB is not necessary for DNA binding activity,

which was similarly observed for *Drosophila* Dorsal and mosquito NF-κB homologues (Shin *et al*, 2002).

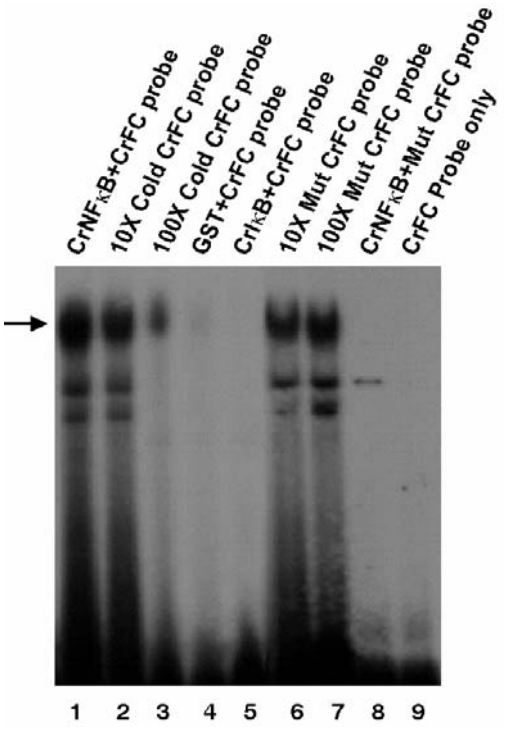

Figure 3.7: Binding of CrNFκB protein to horseshoe crab Factor C (CrFC) κB probe. Sequences of all probes used in this assay are listed in Table 3.2. Complex formations (lane 1) were significantly abolished by cold CrFC probes (lanes 2 & 3), but not by an excess of unlabeled mutant CrFC (Mut CrFC) probes (lanes 6 & 7). As a negative control, GST alone or recombinant CrIκB showed no binding to the CrFC probe (lanes 4 & 5). Almost no complex was formed when mutant CrFC probe was used (lane 8). The NF-κB-DNA complexes are indicated by an arrow.

Further analysis of the CrFC promoter revealed other potential Dorsal-like binding sites: Prox3Dor (-219 to -209; -200 to -190; -193 to -183), Dor348 (-359 to -348), Dor586 (-596 to -586) and Dor788 (-798 to -788) (Wang *et al*, 2003). Previous studies have shown that the Prox3Dor and the Dor788 site can be recognized by the *Drosophila* Dorsal protein. Therefore, we examined the binding ability of CrNFκB on those potential κB sites. As shown in Figure 3.8A, the EMSA results indicated that

except for Prox3Dor site, the recombinant CrNFκB protein showed no obvious binding to the other individual dorsal sites. This is different with the *Drosophila* Dorsal protein. The probe sequences and the binding characteristics of all the probes with CrNFκB are listed in Table 3.2. Interestingly, CrNFκB also recognizes the consensus mammalian NF-κB binding motif, 5′-AGTTGAGGGGACTTTCCCAGGC-3′ (Figure 3.8B), and thus CrNFκB may serve as a functional substitute for the vertebrate NF-κB or vice versa. Furthermore, our results also suggest that the specific sequence recognition of NF-κB transcription factor was acquired early and maintained during evolution.

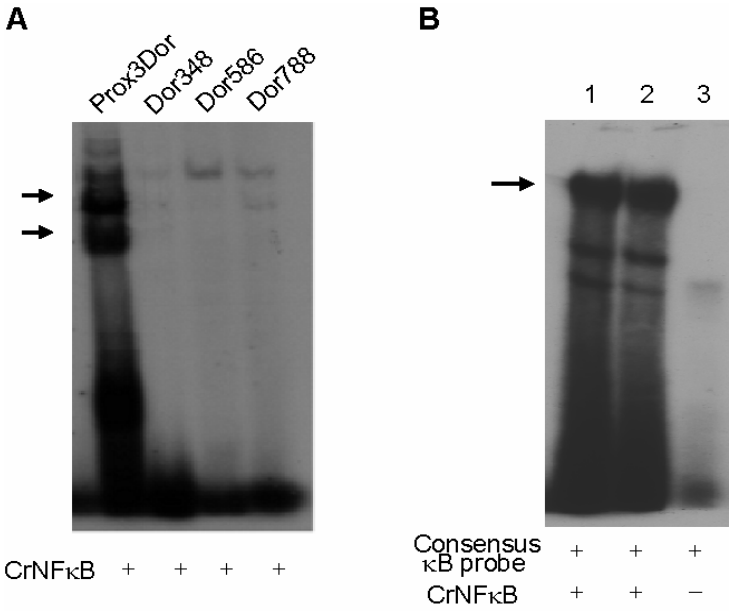

Figure 3.8: Binding ability of CrNFκB on potential κB sites on Factor C promoter and mammalian consensus κB sites. **(A)** The CrNFκB can form stable complexs with Prox3Dor probe. The possible NF-κB-DNA complexes are indicated by arrows. Almost no complex was formed when Dor348, Dor586, Dor788 probe was used. **(B)** The CrNFκB binds with mammalian consensus κB probe. The bacteria expressing CrNFκB were sonicated in the binding buffer. The bacterial lysate was used for EMSA (lane 1 & lane 2). The NF-κB-DNA complexes are indicated by an arrow. Almost no complex was formed when bacterial lyste without expressing CrNFκB was used (lane 3). Sequences of all probes used in this assay are listed in Table 3.2.

Table 3.2: Probes used in EMSA and binding characteristics of CrNFκB and Dorsal to various probes

Probes	DNA Sequence	Potential NF-κB or Dorsal-like binding sites	Binding characteristics	
			CrNFκB	Dorsal[#]
CrFC κB	5'-AAAAGCCGGGAAATCCATTAGA-3'	(-143) 5'-GGGAAATCCA-3' (-133)	+	+
Prox3Dor	5'-AAATTTTTCCTTCTTGTACATTGG AAAACGTTTTCACGTGACGTACTG ATTTGTCTGTCATGCA-3'	(-200) 5'-TTGGAAAACGT-3' (-190)	+	+
		(-183) 5'-CGTGAAAACGT-3' (-193)*		
		(-209) 5'-AAGGAAAAATT-3' (-219)*		
Dor348	5'-GTTGTTGTTTTCTTGTAACAG-3'	(-348) 5'-CAAGAAAACAA-3' (-359)*	–	–
Dor586	5'-GTGTGTGTTTTCTTATAGCA-3'	(-586) 5'-TAAGAAAACAC-3' (-596)*	–	–
Dor788	5'-CAAACGAAGAAAAAACTTCC-3	(-798) 5'-GAAGAAAAAAC-3' (-788)	–	+

*Sequences shown are in the antisense strand. # Adapted from Wang *et al* (2003).

3.2.2 CrNFκB interacts with CrIκB

By binding to the RHD and masking the NLS of NF-κB, the IκB is the natural endogenous inhibitor of the NF-κB activity (Karin and Ben-Neriah, 2000). To investigate whether CrIκB can interact with CrNFκB, pull-down assay and immunoprecipitation were performed. *In vitro* GST pull-down was performed using recombinant His-tagged RHD of CrNFκB (amino acids: 1-353) and full length GST-tagged CrIκB. First, we purified the recombinant GST-CrIκB fusion protein and the purified GST-CrIκB fusion protein was resolved on SDS-PAGE (Figure 3.9, lane 1). The molecular weight of the purified protein (75 kDa) is consistent with the predicted size of

the recombinant GST-CrIκB fusion protein. The His-fusion CrNFκB protein was expressed in bacteria as well. The expression of CrNFκB was confirmed by probing bacteria lysates with anti-His antibody (Figure 3.9, lane 2). Next, the GST-CrIκB fusion protein was immobilized on glutathione beads and assessed for its ability to retain recombinant His-fusion CrNFκB. As shown in Figure 3.9, the pull-down assay showed a stable complex between these two recombinant proteins (lane 5). This interaction between CrNFκB-RHD and CrIκB was specific as no interaction was observed between either control Sepharose beads or GST protein with CrNFκB-RHD (Figure 3.9, lane 3-4).

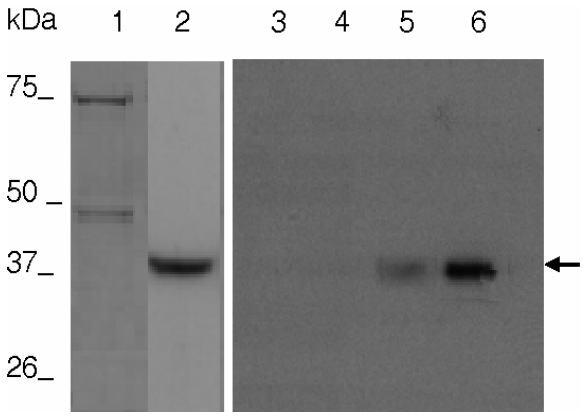

Figure 3.9: *In vitro* interaction of CrNFκB and CrIκB. GST pull-down assay. The purified GST-CrIκB fusion protein was resolved on SDS-PAGE (lane 1). His-fusion CrNFκB protein was recombinantly expressed in bacteria. The expression of CrNFκB was confirmed by probing bacteria lysates with anti-His antibody (lane 2). His-fusion CrNFκB expression bacteria lysates were incubated with glutathione-Sepharose beads loaded with GST-IκB. After washing the beads, the eluted proteins were analyzed by SDS-PAGE and detected by anti-His antibody (lane 5). One-tenth volume of the His-CrNFκB was also electrophoresed as positive control (lane 6). Negative control included Sepharose beads alone (lane 3) and Sepharose beads with GST (lane 4). His-CrNFκB band is indicated by an arrow.

To determine whether CrNFκB interacts with CrIκB *in vivo*, we performed the immunoprecipitation assay. First, we transiently co-expressed full length V5-tagged CrNFκB and c-Myc-tagged CrIκB in *Drosophila* S2 cells. As shown in Figure 3.10, the expression of CrNFκB and CrIκB was confirmed by Western blot using anti-V5 and anti-c-Myc antibodies. Then the extracts of transfected cells were subjected to immunoprecipitation using anti-V5 antibody. The immunecomplexes were resolved in SDS-PAGE and subjected to Western blotting analysis with anti-c-Myc antibody to detect interaction. The CrIκB was confirmed to interact with CrNFκB to form an immunoprecipitated complex (Figure 3.10). This interaction between CrNFκB and CrIκB was specific as no interaction was observed without the expression of CrNFκB.

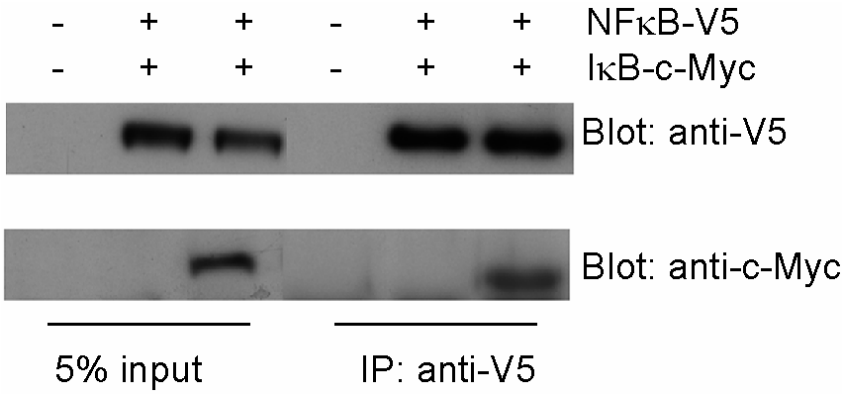

Figure 3.10: Immunoprecipitation (IP) of CrNFκB and CrIκB in *Drosophila* S2 cell. S2 cells were transiently transfected with the indicated combination of CrNFκB-V5 and CrIκB-c-Myc expression plasmids. The cell lysates were subjected to IP using anti-V5 antibody 48 h after transfection. The beads were washed 3 times with lysis buffer and subjected to Western analysis with antibodies against V5 and c-Myc. 5 % volume of the cell lysates used for IP was electrophoresed as control.

3.2.3 CrIκB inhibits CrNFκB DNA-binding activity

It has been shown that the human IκBα but not IκBβ can efficiently remove NF-κB from the DNA (Tran *et al*, 1997). To verify whether CrIκB could also inhibit the DNA-binding activity of CrNFκB, we performed EMSA with or without purified CrIκB proteins. The EMSA results showed that the presence of CrIκB inhibited the DNA-binding activity of CrNFκB in a dose-dependent manner (Figure 3.11). However, the adding of excess amount of GST did not affect CrNFκB DNA-binding ability. This suggests that CrIκB can specifically inhibit the DNA-binding activity of CrNFκB, which was similarly observed in IκBα (Karin and Ben-Neriah, 2000). We noticed that the adding of CrIκB increased the intensity of the nonspecific binding complexes (Figure 3.11, arrowhead). This is probably caused by the contaminant in the purified CrIκB or the increased amount of free κB probe because CrIκB significantly inhibited the binding of CrNFκB to the κB probe. Altogether, the results demonstrate that CrIκB interacts with and specifically inhibits the DNA binding activity of CrNFκB. In addition, in spite of their ancient origin, this familiar relationship between the two homologues forming the NF-κB/IκB cascade suggests that they probably underwent co-evolution.

3.3 Functional activation of the CrNFκB/CrIκB cascade

Sequence analysis of the CrNFκB showed strong similarities between NFκB proteins in the horseshoe crab and insects. The effect of CrNFκB on the gene transcription was analyzed in *Drosophila* S2 cell line. First, we examined whether

overexpression of CrNFκB might activate the expression of an NFκB-controlled reporter gene.

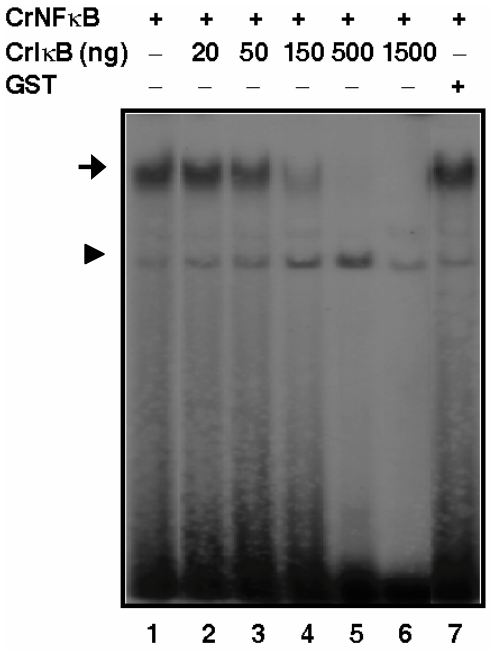

Figure 3.11: CrIκB protein inhibits the CrNFκB DNA-binding activity. A known amount of CrNFκB was titrated with increasing amounts of CrIκB (lanes 2-6). As a negative control, GST (3 μg) alone does not inhibit the CrNFκB binding to the CrFC κB probe (lane 7). The NF-κB-DNA complexes are indicated by an arrow. The unspecific bindings are marked by an arrowhead.

3.3.1 Overexpression of CrNFκB activates κB reporter expression

Previously, it has been shown that the horseshoe crab Factor C promoter contains several potential NF-κB binding motifs which can be recognized by *Drosophila* Dorsal protein (Wang *et al*, 2003). Therefore, we examined the ability of CrNFκB to regulate gene transcription of CrFC promoter (-186 to +1)-CAT reporter using transient co-transfection studies with the horseshoe crab wild-type or truncated V5-tagged CrNFκB expression constructs. The schematic representation of the expression vectors and reporters used in transfection experiments are shown in Figure 3.12.

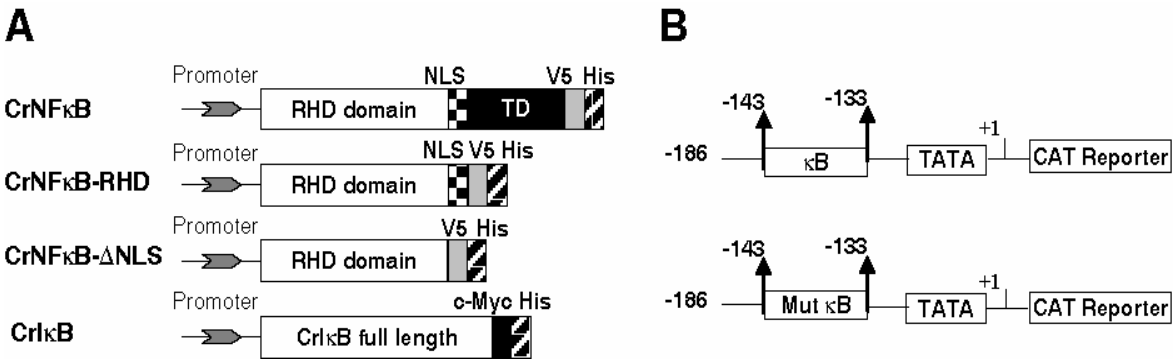

Figure 3.12: Schematic representation of the expression vectors and reporters used in transfection experiments. (A) Schematic representation of the expression vectors used in transfection experiments: CrNFκB (full-length); CrNFκB-RHD (lacks the C-terminal transactivation domain, TD); CrNFκB-ΔNLS (lacks the C-terminal TD and nuclear localization signal, NLS); **(B)** Schematic representation of the wild type (κB) and mutant CrFC-CAT (Mut κB) reporter vectors.

As shown in Figure 3.13, the overexpression of full-length CrNFκB resulted in 10-fold increase in CAT reporter expression compared to the control vector suggesting that the CrNFκB has the gene transactivation ability. However the CrNFκB-RHD (amino acids: 1-321) and CrNFκB-ΔNLS (amino acids: 1-266) led to significantly reduced CAT expression. This suggests that the C-terminal TD of CrNFκB, which is not necessary for DNA-binding (Figure 3.7), is essential for reporter gene activation. The transactivation activity of CrNFκB-ΔNLS was even lower compared with that of CrNFκB-RHD suggesting that the NLS of CrNFκB is also important in regulating NF-κB activity. To show that the κB motif (-143 to -133) of CrFC promoter is responsible for the transcriptional activation, transfection studies were carried out using a CrFC promoter

(-186 to +1)-CAT reporter where the 5′ end of the potential NF-κB binding motif, GGGAAA (-143 to -138), was deleted. The mutant κB reporter showed significantly reduced CAT expression suggesting that the putative κB motif of Factor C promoter is functional and necessary for transactivation. The slight induction by the mutant promoter construct (Figure 3.13) is likely due to the presence of putative non-canonical κB response element (-156 to -146) in the reporter (Wang *et al*, 2003). These results demonstrated that CrNFκB is able to trigger the expression of κB reporter. This transactivation capacity relied primarily on the integrity of the C-terminal domain and NLS of CrNFκB and on the presence of functional κB binding sites in the reporter gene promoter.

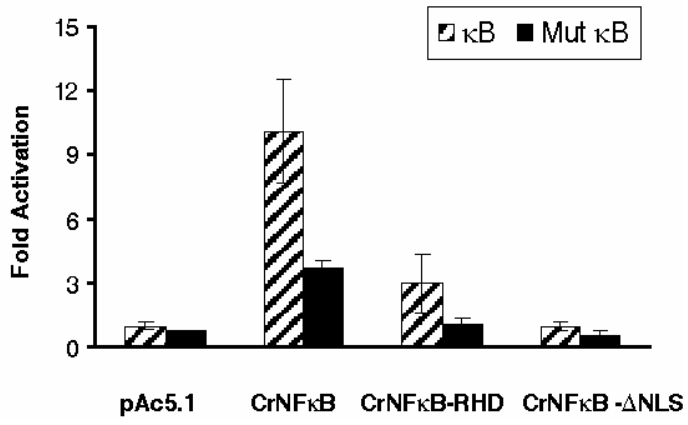

Figure 3.13: The transactivation ability of CrNFκB. S2 cells were transiently co-transfected with wild type and mutant CrFC-CAT reporters (1 μg), a β-galactosidase expression plasmid (50 ng), together with full length or truncated CrNFκB constructs (500 ng). CAT expression level was normalized against the levels of β-galactosidase expression.

3.3.2 CrIκB inhibits CrNFκB transactivation ability

To examine the effect of CrIκB on CrNFκB transactivation ability, similar transfection studies were also performed in the presence of increasing amounts of CrIκB. Consistent with the role of IκB, which is the natural inhibitor of NF-κB, the overexpression of CrIκB caused a dose-dependent reduction in CAT reporter expression (Figure 3.14). Therefore, functional analysis of the CrNFκB and CrIκB revealed that the CrNFκB was an efficient NF-κB like activating transcription factor and the CrIκB can interact with CrNFκB and inhibited its transactivation activity. Taken together, these results strengthen the idea that horseshoe crab IκB proteins are functionally identical to mammalian IκBα.

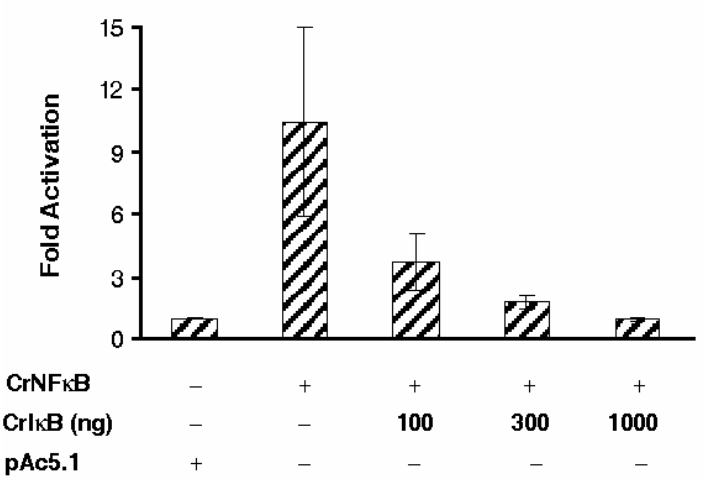

Figure 3.14: The transactivation ability of CrNFκB is inhibited by CrIκB. Co-transfection of CrNFκB (500 ng) and increasing amounts of CrIκB in S2 cells. Results are expressed as relative fold-induction in CAT expression as compared to control cells transfected with vector backbone. Data are presented as mean ± S.D. of three independent experiments.

3.3.3 Subcellular localization of CrNFκB and CrIκB

To verify whether the decreased gene activation ability of truncated CrNFκB (CrNFκB-RHD and CrNFκB-ΔNLS) was attributable to the lack of transactivation activity or to impaired nuclear translocation, the subcellular localization of full-length and truncated CrNFκB was examined. Expression vectors for wild type and truncated V5-tagged CrNFκB were transiently transfected into S2 cells. The subcellular localization of the CrNFκB proteins in *Drosophila* S2 cells was examined by immunofluorescence using anti-V5 antibody.

As shown in Figure 3.15, the immunofluorescence images demonstrated that both the full-length CrNFκB and CrNFκB-RHD (amino acids: 1–321) were evenly distributed in the cytoplasm as well as in the nucleus indicating that the TD did not affect the nuclear localization of CrNFκB. This suggests that the decrease in transactivation ability of CrNFκB-RHD (Figure 3.13) was not due to the subcellular localization. Taken together, it indicates that despite CrNFκB harboring an atypical carboxy-terminal TD, as compared to that of vertebrate or insect homologues (Shin *et al*, 2005), it is still essential and functional for transcriptional activation. On the other hand, the truncated CrNFκB-ΔNLS (amino acids: 1-266) lacking the NLS remained localized to the cytoplasm (Figure 3.15). This result indicates that the NLS (RKRQK) of CrNFκB is functional and necessary for the nuclear localization. It is also consistent with the negligible transactivation ability observed with the CrNFκB-ΔNLS.

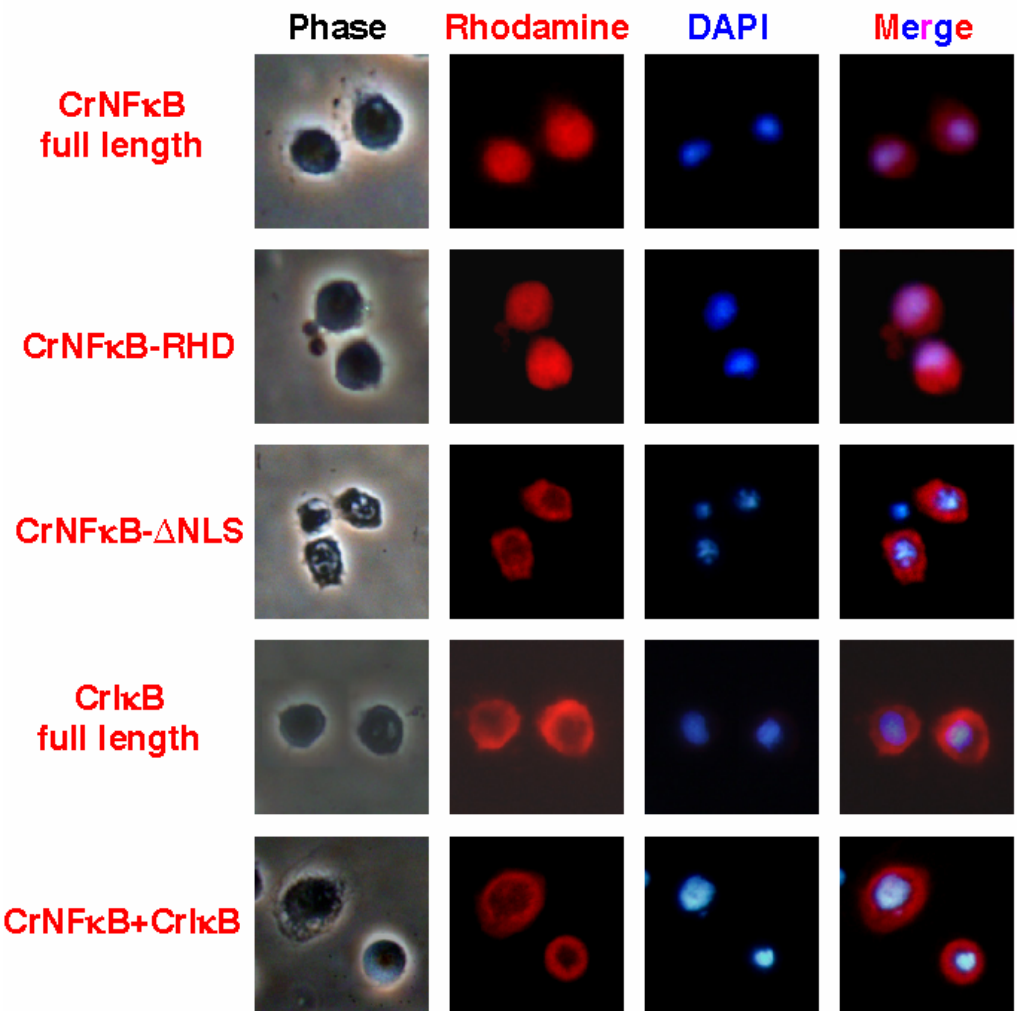

Figure 3.15: Localization of full length and truncated CrNFκB and CrIκB in S2 cells. S2 cells were transfected with plasmids (1 μg) expressing various CrNFκB-V5 or CrIκB-c-Myc proteins. Full length CrNFκB and CrNFκB-RHD are evenly distributed in the cytoplasm as well as in the nucleus when expressed alone. CrNFκB-ΔNLS and CrIκB localized to the cytoplasm. Co-expression of CrIκB results in the re-localization of full-length CrNFκB to the cytoplasm.

Next, we examined the subcellular localization of CrIκB using anti-c-Myc antibodies. The immunofluorescence revealed that the overexpressed CrIκB was exclusively located in the cytoplasm, which is consistent with the role of IκB proteins. To determine the effect CrIκB on the localization of CrNFκB, we co-expressed these two proteins. As shown in Figure 3.15, the overexpression of CrIκB resulted in the sequestration of CrNFκB exclusively to the cytoplasmic compartment which is similar to mammalian IκBα (Huang *et al*, 2000).

Taken together, the results show that the interaction between CrIκB and CrNFκB interferes with the latter's ability to translocate into the nucleus and consequential DNA-binding and gene transactivation. Interestingly, the activation of CrNFκB is analogous to the canonical activation cascade observed in the vertebrate (Chen and Greene, 2004), thus lending support to our proposal that the NF-κB/IκB signaling co-evolved early during evolution.

3.4 Biological significance of a primitive CrNFκB/CrIκB cascade

Thus far, our studies have utilized purified recombinant proteins and over-expression of CrNFκB and CrIκB. However, the relevance of this cascade *in vivo* is still unclear. To this end, we examined CrNFκB DNA-binding and gene regulation activity in the hemocytes, the major immune cell in this invertebrate. First, to examine the relevance of the NF-κB cascade *in vivo*, we investigated the κB-binding activity in the hemocytes – the major immune cells in this invertebrate. Horseshoe crab hemocyte

extracts were tested to see whether they contained proteins that could bind specifically to the κB site of the CrFC promoter. EMSA using whole hemocyte lysates and CrFC κB motif showed a stable complex; however mutation of the 5'-end of the CrFC κB motif from GGG to ATT abolished the binding. It suggests the presence of proteins in hemocytes which bind specifically to the κB site of CrFC promoter (Figure 3.16).

To investigate the identity of the proteins that were bound to the CrFC κB motif, we incubated CrNFκB with helenalin, which specifically inhibits human NF-κB p65 DNA-binding activity (Lyss *et al*, 1998), during the EMSA. As shown in Figure 3.16, the EMSA results indicated that the gel shift complexes were partially reduced by increasing doses of helenalin, further suggesting that the complexes were formed by NF-κB related proteins. To examine whether CrIκB, the natural inhibitor of CrNFκB, could inhibit the formation of DNA-binding complex, we performed similar EMSA in the presence of increasing doses of CrIκB. The EMSA results clearly demonstrate that increasing amounts of recombinant CrIκB protein disrupted the formation of CrNFκB-DNA complex in the horseshoe crab hemocytes (lane 3-6) providing further support to the conclusion that the complexes were formed by NF-κB related proteins. The inhibitory effects of CrIκB were specific as no inhibition was observed when recombinant GST protein was added (Figure 3.16; lane 7). This suggests that CrIκB can specifically inhibit the DNA-binding activity of NF-κB, which was similarly observed in IκBα (Karin and Ben-Neriah, 2000). Similar to previous observation (Figure 3.11), the addition of CrIκB also increased the intensity of the unspecific binding as indicated in Figure 3.16 by an arrowhead (lanes 4-6). This unspecificity is probably caused by the contaminant from the CrIκB, as without CrIκB, this complex is undetectable.

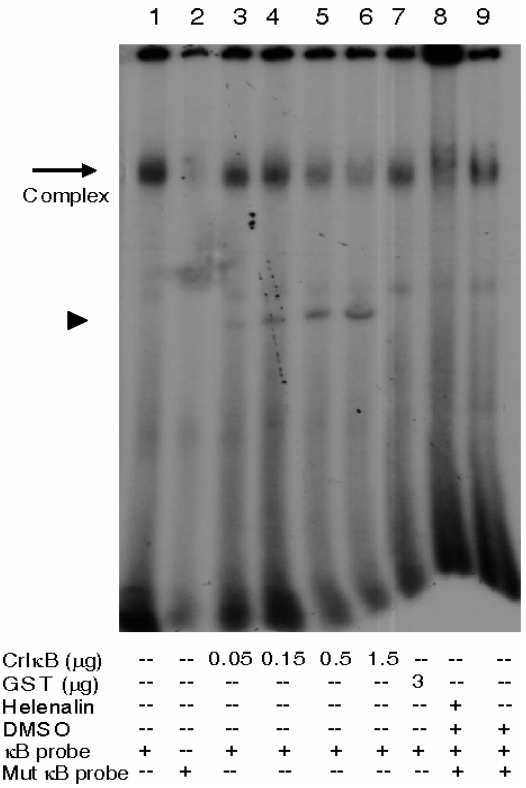

Figure 3.16: EMSA of hemocyte extracts incubated with the CrFC κB probe. Hemocyte extracts from adult horseshoe crab were used for EMSA. Approximately 20 mg of extract was incubated with CrFC κB probe (lanes 1 & 3-9) or mutant (Mut) CrFC κB probe (lane 2). Binding complexes were progressively abolished by addition of increasing amounts of recombinant CrIκB (lanes 3-6) compared to GST (lane 7), which remained unaffected. Helenalin, a specific inhibitor of NF-κB, partially decreases the intensity of the binding which remained unaffected by DMSO (vehicle) (lanes 8, 9). The NF-κB-DNA complexes are indicated by an arrow. The unspecific binding caused by the adding of CrIκB is marked by an arrowhead.

Next, we carried out super-shift assay using anti-CrNFκB antibodies which were produced from synthetic peptides (Biogenes, Germany), and purified using affinity column coupled with the peptide. As shown in Figure 3.17A, anti-CrNFκB antibodies caused a partial supershift of the κB-binding-complex confirming that the CrNFκB binds κB probe. We noticed that the majority of the κB-binding complex cannot be

supershifted by anti-CrNFκB antibody suggesting that there might be other κB motif-binding proteins in the horseshoe crab hemocytes. Indeed, we have cloned another NF-κB homologue, CrRelish, which shows high homology to the *Drosophila* Relish and mammalian NF-κB p100 and p105. Previous study has shown that amongst the three *Drosophila* NF-κB homologues (Dorsal, Dif and Relish), Relish has relatively higher and broader binding activity to κB motifs (Han and Ip, 1999). The similar mechanism probably also exists in horseshoe crab indicating that CrRelish may play a major role in forming the κB complex. Nevertheless, the partial supershift with anti-CrNFκB antibody suggests that the DNA–protein complex formed with κB motif at least involves the presence of CrNFκB. Furthermore, although the exact identity of the unshifted complexes is unknown at this juncture, the data in Figure 3.16 provide evidence to show that the complexes are formed by κB motif binding proteins.

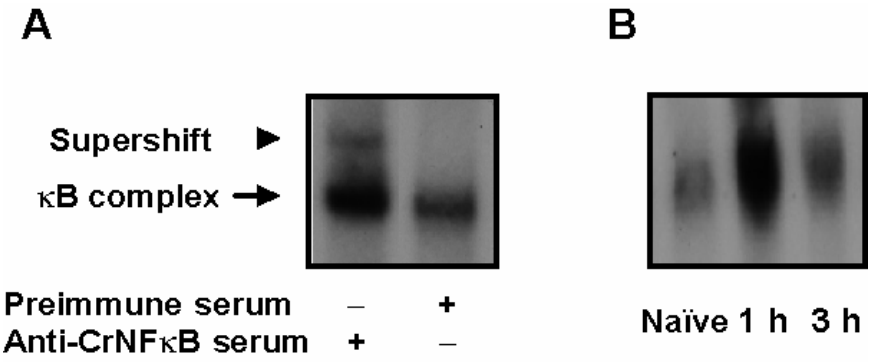

Figure 3.17: Bacterial infection activates CrNFκB DNA-binding activity. (A) Supershift of κB-binding complex by anti-CrNFκB antibody. The supershift was indicated by an arrow and the κB complex was marked by an arrow. **(B)** The naïve, 1 and 3 hpi *Pseudomonas*-challenged horseshoe crab hemocyte nuclear extracts were incubated with CrFC κB probe. The intensity of the DNA-binding complexes increased significantly after bacterial challenge.

To examine the *in vivo* activation of CrNFκB by infection, horseshoe crabs were injected with 1.2×10^7 cfu of *P. aeruginosa* per kg of body weight. After infection, the hemocytes were isolated at indicated time points and the nuclear extracts were prepared to perform EMSA. As shown in Figure 3.17B, upon infection, the EMSA signal increased markedly in the hemocyte nuclear extract suggesting that bacterial infection activates the NF-κB pathway.

We also examined if bacterial infection could cause the degradation of CrIκB proteins using anti-CrIκB antibodies. After infection, the hemocytes were isolated at indicated time points and the protein extracts were prepared to perform Western blot. As shown in Figure 3.18, the CrIκB protein was rapidly degraded upon *P. aeruginosa* infection providing further support to our suggestion that bacterial infection can activate the CrNFκB signaling pathway.

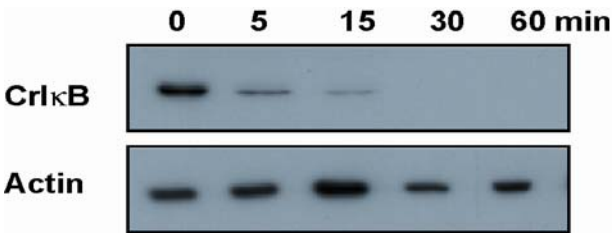

Figure 3.18: Degradation of CrIκB after bacterial infection. Hemocyte extracts were prepared from naïve and infected animals according to Materials and Methods. Western blots show proteins extracted from hemocytes over time (min) of infection. Equal protein loading and transfer was verified using *Limulus* actin as a control.

We next examined the subcellular localization of CrNFκB and CrIκB in the hemocytes upon bacterial challenge. The cytoplasmic CrNFκB in the naïve hemocytes was enriched in the nucleus 30 min after bacterial infection (Figure 3.19) indicating the activation of CrNFκB. Although, the CrIκB remained in the cytoplasm with or without bacterial challenge, its intensity decreased significantly upon infection (Figure 3.19). This is in agreement with the Western blot (Figure 3.18); which further lends support that bacteria infection activates the CrNFκB signaling pathway.

We also noticed that, in the overexpressed S2 cells, the CrNFκB was evenly distributed in the cytoplasm and nucleus (Figure 3.15); however the endogenous CrNFκB was exclusively located at the cytoplasm (Figure 3.19). The overexpression may be responsible for the discrepancy, in which the endogenous IκB protein is insufficient to capture all of the CrNFκB in the cytoplasm. Accordingly, coexpression of CrNFκB with CrIκB sequesters all of the CrNFκB in the cytoplasm.

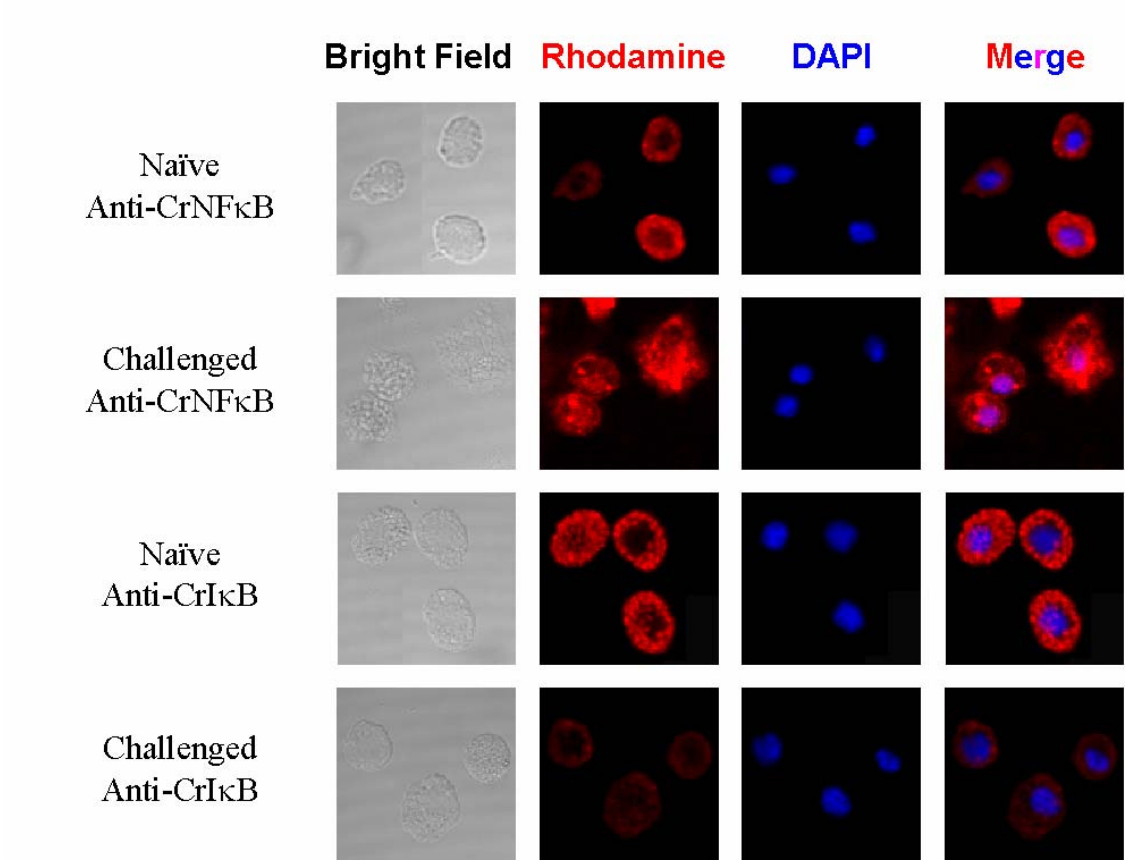

Figure 3.19: Localization of CrNFκB and CrIκB in horseshoe crab hemocytes. Hemocytes from naïve horseshoe crab or 30 min challenged with *P. aeruginosa* were collected into 3 % saline at 42 °C. The diluted hemocytes were spread on pyrogen free cover slip for cell attachment and stained with anti-CrNFκB and CrIκB antibodies. Confocol microscopy showed that the CrNFκB and CrIκB exclusively distributed in the cytoplasm in the naïve hemocytes. The CrNFκB was enriched in the nucleus after bacterial infection. The CrIκB protein significantly decreased 30 min after infection. All the images of CrIκB were taken under the identical parameters.

In order to determine the expression pattern of CrNFκB and CrIκB upon *P. aeruginosa* infection, RT-PCR was performed with total RNA from hemocytes collected at indicated time points post challenge (hpi). CrNFκB and CrIκB mRNA expression were normalized against actin-11 gene for each time point. As shown in Figure 3.20, the RT-PCR results indicated that CrNFκB mRNA was constitutively expressed in the hemocytes and remained unchanged throughout the course of infection. In contrast to CrNFκB, the expression of CrIκB was significantly induced after bacterial challenge (Figure 3.20). This is consistent with studies on *Drosophila* and humans in which activation of the NF-κB pathway increases the expression of IκB and negatively autoregulates the NF-κB activity (Ghosh *et al*, 1998). In comparison, CrFC exhibited a slight up-regulation over the same time frame as CrIκB, suggesting that both CrIκB and CrFC are NF-κB-responsive genes (Figure 3.20).

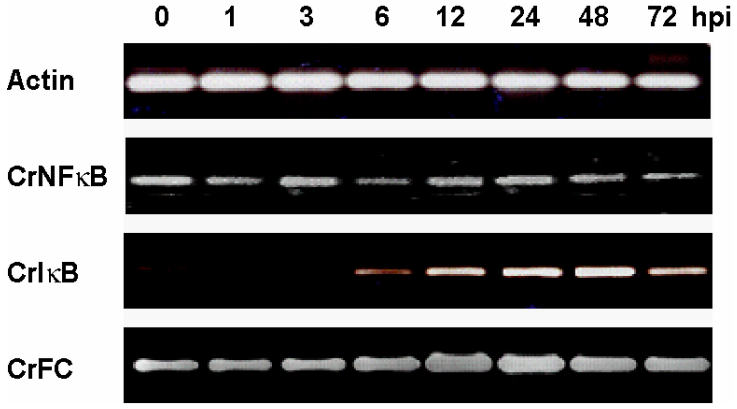

Figure 3.20: Expression of CrNFκB, CrIκB and CrFC. The hemocytes were collected from adult horseshoe crab 1-72 h post-infection (hpi) with *P. aeruginosa*. The mRNA was reverse transcribed as described in "Materials and Methods". The cDNA was used as template for PCR analysis with specific primers. The horseshoe crab actin-11 gene was analyzed under the same conditions as the internal control.

To examine whether the expression of CrIκB is indeed affected by NF-κB pathway, we studied the effect of NF-κB specific inhibitors on the up-regulation of CrIκB. Two different types of NF-κB inhibitors, MG-132 and helenalin were used in this experiment. MG-132 is a proteasome inhibitor which will block the degradation of IκB proteins (Gao *et al*, 2000). Helenalin is a more specific inhibitor for NF-κB. It acts by alkylating the p65 subunit of NF-κB and prevents its DNA-binding (Lyss *et al*, 1998). As shown in Figure 3.21A, the injection of DMSO (vehicle) did not affect the activation of CrIκB during infection, whereas treatment with two unrelated NF-κB specific inhibitors, helenalin or MG-132, prior to infection consistently suppressed the up-regulation of CrIκB. This indicates a possible role of NF-κB pathway in the regulation of CrIκB expression *in vivo*.

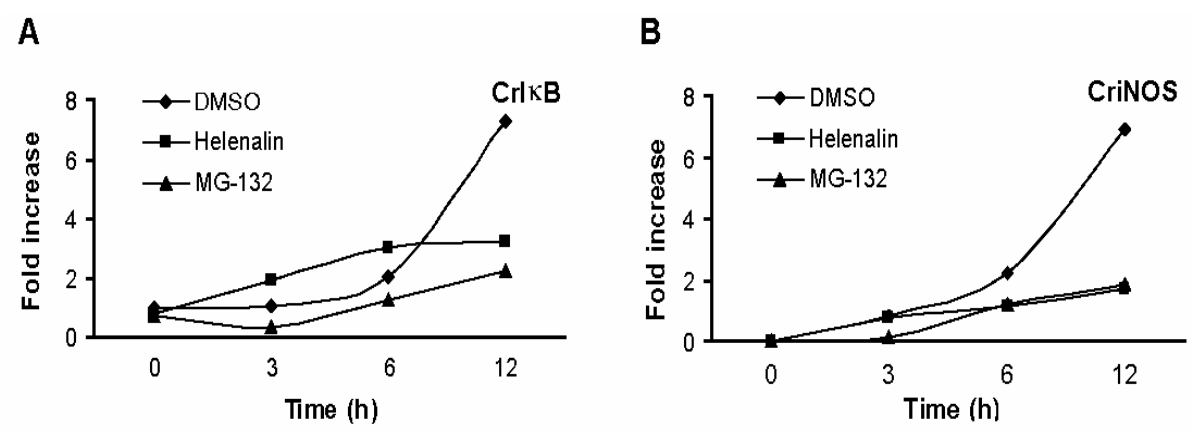

Figure 3.21: Involvement of NF-κB signaling pathway in the transcription of CrIκB and CriNOS. The expression of these genes were examined in horseshoe crab hemocytes that were administered with a vehicle, DMSO (•), helenalin (■) or MG-132 (▲) before challenge with *P. aeruginosa*. One hour after treatment with DMSO, helenalin or MG-132, the horseshoe crabs were either left unstimulated (0 h) or challenged with *P. aeruginosa* and the hemocytes were collected at the indicated time points (in h). The RT-PCR products were analyzed on gels and quantified relative to the levels of *Limulus* actin-11 mRNA. Results are expressed as relative fold increase as compared to naïve control (0 h) which was set to 1 **(A)**. Without infection of *P. aeruginosa*, the expression of CriNOS was undetectable. Therefore, the expression level of CriNOS at 3 h post infection was set to 1 **(B)**.

To investigate whether NF-κB signaling also plays a role in regulating other immune–related gene transcription, we analyzed the expression of *C. rotundicauda* inducible nitric oxide synthase, CriNOS. iNOS is a classical NF-κB target gene required for a robust innate immune response both in the *Drosophila* and vertebrates (Bogdan, 2001; Foley and O'Farrell, 2003). The iNOS activity has been detected in horseshoe crab hemocytes and it has been shown to regulate the aggregation of hemocytes (Radomski *et al*, 1991). As shown in Figure 3.21B, the expression of CriNOS was significantly induced after infection by *P. aeruginosa*. When cells were treated with the NF-κB specific inhibitors, there was negligible increase of CriNOS mRNA clearly showing that NF-κB inhibitors blocked the increase of CriNOS gene transcription (Figure 3.21B). It suggests that, like the iNOS in the vertebrates (Lin *et al*, 1996), the expression of horseshoe crab iNOS mRNA is probably under the control of NF-κB signaling pathway.

Next, we analyzed the expression of horseshoe crab coagulogen and CrC3, a functional homologue of vertebrate complement 3 (Zhu *et al*, 2005), with or without NF-κB inhibitors. The observation that the expression levels of coagulogen and CrC3 remained unchanged during the bacterial challenge with or without NF-κB inhibitors (Figure 3.22A & B) suggests that they are probably not target genes of CrNFκB and that these NF-κB inhibitors do not exert a non-specific global effect on gene transcription. To further demonstrate that the NF-κB inhibitors only affect NF-κB pathway, we analyzed the expression of transglutaminase, which has been shown to be under the control of Sp1 and CREB/AP-1 in the vertebrate (Medvedev *et al*, 1999). Indeed, injection of NF-κB inhibitors did not affect the activation of transglutaminase transcription upon infection (Figure 3.22C).

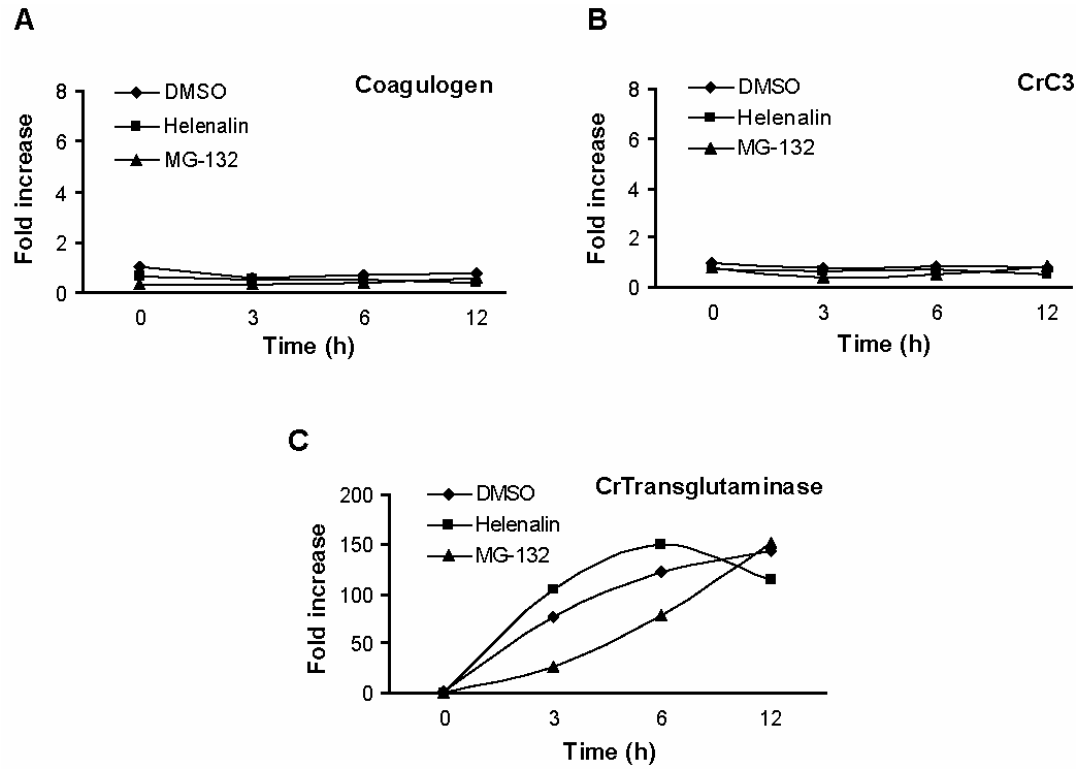

Figure 3.22: The effects of NF-κB inhibitors on the transcription of horseshoe crab coagulogen, CrC3 and transglutaminase. The expression of these genes were examined in horseshoe crab hemocytes that were administered with a vehicle, DMSO (•), helenalin (■) or MG-132 (▲) before challenge with *P. aeruginosa*. The RT-PCR products were analyzed on gels and quantified relative to the levels of *Limulus* actin-11 mRNA. Results are expressed as relative fold increase as compared to naïve control (0 h) which was set to 1.

Taken together, in this part of the thesis, we have revealed the presence of a primitive but functional CrNFκB/CrIκB signaling cascade and demonstrated its relevance to the immune defense of the horseshoe crab, *C. rotundicauda*. We showed that the CrNFκB and CrIκB displayed similar signature motifs found in the vertebrate orthologues, despite the huge evolutionary distance between horseshoe crab and vertebrates. The functional studies indicate that the NF-κB activation pathway of

horseshoe crab is functionally comparable to that of the *Drosophila* and mammals, suggesting that the roles of NF-κB and its natural inhibitor IκB have co-evolved and remained conserved through evolution. Its ubiquitous regulatory role over many downstream immune response genes studied strongly suggests the global function of horseshoe crab NF-κB signaling pathway in infection and immunity. In conclusion, although incomplete and non-functional in the *C. elegans*, the NF-κB/IκB signaling pathway has co-evolved and remained well-conserved from horseshoe crab to human, playing an archaic but crucial and fundamentally role in innate immune response to regulate the expression of critical immune defense molecules.

3.5 Isolation and sequence analysis of the horseshoe crab TRX

The development of high-throughput methods of gene identification by EST analysis has become a commonly used approach to identify genes involved in specific biological functions. This is especially so in organisms where genome data is unavailable or limited (Aaronson *et al*, 1996) and has accelerated the pace at which new immune functions can be discovered. Recently, our lab has used the subtractive cDNA hybridization approach, to isolate and identify differentially expressed genes from the horseshoe crab, *C. rotundicauda*, in response to *P. aeruginosa* infection (Ding *et al*, 2005). Using this approach, we identified one cDNA clone that was differentially expressed in the hepatopancreas (equivalent to liver in mammals) when stimulated with *P. aeruginosa*. Sequence analysis revealed that this gene encodes a protein possessing the characteristic organization of TRX proteins, henceforth referred to as *C. rotundicauda* TRX, Cr-TRX1 (Wang *et al*, 2007).

Thioredoxin (TRX), which functions as a general protein-disulfide reductase, is commonly known to be a small ubiquitous protein of 12 kDa. Up to now, no TRX protein has been identified in the horseshoe crab and the function of TRX proteins in this ancient species is still unknown. Previously, it has been shown that the human 12 kDa TRX1 enhances the DNA-binding of NF-κB by directly reducing the cysteine groups in the DNA-binding motif of NF-κB (Figure 1.7). Therefore, it is interesting to examine if the horseshoe crab TRX functions as an NF-κB regulator in this "living fossil". In order to understand the ancient functions of TRX in the horseshoe crab anti-oxidant system and

NF-κB signaling pathway, we decided to first examine the biochemical characteristics of the Cr-TRX1 followed by investigating its roles in regulating the NF-κB signaling pathway.

3.5.1 Sequence analysis of Cr-TRX1

Sequence analysis showed that the complete sequence of the Cr-TRX1 cDNA encompasses an ORF of 429 bp, a 5'-UTR of 40 bp and a 3'-UTR of 353 bp upstream of the poly A tail. The deduced sequence of Cr-TRX1 encodes a protein of 143 residues with a predicted molecular mass of 16 kDa and predicted pI of 5.2. The overall similarity to other 12 kDa TRXs from mammalian, insect and bacterial species were approximately 18 % suggesting that the 16 kDa and 12 kDa TRX molecules have diverged early during evolution (Figure 3.23). A majority of this homology is clustered in the region surrounding the respective active sites which are involved in the interaction with substrates (Figure 3.23). Compared with the 12 kDa TRXs, the Cr-TRX1 is about 35 residues longer. The sequence alignment shows that most of the additional residues appear as an insertion downstream of the active site (Figure 3.23, black line). The classical 12 kDa TRXs are characterized by a conserved WCGPC motif in the active site, which is clearly different from the WCPPC motif in the 16 kDa Cr-TRX1 (Figure 3.23).

Hitherto, two clusters of 16 kDa TRXs have been identified from the nematodes and the trypanosomes (Kunchithapautham *et al*, 2003; Ludemann *et al*, 1998), which also contain the putative WCPPC active site, and these sequences are 42 % and 25 % identical respectively, to Cr-TRX1 (Figure 3.24). Interestingly, except for the 16 kDa TRXs found in the nematodes and trypanosomes, several other 16 kDa TRXs containing WCPPC

active site can be identified from the zebrafish, pufferfish and frog (Figure 3.25). However, a search of the fully sequenced genomes of the *Drosophila* and mosquito showed that such a 16 kDa TRX is absent in these arthropods. This provides further support to the notion that antioxidant defense in insects differs fundamentally from that in other organisms (Kanzok *et al*, 2001). Furthermore, the Cr-TRX1 also shows high homology (18 % to 29 %) to protein disulfide isomerases (PDI) from several plants, which also contain the WCPPC active site sequences (Figure 3.25).

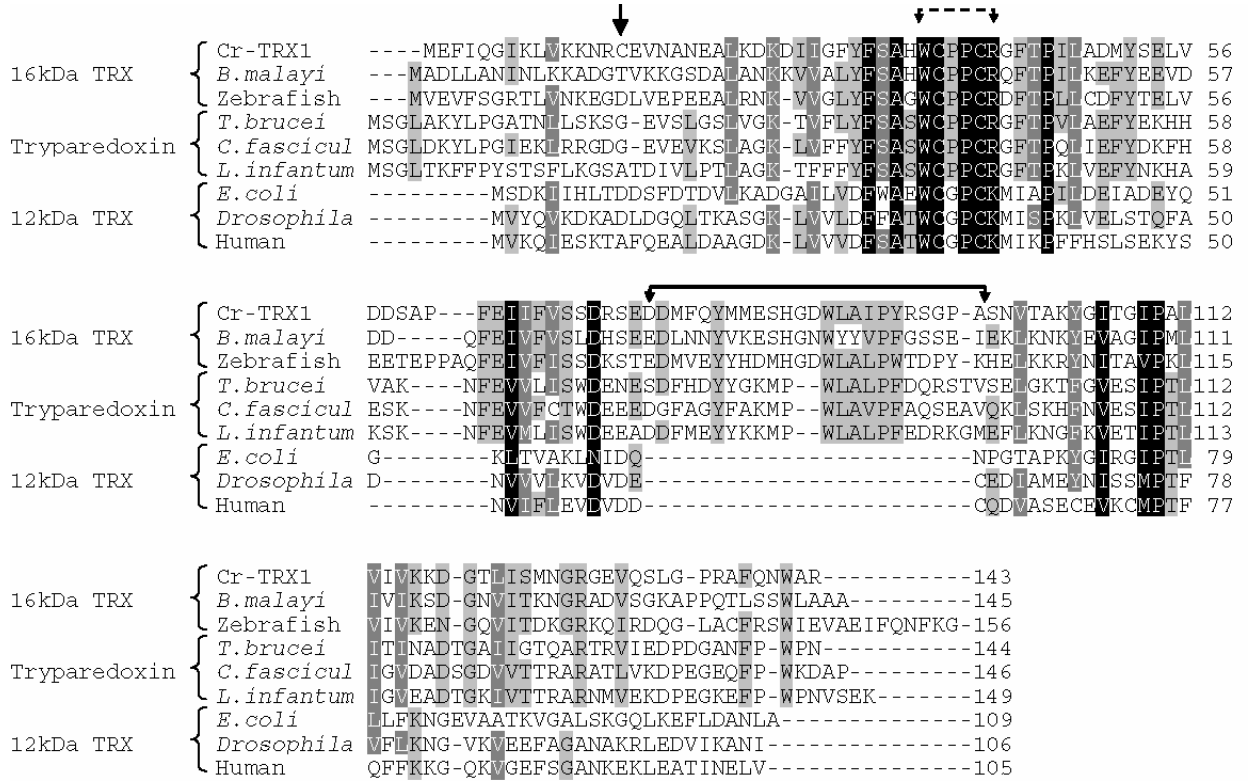

Figure 3.23: Amino acid sequence comparison between Cr-TRX1 and the 16 kDa TRX, Tryparedoxin and 12 kDa TRX. Alignments were done by Clustal X. The active sites are demarcated by a dashed line. The extra sequence of 16 kDa TRX is indicated by a black line. The additional C-terminal Cys residue of Cr-TRX1 is marked by a big arrow. Residues highlighted in black box are invariant for all of the sequences tested. The GenBank accession numbers of the sequences used in this study are listed in Table 3.3.

A phylogenetic analysis demonstrates that Cr-TRX1 clustered amongst the 16 kDa TRX proteins (Figure 3.25). This cluster differs from the common 12 kDa TRX and the 16 kDa Tryparedoxin from parasitic trypanosomes. The phylogenetic analysis clearly shows that the 16 kDa Cr-TRX1 shares a common ancestor with the nematode 16 kDa TRX which is consistent with their high sequence similarity. This observation suggests that the 16 kDa TRXs has evolutionarily diverged from the 12 kDa TRXs at an early stage.

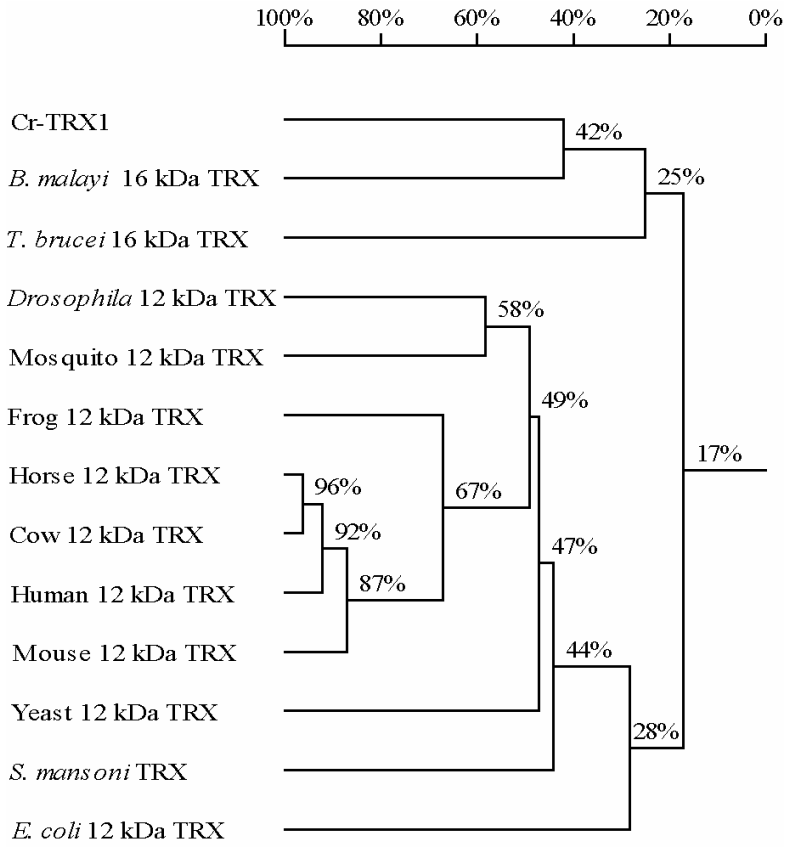

Figure 3.24: The homology analysis of Cr-TRX1 and related TRX proteins. The homology tree was produced with DNAMAN. The sequence homology (in %) of TRX proteins are indicated at the branching nodes. GenBank accession numbers of the sequences are listed in Table 3.3.

Table 3.3: The sequences used for phylogenetic analysis of the Cr-TRX1 and TRX6 proteins

16 kDa TRX		
Name	**Accession Number**	**Organism**
Cr-TRX1	DQ489712	*Carcinoscorpius rotundicauda*
B. malayi	AY117545	*Brugia malayi*
C. elegans	AAB37590	*Caenorhabditis elegans*
Roundworm	AAS78778	*Ascaris suum*
Frog	AAH71162	*Xenopus laevis*
Zebrafish	AAH86727	*Danio rerio*
Pufferfish	CAF97179	*Tetraodon nigroviridis*
Mouse	NP_083449	*Mus musculus*
Human	CAH71401	*Homo sapiens*
Tryparedoxin (16 kDa)		
T. brucei	AJ006403	*Trypanosoma brucei*
C. fascicul	AAD20445	*Crithidia fasciculata*
L. infantum	AAS48351	*Leishmania infantum*
24 kDa TRX (TRX6)		
Zebrafish	XP_696316	*Danio rerio*
Frog	AAH80091	*Xenopus laevis*
Dog	XM_541952	*Canis familiaris*
Mouse	NP_663573	*Mus musculus*
Human	BC014127	*Homo sapiens*
12 kDa TRX		
E. coli	P00274	*Escherichia coli*
Yeast	TXBY1	*Saccharomyces cerevisiae*
Drosophila	AF220362	*Drosophila melanogaster*
Mosquito	AAK70900	*Aedes aegypti*
Zebrafish	AAH49031	*Danio rerio*
Frog	AAH72884	*Xenopus laevis*
Mouse	X77585	*Mus musculus*
Human	JH0568	*Homo sapiens*
Plant protein disulfide isomerase (PDI)-like proteins		
Z. mays	AAD04231	*Zea mays*
Muskmelon	AAU04766	*Cucumis melo*
Oak	CAC87937	*Quercus suber*
A. thaliana	AAM64945	*Arabidopsis thaliana*

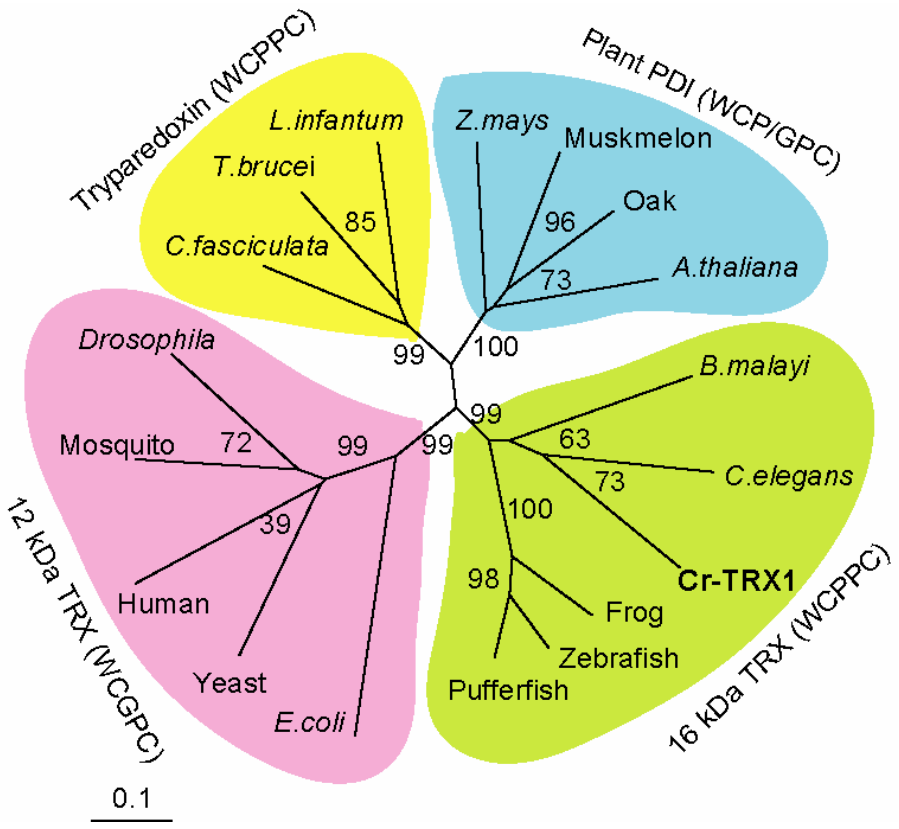

Figure 3.25: Phylogeny of Cr-TRX1 and related TRX proteins. Multiple sequence alignments were produced with Clustal X using Gonnet series protein weight matrix. An unrooted phylogenetic tree was constructed using neighbor-joining method based on the alignments. The confidence scores (in %) of a bootstrap test of 1000 replicates are indicated for major branching nodes. GenBank accession numbers of the sequences are listed in Table 3.3.

3.5.2 Bacterial expression and purification of recombinant Cr-TRX1

To obtain large quantities of pure Cr-TRX1 protein for functional studies, the full-length Cr-TRX1 was cloned into the pGEX-4T-1 plasmid for bacterial expression of GST fusion protein. The cell extract from *E. coli* transformed with pGEX-TRX and induced with IPTG showed a major protein band of 42 kDa in the SDS-PAGE analysis. The molecular weight of this protein agreed well with that predicted for the fusion protein

indicating that the GST-Cr-TRX1 fusion protein was successfully expressed. The cell-free extract containing the fusion proteins was loaded onto a glutathione-Sepharose 4B column and the bound fusion protein was eluted from the matrix with glutathione buffer. The purified fusion protein was analyzed with SDS-PAGE. As shown in Figure 3.26 (lane 1), the GST-Cr-TRX1 fusion protein was purified satisfactorily. To obtain the Cr-TRX1 protein without the GST tag, we digested the fusion protein on the column with thrombin. The eluted Cr-TRX1 was then extensively dialyzed against PBS and analyzed by SDS-PAGE (Figure 3.26, lanes 2-4). The results suggest that the recombinant Cr-TRX1 has been purified successfully and the purified protein was suitable for functional studies.

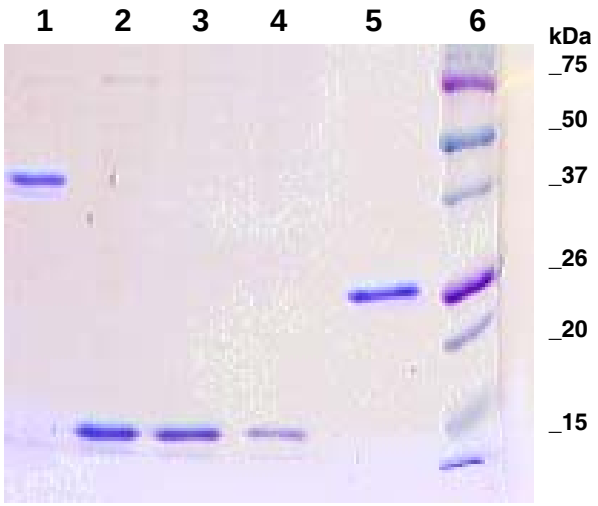

Figure 3.26: SDS-PAGE analysis of purified GST-Cr-TRX1 and Cr-TRX1 protein. Lane 1: purifed GST-Cr-TRX1 protein. Lanes 2-4: Different amounts of purified Cr-TRX1 after digestion with thrombin. Recombinant GST protein was run as a control (lane 5). Lane 6: Protein marker.

3.5.3 The CPPC motif of Cr-TRX1 is the redox-active site

In addition to the two conserved cysteines in the active site, mammalian TRXs have three conserved cysteines at their C-terminus. Those Cys residues may impart unique biological properties to the mammalian 12 kDa TRXs (Holmgren, 1985). The crystal structure also revealed that human TRX1 can form a dimer via the Cys^{73} at the C-terminus (Weichsel *et al*, 1996). However all of these conserved Cys residues are absent from the bacterial TRXs and the 16 kDa TRX proteins in *C. elegans* and the parasite trypanosomes (Figure 3.27). Similar to these 16 kDa TRXs, the Cr-TRX1 also does not contain the extra C-terminal cysteines.

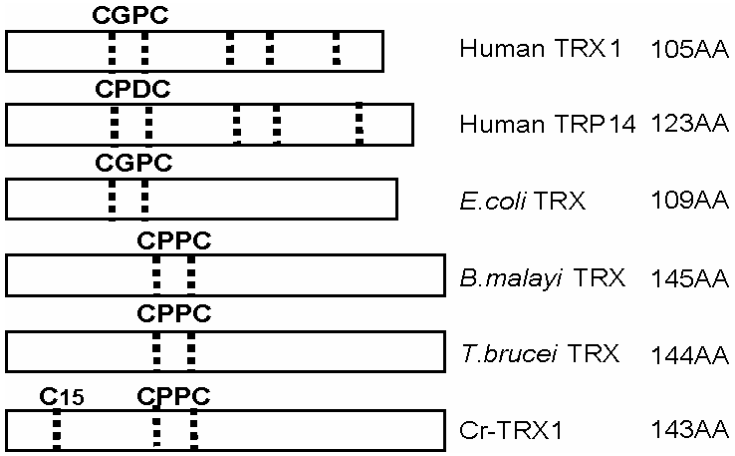

Figure 3.27 Comparison of CXXC motif, numbers and positions of cysteine residues in various TRXs. The Cys residues are indicated by dashed lines. The sequences of catalytic motif are indicated as well. TRP14: human 14 kDa TRX-related protein. The GenBank accession numbers of the sequences used in this analysis are listed in Table 3.3.

Interestingly, in addition to the conserved Cys^{38} and Cys^{41}, the Cr-TRX1 contains 1 extra Cys residues (Cys^{15}) at the N-terminus (Figure 3.23, big arrow & Figure 3.27). To our knowledge, Cr-TRX1 is the first 16 kDa TRX reported to contain an extra Cys at the N-terminus of the active site (Figure 3.27). Therefore, it is important to identify which Cys residue is redox sensitive in Cr-TRX1. To achieve this, we firstly determined the number of active Cys residues in Cr-TRX1 molecule using mass spectrometry. It has been demonstrated that the free SH groups in TRX can be modified with iodoacetamide, IAM, however the IAM dose not react with the cysteines that are engaged in the disulfide bond. Therefore, the number of free Cys can be deduced from the molecular weight change before and after treatment with IAM (Gommel *et al*, 1997).

To determine the number of active Cys residues, we treated oxidized and reduced Cr-TRX1 with IAM and compared their molecular masses by MALDI-TOF mass spectrum. As shown in Figure 3.28, the molecular mass of the oxidized Cr-TRX1 was not changed on exposure to IAM suggesting none of the three Cys residue is active in the oxidized Cr-TRX1. However the molecular mass of the reduced form of Cr-TRX1 was increased from 16,209 Da to 16,323 Da after adding IAM. The molecular mass difference (114 Da) precisely corresponds to the addition of two carboxyamidomethyl residues (57 Da) indicating that only two Cys can be reduced by DTT and modified by IAM and the remaining one Cys residues remained unmodified. These results indicate that the DTT can reduce the disulfide bond of the oxidized Cr-TRX1 which is comparable to the observations in human and bacterial homologues (Holmgren, 1985; Powis and Montfort, 2001).

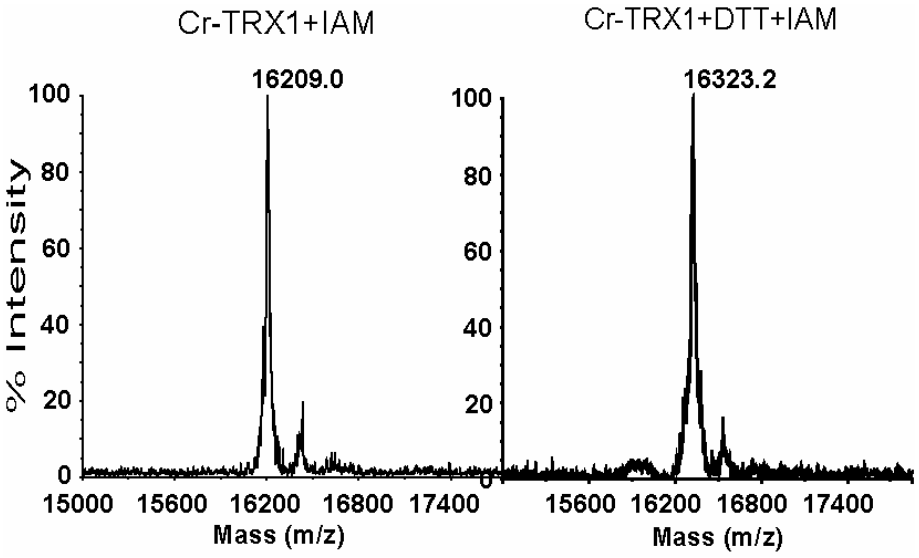

Figure 3.28: Identification of the number of active Cys in Cr-TRX1 by MALDI-TOF. The mass increment (114 Da) shown in oxidized Cr-TRX1 (left) and reduced Cr-TRX1 (right), which are derivatized with iodoacetamide (IAM) correspond to the addition of two caboxyamidomethyl groups (57 Da). The molecular mass difference (114 Da) precisely corresponds to the addition of two carboxyamidomethyl residues (57 Da) indicating that two Cys residues can be reduced by DTT and modified by IAM.

To investigate which of the Cys residues are redox sensitive, the unmodified and modified Cr-TRX1(s) were digested by trypsin and the digested peptides were analyzed using mass spectrum. From the mass differences of the peptides, we can determine which peptide is modified by IAM and deduce the position of active cysteines. As shown in Figure 3.29, both the unmodified and modified samples showed characteristic peaks of Cr-TRX1. However, the IAM-modified sample contained 2 additional peaks with molecular masses of 2,027 and 2,270 Da, respectively, which are absent from the list of trypsin-digested peaks (Table 3.4). Further examination revealed that these two peaks corresponded to the peptides 25-42 and 27-42, in which the two Cys residues have been

modified by IAM (Table 3.4) suggesting that the two Cys residues in the active motif WCPPCR are redox active and can be modified by IAM. The formation of the peptide 25-42 is probably due to the missing cleavage by the trypsin at Lys[26].

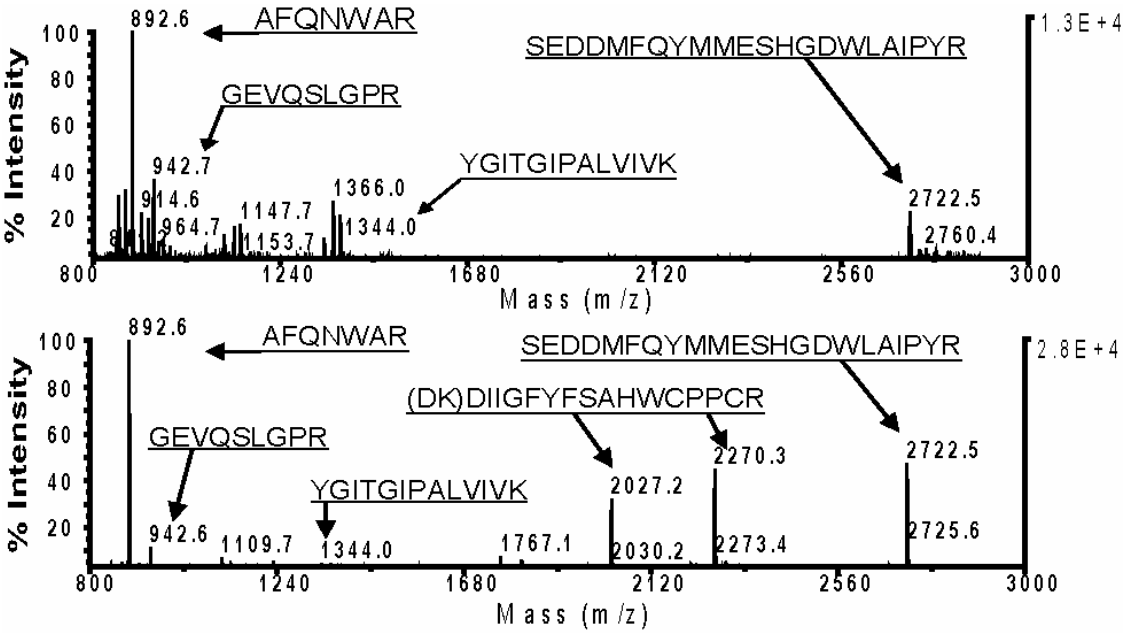

Figure 3.29: MALDI-TOF analysis of peptides generated by trypsin from IAM-labeled Cr-TRX1. Oxidized (top panel) and reduced (lower panel) forms of Cr-TRX1 were labeled with IAM and digested before mass spectrometry. The two additional peaks in lower panel corresponded to the peptides 25-42 and 27-42, with the two Cys residues modified by IAM. Compared to peak 2027.2, peak 2270.3 contains two additional amino acids (DK) because of one missed cleavage.

Further confirmation was obtained from the MS/MS sequencing spectrum. The results clearly showed that both peptide sequences of 25-42 and 27-42 fit unambiguously with the active site containing peptide (DKDIIGFYFSAHWCPPCR) and the two Cys residues were modified by IAM (Figure 3.30). Taken together, these results confirmed that the conserved Cys residues in the active site of Cr-TRX1 are redox active.

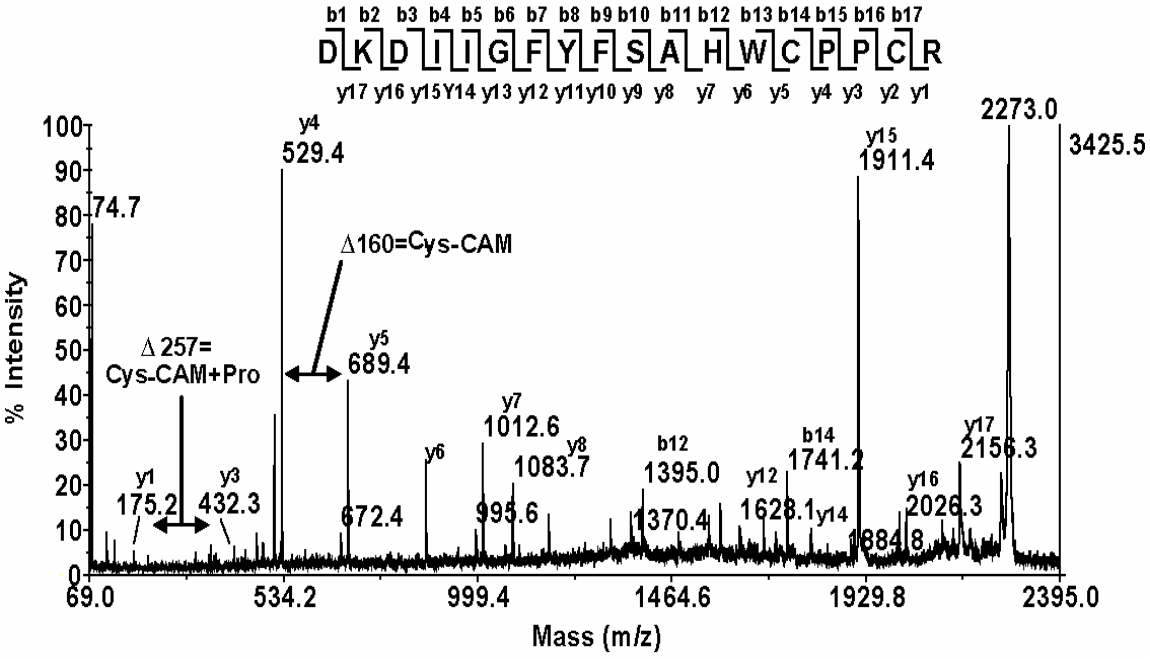

Figure 3.30: Identification the position of active Cys residues by MS/MS sequencing. The amino acid sequence of the peptide could be deduced from two complementary series of N-terminal and C-terminal fragment ions, respectively. The mass difference between the ions y4 and y5 is 160 Da which is almost exactly the molecular weight of Cys with the modification of IAM. Cys_CAM: carbamidomethyl-cysteine. Although the y2 ion cannot be identified, the mass difference between y1 and y3 ions (257 Da) is just the molecular weight of IAM-modified Cys plus Pro (Cys_CAM+Pro) indicating that the Cys[38] was modified by IAM as well.

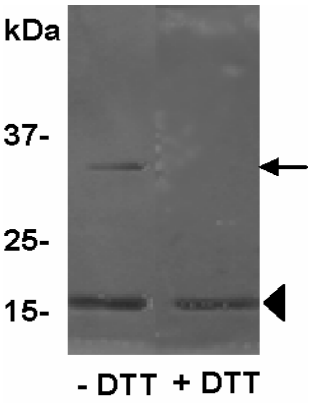

Figure 3.31: SDS-PAGE electrophoretic analysis of Cr-TRX1 in non-reducing (-DTT) and reducing (+DTT) conditions. The dimer formed in non-reducing condition is indicated by an arrow. The Cr-TRX1 monomer is indicated by an arrowhead.

Table 3.4: The list of trypsin digestion peaks of Cr-TRX1

mass	position	#MC	modification(s)	peptide sequence
966.1829	1-8	0		MEFIQGIK
1091.2238	15-24	0	Cys_CAM*: 15 1148.2750	CEVNANEALK
1913.2210	27-42	0	Cys_CAM: 38, 41 2027.3250	DIIGFYFSAHWCPPCR
2156.4837	25-42	1	Cys_CAM: 38, 41 2270.5877	DKDIIGFYFSAHWCPPCR
3236.6170	43-71	0		GFTPILADMYSELVDDSAPF EIIFVSSDR
2723.0210	72-93	0		SEDDMFQYMMESHGDWLAIPYR
932.0209	94-103	0		SGPASNVTAK
1344.6800	104-116	0		YGITGIPALVIVK
1064.2011	118-127	0		DGTLISMNGR
943.0471	128-136	0		GEVQSLGPR
892.9921	137-143	0		AFQNWAR

The list of trypsin digestion peaks of Cr-TRX1 was predicted with PeptideMass of ExPASy at http://kr.expasy.org/tools/peptide-mass.html using average masses of the occurring amino acid residues and giving peptide masses as $[M+H]^+$. The two cysteines containing peptides which can be modified by iodoacetamide (IAM) were underlined. *Cys_CAM: cysteines have been treated with iodoacetamide to form carbamidomethyl-cysteine. #MC: number of missed cleavages.

It has been reported that the 12 kDa human TRX1 forms covalently linked homodimers in solution through intermolecular disulfide bonding via Cys^{73} (Powis and Montfort, 2001). Interestingly, although it lacks the C-terminal extra Cys residue, the 16 kDa Cr-TRX1 molecule could also form a stable dimer, yielding a molecular mass of 32 kDa (Figure 3.31). To confirm the identity of the 32 kDa band, we performed the mass spectrum analysis. As shown in Figure 3.32, the identity of the 32 kDa Cr-TRX1 dimer

was confirmed by mass spectrometry. It is still unclear if such dimer also exists under physiological conditions, and therefore, the role of the extra Cys in the dimer formation needs further examination. Further mutation and structure studies would be useful to define the function of the extra N-terminal Cys residue.

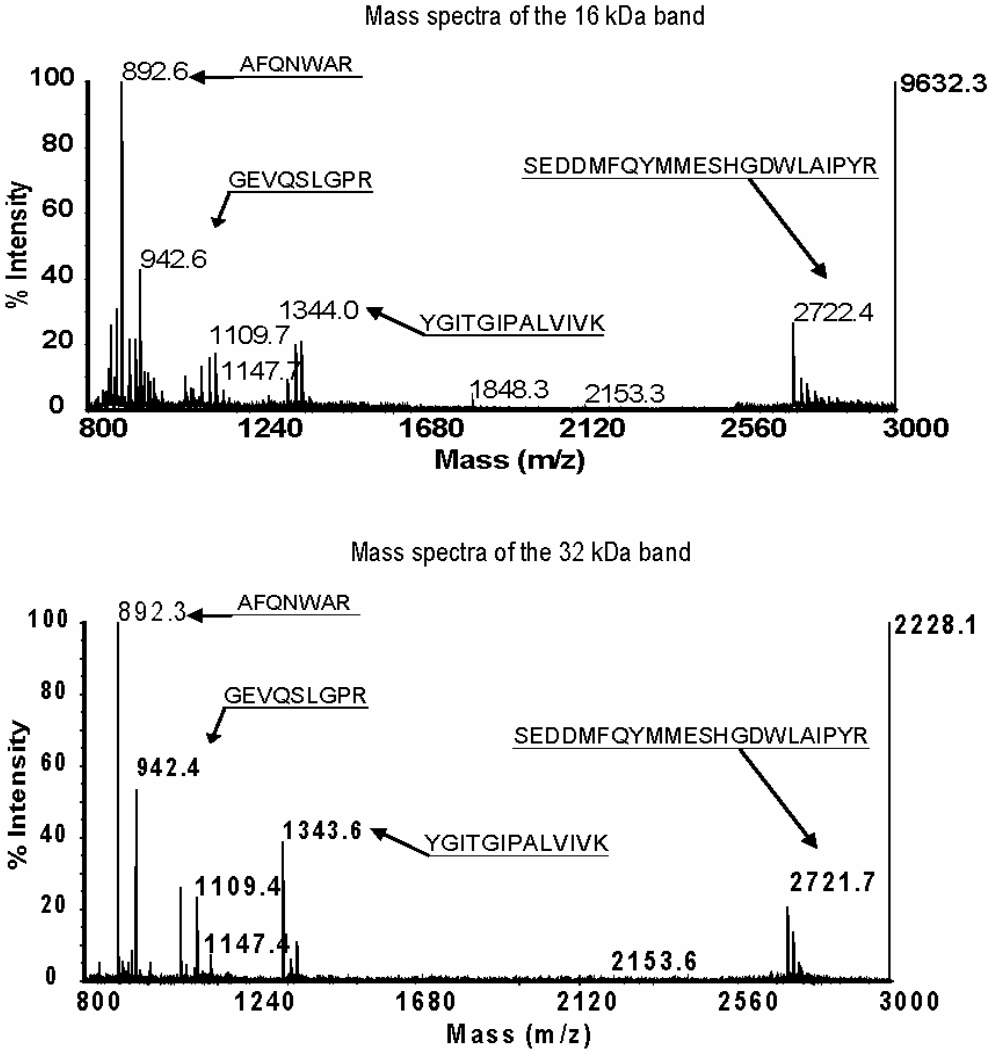

Figure 3.32: MALDI-TOF Mass Spectrum of 16 kDa and 32 kDa bands of Cr-TRX1. The purified Cr-TRX1 was run in SDS-PAGE in non-reducing (-DTT) condition. As shown in Figure 3.26, the 16 kDa (upper panel) and 32 kDa bands (lower panel) were cut out and digested with trypsin prior to MALDI-TOF analysis. The fingerprints of the two bands suggest that both of them are Cr-TRX1.

3.6 Biochemical characterization of Cr-TRX1

3.6.1 The spectral properties of Cr-TRX1

It has been demonstrated previously that the classic 12 kDa TRX from the *E. coli* shows a 3.5-fold increase in fluorescence intensity upon reduction of the active site Cys residue(s) due to the quenching effect of the active site disulfide bond on the fluorescence of two adjacent Trp (W) residues, Trp^{26} and Trp^{28} (Windle *et al*, 2000). Here, we found that the 16 kDa Cr-TRX1 also contains a Trp residue in the active site motif, WCPPC, although it lacks the Trp^{26} residue that is found in the *E. coli* TRX (Figure 3.23). To confirm whether the 16 kDa Cr-TRX1 displays a similar intrinsic fluorescence characteristic, the recombinant Cr-TRX1 was reduced by 1 mM DTT. The reduction of Cr-TRX1 resulted in a 2-fold increase in the Trp fluorescence intensity at 340 nm (Figure 3.33), suggesting changes in the microenvironment around the Trp residue juxtaposing the CXXC active site. The slightly lower increase in fluorescence intensity (2-fold) compared with that of *E. coli* TRX (3.5-fold) may be attributable to the absence of Trp^{26} in Cr-TRX1.

3.6.2 Insulin reduction activity of Cr-TRX1

The interchain disulfide bonds of insulin are substrates of thioredoxin. Reduction of the disulfide linkage releases the A and B chains of insulin, the latter of which precipitates. Therefore, the insulin reduction can be measured turbidometrically due to the precipitation of the free insulin B chain (Kunchithapautham *et al*, 2003). To investigate the activity of Cr-TRX1 in catalyzing the reduction of insulin, we compared the rates of insulin reduction by DTT in the presence and absence of Cr-TRX1 and *E. coli*

TRX. In the reactions containing only DTT or DTT plus 5 μM recombinant GST, measurable precipitation was observed through 30 min. With the addition of Cr-TRX1 or *E. coli* TRX, precipitates were detected within 5 min indicating that both TRXs have the disulfide reductase activities targetting insulin as a substrate (Figure 3.34). Interestingly, the kinetics of disulfide reduction observed for Cr-TRX1 was approximately 2-fold more efficient at reducing insulin than the equivalent amounts of *E. coli* TRX (Figure 3.34). In addition, the initial rate of insulin reduction was greater with Cr-TRX1. These observed redox activities of Cr-TRX1 (Figure 3.34) and the differential spectral properties of reduced and oxidized Cr-TRX1 (Figure 3.33) indicate that the Cr-TRX1 is not only functional, but it appears more efficacious than the *E. coli* counterpart.

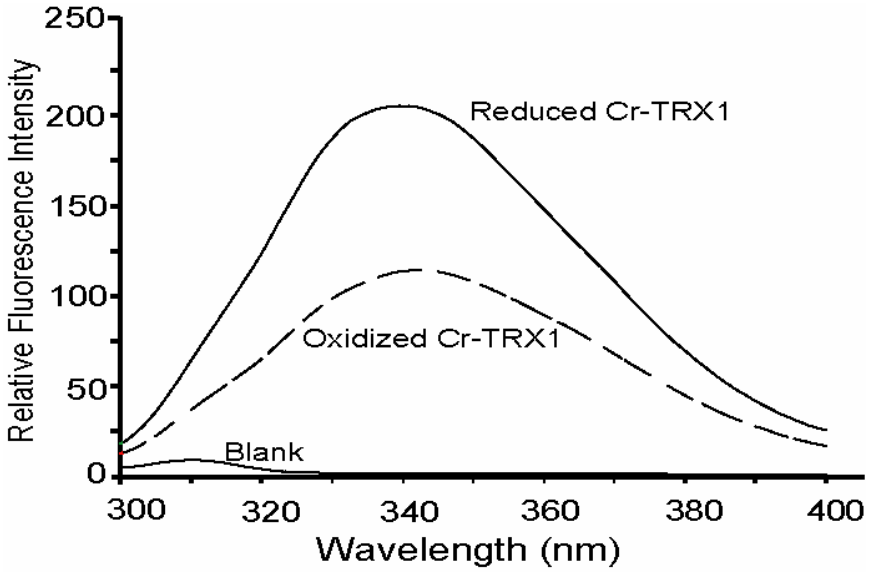

Figure 3.33: Fluorescence emission spectra of reduced and oxidized Cr-TRX1. Reduction of oxidized Cr-TRX1 was achieved by addition of DTT to a final concentration 1 mM. The Tris solution without Cr-TRX1 was run as control (blank).

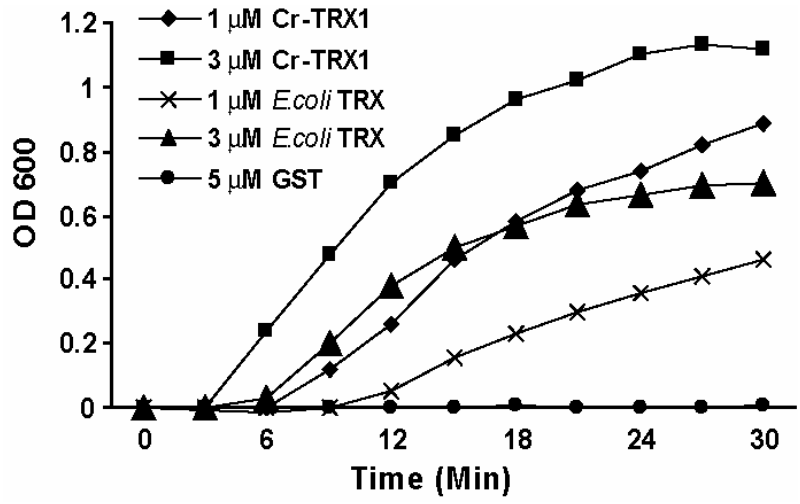

Figure 3.34: Reduction of insulin by recombinant Cr-TRX1. The increase in turbidity measured at OD_{600} nm was plotted against reaction time. *E. coli* TRX was used as a positive control (× and ▲). Recombinant GST was included as a negative control (•).

3.6.3 Reduction of Cr-TRX1 by mammalian thioredoxin reductase

The TRX function requires a reversible change in the redox status of the CXXC motif, and the reduction of oxidized TRX molecules is catalyzed by the NADPH-dependent enzyme, TRX reductase (TRXR). To test the cross-species (cross-phylum in this case) functionality of Cr-TRX1, we examined whether oxidized Cr-TRX1 can be reduced by rat TRXR in the presence of NADPH, by monitoring NADPH oxidation at 340 nm. As shown in Figure 3.35, the oxidized Cr-TRX1 was reduced by the rat TRXR and the reduction rate was slightly faster than that of the oxidized *E. coli* TRX, suggesting the 16 kDa Cr-TRX1 is functionally conserved with the classical 12 kDa TRX. As negative controls, the recombinant GST and commercial BSA cannot be reduce by the rat TRX reductase.

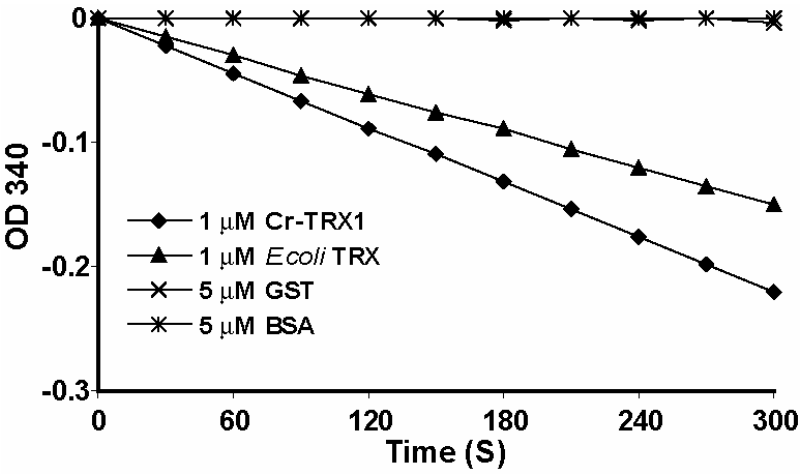

Figure 3.35: Reduction of Cr-TRX1 by rat TRX reductase (TRXR). Reduction of Cr-TRX1 by TRXR was assayed at room temperature by monitoring A_{340} nm in the presence of GST 5 mM (×), BSA 5 mM (∗), Cr-TRX1 1 mM (•) and *E. coli* TRX 1 mM (▲).

3.6.4 The horseshoe crab thioredoxin functions as an antioxidant

Normal cellular processes that involve oxygen result in the production of reactive oxygen species (ROS) such as singlet oxygen, hydroxyl radical and hydrogen peroxide, (H_2O_2). Each of these species has the ability to oxidize macromolecules and thereby to induce mutation of DNA, impairment of protein function, and lipid peroxidation. Intracellular ROS is removed mostly by superoxide dismutase (SOD), catalase, glutathione peroxidase and peroxiredoxin (Chang *et al*, 2004). It has been suggested that TRX also plays a direct role as an antioxidant or scavenger of ROS. TRX by itself can scavenge singlet oxygen, hydroxyl radical and hydrogen peroxide, H_2O_2 (Hirota *et al*,

2002), thereby buffering the effect of the avalanche of ROS. To test whether the novel Cr-TRX1 is capable of functioning as an antioxidant to scavenge H_2O_2, the peroxidase activity assay (Jeong *et al*, 2004b) was performed using the recombinant Cr-TRX1. Indeed, Cr-TRX1 was capable of reducing H_2O_2 with an activity comparable to that of TRX from *E. coli* (Figure 3.36). Like the *E. coli* TRX, the peroxidase activity of Cr-TRX1 was also dependent on the enzyme concentration.

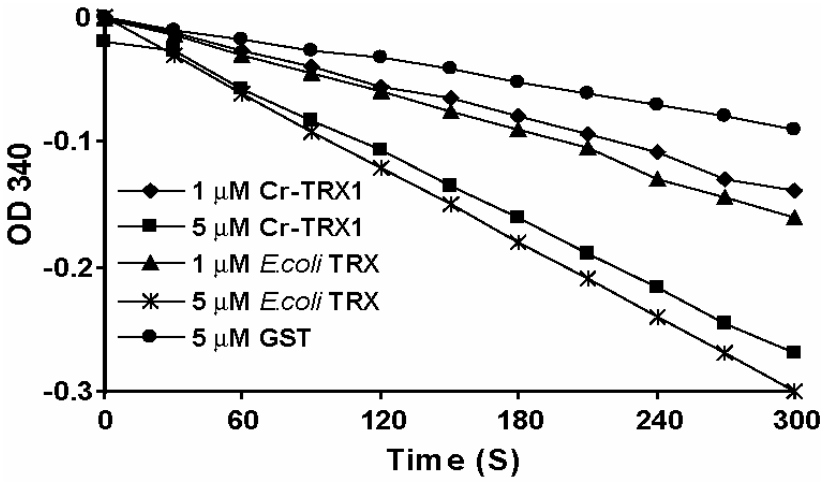

Figure 3.36: Peroxidase activities of Cr-TRX1. Peroxidase reactions were performed at 30 ℃ and monitored on the basis of A_{340}. Assay mixtures containing GST (•) served as negative controls.

To further confirm that Cr-TRX1 can function by itself as an antioxidant and protect DNA, we performed the DNA nicking assay (Kunchithapautham *et al*, 2003). The assay employed the mixed function oxidation (MFO) system that generates hydroxyl (OH-) and thiol (RS*) radicals capable of damaging a DNA template. The extent of DNA damage was evaluated by assessing the shift in gel mobility of a plasmid as it was

converted from the supercoiled to the nicked form (Kunchithapautham *et al*, 2003). In the DNA nicking assay, when the plasmid DNA was exposed to the MFO system, all of the plasmid DNA was converted to the nicked form within 60 min. The recombinant Cr-TRX1 proteins rescued the nicking reaction in a dose-dependent manner (Figure 3.37, lanes 2 to 5). As a control, GST or BSA showed no marked effect on rescuing the plasmid DNA nicking activity (Figure 3.37, lanes 6 & 7) suggesting that the protection effect was specific to Cr-TRX1 and not simply due to the presence of proteins in the reaction.

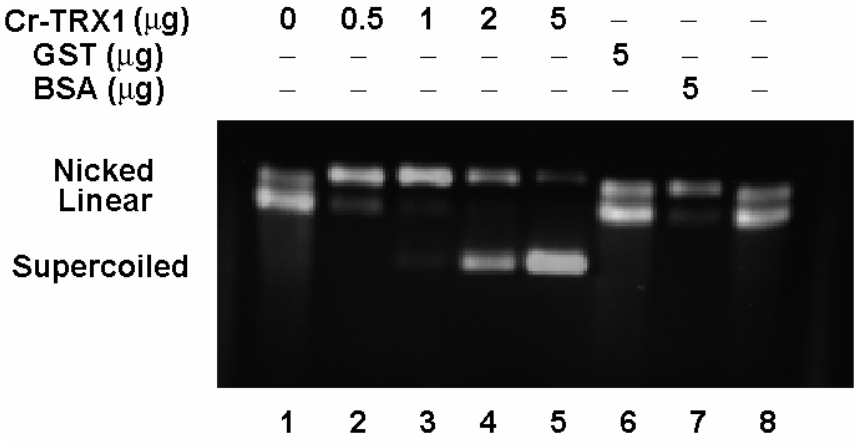

Figure 3.37: Cr-TRX1 functions as an antioxidant to protect DNA from being nicked by MFO. DNA nicking assays were performed in the MFO system with or without Cr-TRX1. The extent of protection against MFO-mediated nicking was evaluated with increasing concentrations of Cr-TRX1. Recombinant glutathione S-transferase (GST) and bovine serum albumin (BSA) were used as negative controls. The supercoiled, nicked and linearized forms of DNA are indicated.

3.7 Involvement of Cr-TRX1 in the NF-κB signaling pathway

It has been shown that the binding of NF-κB to DNA requires the NF-κB to be fully reduced especially the Cys^{62} of the NF-κB p50 subunit (Powis and Montfort, 2001). In the nucleus, the human 12 kDa TRX1 enhances the DNA-binding of NF-κB by directly reducing the cysteine groups in the DNA-binding motif of NF-κB (Figure 1.7) (Flohe *et al*, 1997; Matthews *et al*, 1992). Tumor necrosis factor α (TNFα) was one of the first receptor ligands shown to generate ROS in nonphagocytic cells and is among the ligands whose signaling pathways have been studied most extensively in relation to ROS production (Jeong *et al*, 2004a; Schreck *et al*, 1991). We therefore examined the effect of overexpression of Cr-TRX1 on TNFα-induced NF-κB activation in HeLa cells.

3.7.1 Cr-TRX1 activates NF-κB in HeLa cells

As shown in Figure 3.38, transient overexpression of wild type Cr-TRX1 caused a dose-dependent activation of TNFα-induced κB-reporter expression. However, the overexpression of mutant Cr-TRX1 caused a slight decrease of κB-reporter expression suggesting that the oxidoreductive activity of Cr-TRX1 is essential to enhance the NF-κB activity. Furthermore, the Western blot with anti-p50 antibody revealed equal expression of NF-κB p50 protein suggesting that the overexpression of Cr-TRX1 did not affect the protein synthesis of p50 (Figure 3.39A). The overexpression of the 12 kDa TRX has been shown to affect TNFα-induced degradation of IκBα in HeLa cells (Zhu *et al*, 2005). Therefore, we also examined the effects of Cr-TRX1 on the IκBα degradation. Unlike the 12 kDa TRX, the Cr-TRX1-transfected cells showed no obvious effect on the

TNFα–induced degradation of IκBα (Figure 3.39A). Then, we investigated whether the enhanced NF-κB activity is attributable to its nuclear translocation. However, the nuclear localization of NF-κB p50 was not affected by overexpression of Cr-TRX1 (Figure 3.39B).

Subsequently, to examine whether Cr-TRX1 affects the NF-κB DNA-binding activity, electrophoretic mobility-shift assay (EMSA) was applied. As demonstrated in Figure 3.40, the wild type Cr-TRX1 slightly enhanced NF-κB DNA-binding activity. In contrast, the mutant form of Cr-TRX1 inhibited the NF-κB DNA-binding activity (Figure 3.40). This result is consistent with the κB-reporter assay in which the mutant Cr-TRX1 also slightly inhibited the TNFα-induced NF-κB activity (Figure 3.38), further suggesting that the oxidoreductive activity of Cr-TRX1 is essential in regulating the NF-κB activity.

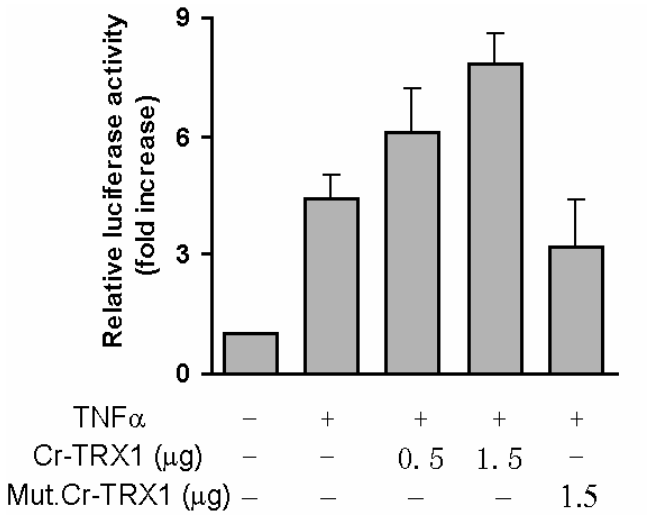

Figure 3.38: Effect of overexpression of Cr-TRX1 on the NF-κB activity. HeLa cells were transfected with indicated amounts of wild type and mutant (Mut) Cr-TRX1 together with 0.5 μg of pκB-Luc & pRL-CMV (internal controls). The luciferase activities were measured with dual-luciferase assay kit and were expressed as fold-increase relative to the internal control. Data are means ± S.D. of values from 3 independent experiments.

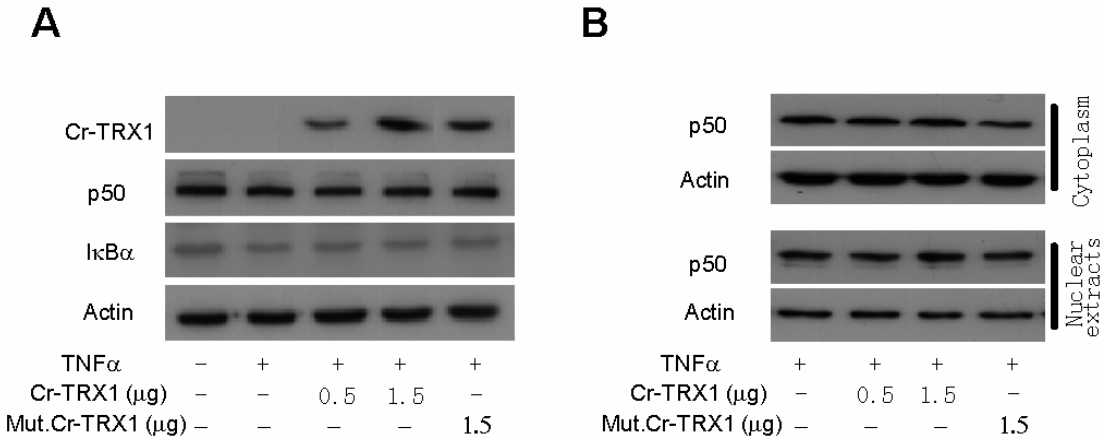

Figure 3.39: Effect of Cr-TRX1 on the expression and subcellular localization of NF-κB. (A) Effects of Cr-TRX1 expression on NF-κB p50 and IκBα expression. HeLa cells were transfected with Cr-TRX1 as mentioned in Figure. 3.38. Cell lysates were subjected to Western blot analysis. The FLAG-tagged Cr-TRX1 was detected with anti-FLAG antibody. **(B)** Cr-TRX1 overexpression did not affect the subcellular localization of NF-κB p50. After transfection with wild-type or mutant Cr-TRX1, cells were treated by TNFα (20ng/ml). The cytoplasmic and nuclear extracts were prepared using NE-PER Nuclear and Cytoplasmic Extraction Reagents (Pierce). The nuclear and cytoplasmic extracts were subjected to Western blot analysis using anti-p50 antibodies. The level of actin was analyzed as control.

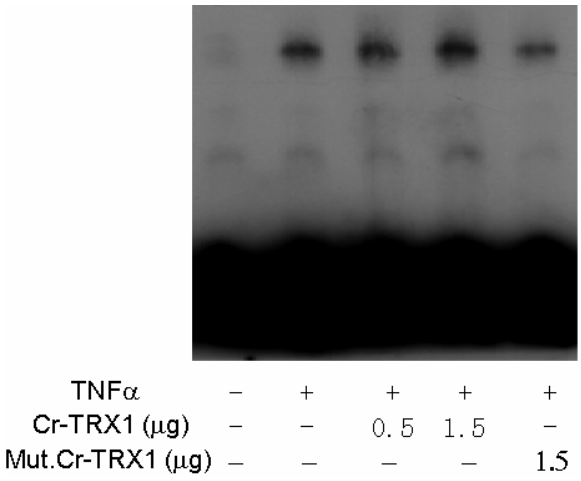

Figure 3.40: Cr-TRX1 increases TNFα-induced NF-κB DNA-binding activity. HeLa cells were transfected with indicated amounts of wild type and mutant (Mut) Cr-TRX1. Cells were harvested at 48 h after transfection. Nuclear extracts were prepared and EMSA was performed as described under "Materials and Methods".

3.7.2 Biological significance of oxidative stress in the regulation of NF-κB signaling pathway

Thus far, our studies have demonstrated that Cr-TRX1 acts as an antioxidant to regulate NF-κB activity in mammalian cells and the regulatory roles of Cr-TRX1 are attributable to its oxidoreductive activity. Therefore, we reasoned that oxidative stress could also play a crucial role in mediating immune response in the horseshoe crab, an ancient protostome species (Zhu *et al*, 2005). In our recent study, we have shown that Gram-negative bacteria infection activates the expression of immune-related genes, such as CriNOS (*C. rotundicauda* inducible nitric oxide synthase) and CrIκB (*C. rotundicauda* inhibitor of NF-κB) via NF-κB signaling pathway in horseshoe crab (Wang *et al*, 2006b).

To examine the potential effect of the antioxidant on the NF-κB-regulated immune gene expression in response to Gram-negative bacterial infection, we treated horseshoe crabs with an antioxidant, pyrrolidine dithiocarbamate (PDTC), before challenging with *P. aeruginosa*. As shown in Figure 3.41A & B, the administration of PDTC consistently suppressed the anticipated up-regulation of immune-responsive genes, CriNOS and CrIκB, indicating a possible role of reactive oxygen species in the activation of NF-κB mediated gene expression *in vivo*. As a positive control, we showed that the expression of CriNOS and CrIκB genes were also suppressed by an inhibitor of NF-κB pathway, MG-132 (Simeonidis *et al*, 2003). Furthermore, we analyzed the expression of horseshoe crab transglutaminase, whose expression in the vertebrate has been shown to be under the control of Sp1 and CREB/AP-1 (Lu *et al*, 1995; Medvedev *et al*, 1999). Injection of the NF-κB inhibitor, MG-132, did not affect the activation of the transglutaminase transcription upon Gram-negative bacterial infection (Figure 3.41C).

However, injection of PDTC inhibited the expression of transglutaminase by 50 % suggesting that the antioxidant also regulates the AP-1 signaling pathway as has been observed in humans (Witte *et al*, 2000). As a negative control, the expression of CALF (*C. rotundicauda* anti-LPS factor) was shown to be unaffected with or without NF-κB inhibitors, suggesting that the action of the antioxidant, PDTC, was specific and did not randomly affect the overall mRNA synthesis (Figure 3.41D).

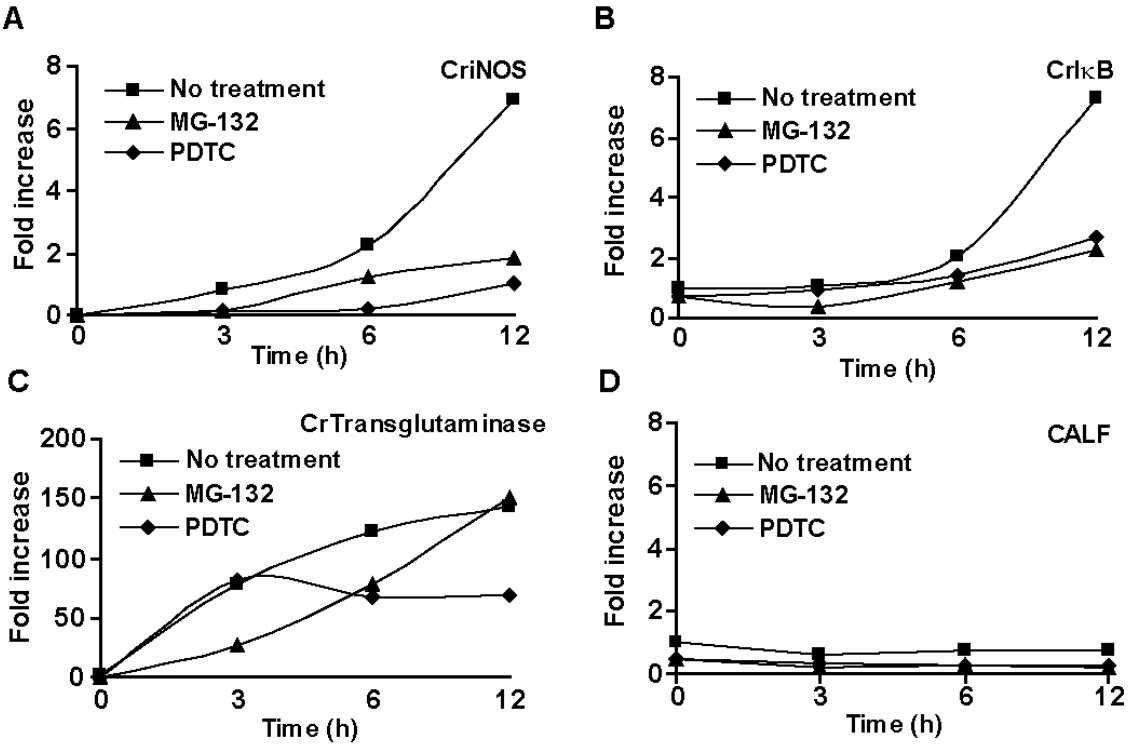

Figure 3.41: Antioxidant regulates NF-κB signaling pathway in horseshoe crab. The expression of horseshoe crab iNOS (CriNOS), IκB (CrIκB), transgultaminase (CrTransgultaminase) and CALF (*C. rotundicauda* anti-LPS factor) genes in hemocytes was examined after challenge with *P. aeruginosa* with or without inhibitors (■). One hour after treatment with PDTC (♦) or MG-132 (▲), the horseshoe crabs were either infected with *P. aeruginosa* or left unchallenged (0 h) and the hemocytes were collected at the indicated time points (in h). The RT-PCR products were analyzed on gels and quantified relative to the levels of horseshoe crab actin-11 mRNA. Results are expressed as relative fold-increase compared to naïve control (0 h) which was set to 1.

To examine whether *P. aeruginosa* infection affects Cr-TRX1 expression, the transcript profile of Cr-TRX1 was monitored using RT-PCR with total RNA extracted from hemocytes collected at indicated time points post *P. aeruginosa* challenge. As shown in Figure 3.42, the expression level of Cr-TRX1 decreased slightly after infection. This is in agreement with our earlier finding that the Cr-TRX1 gene was obtained from the hepatopancreas reverse subtractive library (Ding *et al*, 2005).

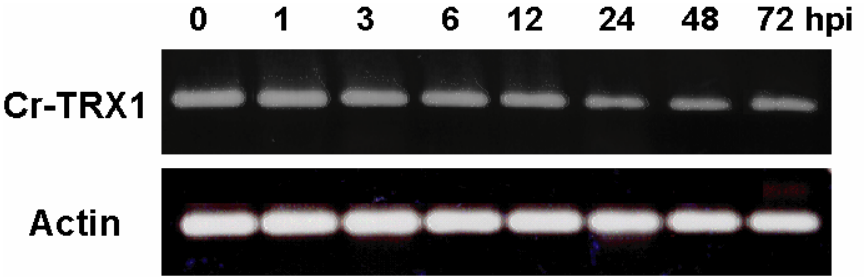

Figure 3.42: RT-PCR analysis of the expression level of Cr-TRX1 during bacterial infection. The mRNA expression of Cr-TRX1 was analyzed 1-72 h post-infection (hpi) with *P. aeruginosa.* The horseshoe crab actin-11 gene was analyzed under the same conditions as the internal control.

3.8 The 16 kDa TRX is conserved from *C. elegans* to human

3.8.1 Evolutionary conservation of 16 kDa TRX

A homology search of the GenBank™ database was conducted using the Cr-TRX1 cDNA as template. Interestingly, a number of putative 16 kDa TRX sequences were revealed from a variety of organisms. As shown in Figure 3.43, the 16 kDa TRXs are present in several nematode species and in the vertebrates, from zebrafish to human suggesting that the 16 kDa TRXs are evolutionary conserved. Sequence alignment of

these homologous proteins revealed that the WCPPC motif was fully conserved amongst the invertebrates (Figure 3.44), indicating the potential importance of this motif in the function of the16 kDa TRX.

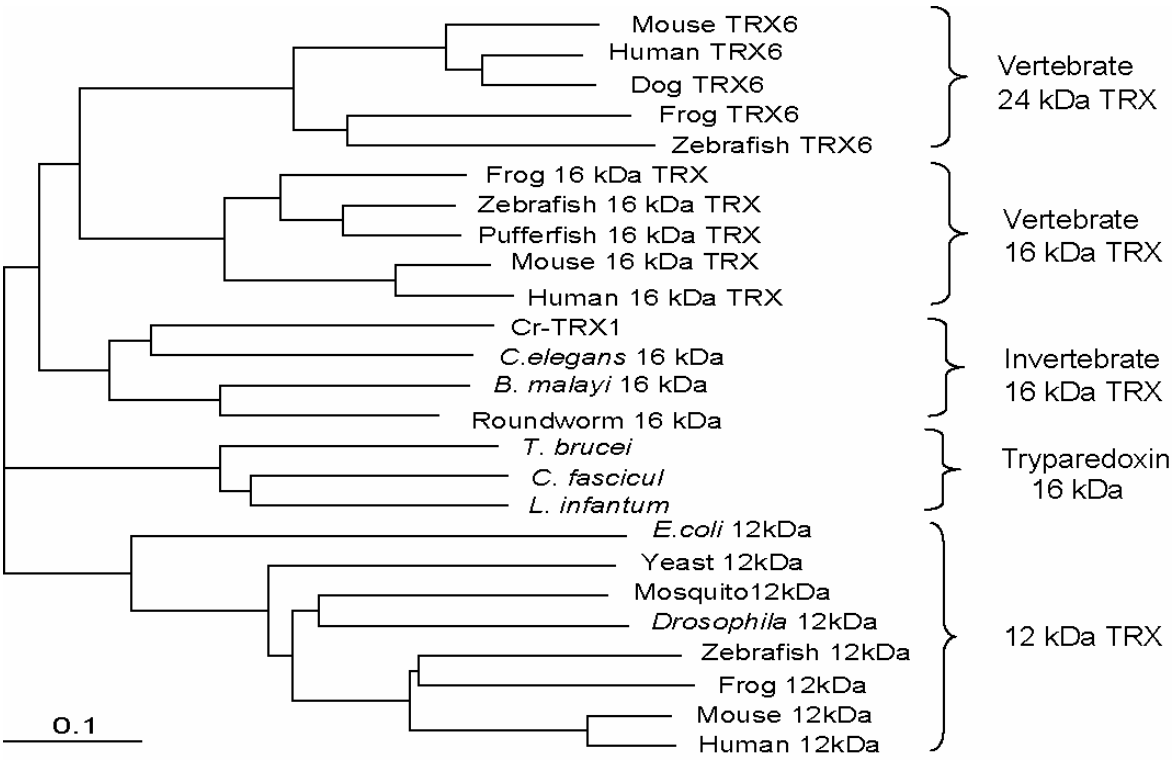

Figure 3.43: Phylogenetic study of the 16 kDa Cr-TRX1 and related TRX proteins. Multiple sequence alignments were produced with Clustal X using Gonnet series protein weight matrix. GenBank accession numbers of the sequences are listed in Table 3.3.

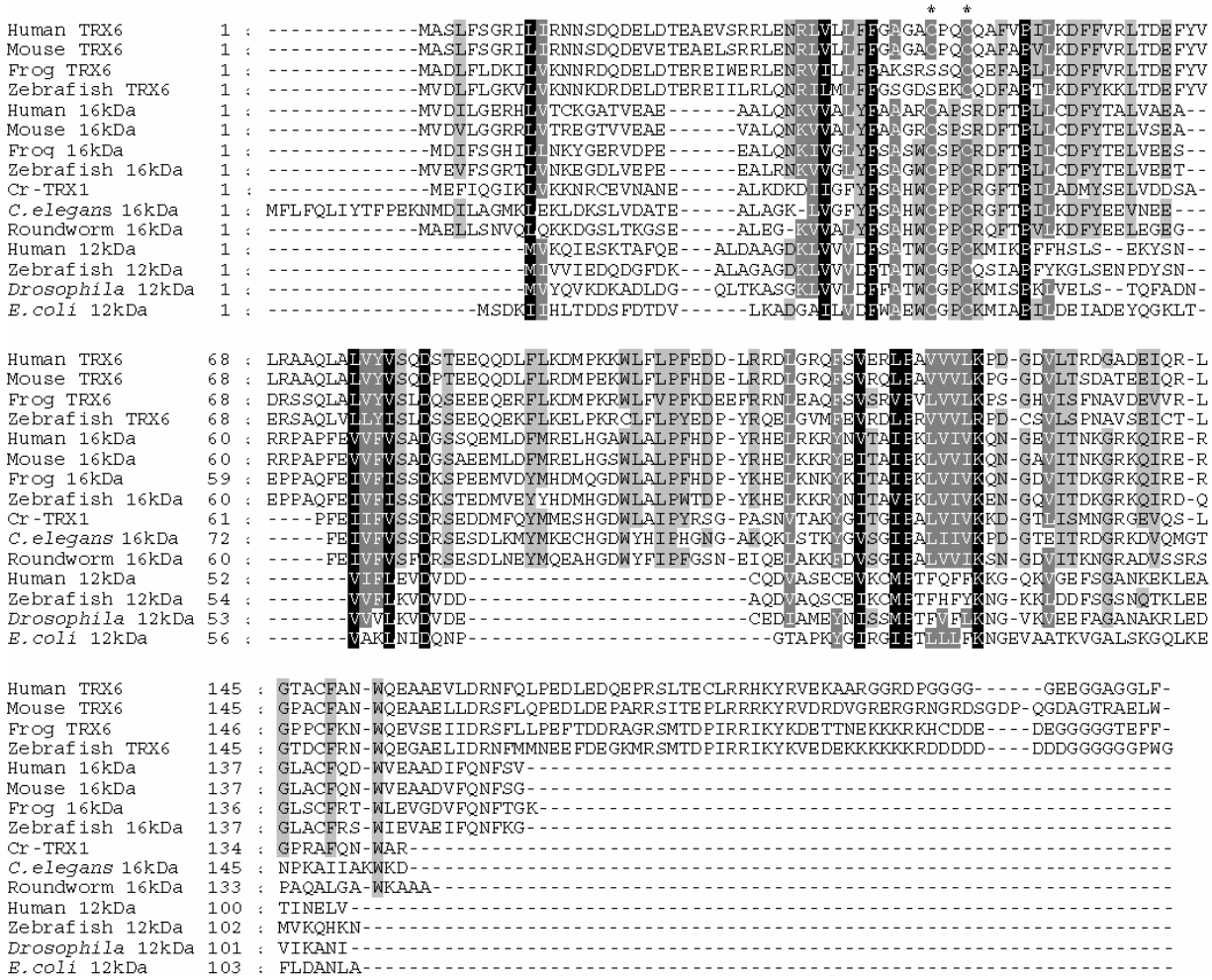

Figure 3.44: Sequence analysis of the 16 kDa Cr-TRX1 and related TRX proteins. Amino acid sequences comparison between Cr-TRX1 and the 16 kDa, 24 kDa and 12 kDa TRXs. Alignments were done by Clustal X. The Cys residues in the active sites are demarcated by *. Black and grey shades indicate identity and similarity of the residues, respectively. GenBank accession numbers of the sequences are listed in Table 3.3.

Surprisingly, in the vertebrates, another family of TRX-like proteins, with a molecular weight of 24 kDa, also shows high homology to the 16 kDa Cr-TRX1 suggesting that the 16 kDa TRX probably underwent gene duplication and divergence in the vertebrates and gave rise to the 24 kDa TRX (Zhang, 2003). An alignment of the 16 kDa and 24 kDa TRXs revealed that the active sites of these TRXs have undergone marked changes (Figure 3.44). Alternative active-site sequences include ACPQCQ and WCSPCR. For several members of the 16 kDa TRXs and 24 kDa TRXs, even the most conserved Cys has been replaced with Ser (Figure 3.44). However, besides the active motif, several other regions remained conserved amongst the 16 kDa TRXs compared with 12 kDa TRXs (Figure 3.44). This observation suggests that the 16 kDa TRX has evolutionary diverged from the 12 kDa TRX at an early stage.

3.8.2 Human TRX6, a homologue of Cr-TRX1, regulates NF-κB DNA binding activity

In order to assess whether the function of this family of TRX are also evolutionarily conserved, we decided to examine the function of a human homologue of Cr-TRX1. There are two highly homologous proteins of the Cr-TRX1 in the human genome, one is 16 kDa and another one is 24 kDa. Because the 16 kDa human TRX harbors a change in one of the two conserved cysteines in the active motif (Cys to Ser) (Figure 3.44), we chose the human 24 kDa TRX protein (GeneBank accession number, BC014127) for further functional studies. The human 24 kDa TRX is henceforth referred to as TRX6 ("thioredoxin-like 6", NCBI). The DNA sequence of TRX6 consists of an ORF of 636 bp, a 5'-untranslated region of 47 bp including an in-frame stop codon.

Compared with the 16 kDa Cr-TRX1, the TRX6 is 8 kDa longer. The predicted protein does not contain a known signal peptide for a specific subcellular localization. A search of the human genome sequence revealed that the gene for TRX6 is located at chromosome 19p13.12 and comprises 2 exons as well as 1 intron. BLAST search using Cr-TRX1 as template indicated the the TRX6 protein shares 27% identities and 54% homology with Cr-TRX1 respectively. The sequence alignment shows that most of the additional residues appear at the extreme C-terminus (Figure 3.44). Next, we predicted the structures of TRX6 and Cr-TRX1 using the Swiss-model program at the Expasy website. The structure of TRX6 is highly superimposable on that of Cr-TRX1 and *Trypanosoma* 16 kDa TRX, despite limited sequence identity. Like other 16 kDa TRXs, the Cr-TRX1 and TRX6 contain a characteristic thioredoxin fold, (Alphey *et al*, 1999; Martin, 1995) consisting of 5 central β-sheets and 4 flanking α-helices (Figure 3.45).

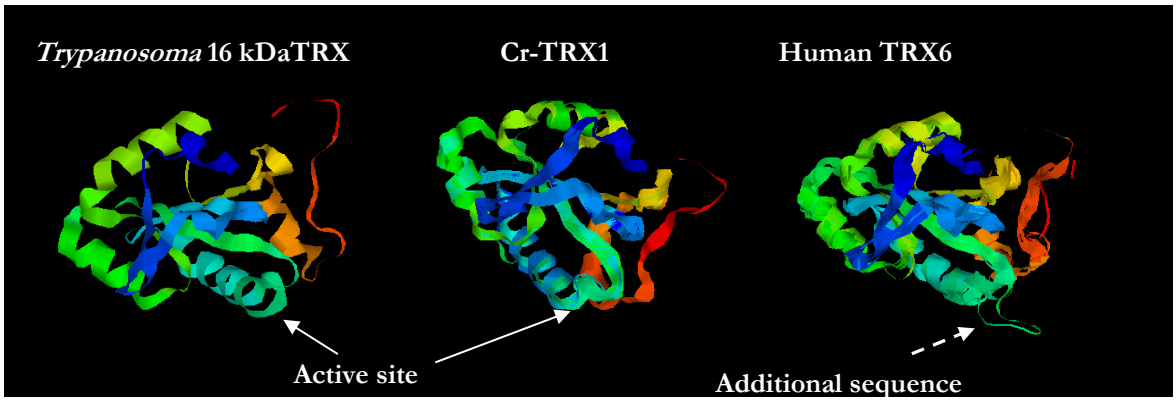

Figure 3.45: The predicted structures of Cr-TRX1 and the human TRX6. The structure of *Trypanosoma* 16 kDa TRX was obtained from the Protein Data Bank (PDB). The structures of Cr-TRX1 and human TRX6 were predicted using the Swiss-model program at the Expasy website: http://swissmodel.expasy.org/SWISS-MODEL.html. The white arrows indicate the active sites of the *Trypanosoma* 16 kDa TRX and Cr-TRX1. The additional sequence after the conserved active site in TRX6 (dashed arrow) is hypothesized to affect the activity of the TRX6.

In order to determine the enzymatic functions of TRX6, we expressed the recombinant TRX6 in *E. coli*. However, when expressed *in vitro*, the TRX6 lacked detectable oxido-reductase activity. This loss of function is probably due to an additional sequence (FYVLRAAQ) after the active site (Figure 3.44), resulting in a different structure around the catalytic site of the TRX6 (Figure 3.45). Furthermore, a highly conserved tryptophan (W) residue, located before the active site motif of TRX6 was replaced by alanine (A) residue (Figure 3.44), which might also have affected the enzymatic activity or substrate specificity of the recombinant TRX6.

To examine if TRX6 has conserved the NF-κB regulatory activity of Cr-TRX1, we expressed the recombinant TRX6 in *E. coli* and examined its ability to regulate horseshoe crab NF-κB, CrNFκB (a homologue of human NF-κB p65), DNA-binding activity by EMSA (Wang *et al*, 2006b). As shown in Figure 3.46, the TRX6 alone did not bind to the κB motif (lane 2). However, it can significantly enhance the DNA-binding activity of CrNFκB (lane 4) suggesting that like Cr-TRX1, the human TRX6 probably also possesses the NF-κB regulatory ability although the recombinant TRX6 has no detectable oxidoreductase activity. The augmentation is specific, as the control recombinant GST showed no effect on the binding activity of CrNFκB (lane 5).

The TRXs that have been characterized to date are nearly uniformly 12 kDa proteins with an active motif of WCGPC. In this thesis, we report the identification of a 16 kDa TRX, with an active motif of WCPPC, in horseshoe crab (an arthropod) and demonstrate that the 16 kDa TRX are evolutionarily conserved from *C. elegans* to human (Wang *et al*, 2007). Despite notable differences in the molecular mass and amino acid sequence of the catalytic site, the 16 kDa Cr-TRX1 appears to be functionally similar to

the classical 12 kDa TRXs. Our studies also showed that the 16 kDa Cr-TRX1 could positively regulate the TNFα-induced NF-κB activation and the enhancement of NF-κB-dependent gene expression was associated with increased NF-κB DNA-binding activity. Although the exact mechanism underlying the regulation of the NF-κB activity by Cr-TRX1 and TRX6 is still unknown; our studies strongly suggest that the NF-κB regulatory activity might be a common characteristic of the 16 kDa TRXs.

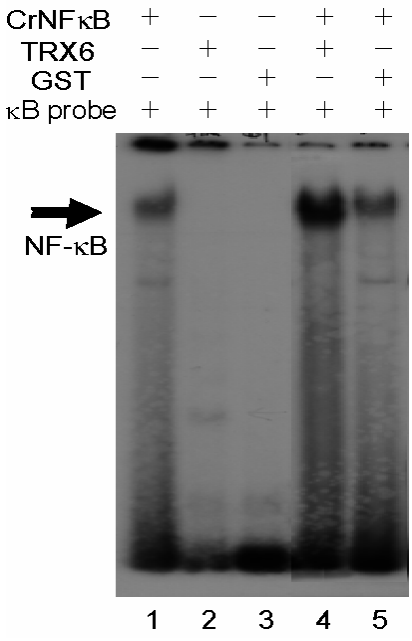

Figure 3.46: TRX6 enhances horseshoe crab NF-κB (CrNFκB) DNA-binding activity. EMSA was performed using the recombinant CrNFκB, TRX6 protein and κB probe. Purified recombinant TRX6 (200 ng) or GST (2 μg) were preincubated with CrNFκB at room temperature for 30 min and mixed with the labeled κB oligonucleotide (lanes 4 & 5). Complex formations were significantly enhanced by TRX6 (lanes 4), but not by recombinant GST (lane 5). The negative control, TRX6 or recombinant GST alone, showed no binding to the κB probe (lanes 2 & 3). The complexes are indicated by an arrow. Experiments were repeated three times with almost identical outcome and a representative result is shown.

CHAPTER 4: DISCUSSION

4.1 The evolutionarily conserved NF-κB signaling pathway

NF-κB family members are transcriptional factors that regulate the expression of a large number of target genes involved in physiological processes such as immune response, inflammation, apoptosis and progression of the cell cycle in different organisms (Bonizzi and Karin, 2004). Since the discovery of NF-κB transcription factors in 1986 (Sen and Baltimore, 1986), a wealth of information in understanding the mechanisms that operate in the NF-κB signaling pathway, and the functions of NF-κB in various diseases, has been generated for the mammalian systems (Hayden and Ghosh, 2004). However, other than evidence of Toll homologues in several insect species, an IKKβ homologue in an oyster and NF-κB homologues in several dipteran insects (Hoffmann and Reichhart, 2002), little is known about the NF-κB signaling pathway in other invertebrates. Therefore, we are in great need of information on the NF-κB signaling pathway in other invertebrates besides the insects. In this study, we have isolated and characterized the NF-κB and IκB from the horseshoe crab (*C. rotundicauda*), and named these homologues CrNFκB and CrIκB, respectively. To the best of our knowledge, except for Cactus in *Drosophila*, CrIκB is the only IκB characterized in invertebrates and CrNFκB is the only NF-κB identified in a non-insect species of arthropods.

4.1.1 The NF-κB/IκB signaling cascade of horseshoe crab is functionally comparable to that of the *Drosophila* and mammals

Phylogenetic analysis showed that CrNFκB and CrIκB share high level of similarities with their mammalian homologues. Despite the huge evolutionary distance between horseshoe crab and vertebrates, we showed that the CrNFκB and CrIκB display similar signature motifs as their respective vertebrate orthologues, notably, the Rel homology domain (RHD), the DNA binding motif and the nuclear localization signal (NLS) of CrNFκB; the 5 ankyrin repeats and the N-terminal potential phosphorylation sites of CrIκB (Figure 3.1 and 3.3). In addition, from a fragment obtained during the cloning of CrIκB, we isolated the horseshoe crab p100 and p105 homologue, CrRelish. Like human p100, p105 and insect Relish proteins, the CrRelish is a mosaic protein which contains both RHD and inhibitory IκB domain (Figure 3.5). It will be important to determine whether CrRelish is proteolytically processed during bacterial challenge. The fact that human p100 and *Drosophila* Relish are cleaved to release its N-terminal activation domains suggests that the CrRelish probably undergoes similar process of activation upon bacterial infection. Also, demonstrating the presence of a compound NF-κB protein (CrRelish contains both RHD and inhibitory IκB domain) in horseshoe crab, insects, as well as mammals provides further support for the postulation that these proteins may serve important regulatory roles that cannot be accomplished by separating Rel/NF-κB and IκB proteins (Dushay *et al*, 1996). Furthermore, the discoveries of CrNFκB, CrIκB and CrRelish in horseshoe crab strengthen the similarity of the mechanisms used by invertebrates and vertebrates to regulate their immune responses.

It has been shown that the RHD of the NF-κB transcription factor is the domain that binds the κB site. Therefore, we examined the specific binding of the recombinant CrNFκB RHD with oligonucleotides harboring κB motif(s). Results of EMSA strongly suggest that the horseshoe crab CrNFκB can bind to the κB site and its binding specificity was also confirmed. Using EMSA, we demonstrated that the DNA recognition mechanism of CrNFκB is reminiscent of that of mammalian and *Drosophila* species. We also observed that horseshoe crab CrNFκB proteins could physically interact with CrIκB proteins, providing evidence that horseshoe crab NF-κB molecules are functionally compatible with their mammalian counterparts.

CrNFκB shows highest homology with NF-κB proteins in insects. Thus, given the lack of horseshoe crab cell lines, it appeared appropriate to investigate the CrNFκB functions by performing transfection experiments in *Drosophila* cell line. To test the transcription activation, the CrNFκB and κB reporter constructs were transfected into the *Drosophila* S2 cell. Our results indicated that overexpression of CrNFκB can activate the *C. rotundicauda* Factor C (CrFC) κB reporter expression and the κB motif on the promoter of the reporter is necessary for the transactivation activity. Furthermore, we demonstrated that CrIκB could specifically inhibit the binding of CrNFκB to the κB motif of the CrFC promoter and reduce its transcriptional activity. Cell imaging also revealed that the NLS of CrNFκB is critical for its translocation into the nucleus. The process can be inhibited by overexpression of CrIκB suggesting that the activity of CrNFκB is modulated by an autoregulatory feedback mechanism akin to that of the mammalian and *Drosophila* systems (Ghosh *et al*, 1998).

Gram-negative bacterial infection caused rapid degradation of CrIκB and nuclear translocation of CrNFκB, suggesting that the horseshoe crab NF-κB signaling pathway can be activated by pathogen infection. Using RT-PCR, we confirmed that CrIκB is a target gene of CrNFκB. This feedback regulation of NF-κB activity has also been observed in the vertebrates and *Drosophila* (Tran *et al*, 1997). Lastly, we demonstrated that CriNOS, a homologue of mammalian iNOS, which is a classical target gene of NF-κB pathway in mammals, is also transcriptionally regulated by CrNFκB in the horseshoe crab. In summary, this study showed that the NF-κB activation pathway of the horseshoe crab is functionally comparable to that of the *Drosophila* and mammals, suggesting that the roles of NF-κB and its natural inhibitor, IκB, have co-evolved and remained conserved through evolution. We anticipate that these findings would provide evolutionary perspectives into the signal transduction of immune response and provoke further interests in the scientific community to understand the origin of innate immunity and how it influences adaptive immunity.

4.1.2 A proposed NF-κB signaling pathway in the horseshoe crab

The phenomenal success of the immune defense of the horseshoe crab, one of the most ancient living arthropods, has contributed to its survival for ~550 million years (Størmer, 1952) and makes this species an excellent model to understand the origin of innate immunity. Previously, the striking similarities between the extracellular *Drosophila* dorsoventral determination cascade and the horseshoe crab LPS-sensitive blood coagulation cascade have been observed (Ding *et al*, 2004). In *Drosophila*, the dorsoventral cascade can activate the Toll-ligand, Spätzle, which then binds to the Toll

on the cell membrane and triggers the intracellular NF-κB signaling pathway. In this work, we have revealed the presence of a primitive but functional CrNFκB/CrIκB signaling cascade and demonstrated its relevance to the immune defense of a horseshoe crab, *C. rotundicauda*.

Our findings herein and the recent cloning of Toll-like receptor in the horseshoe crab (Inamori *et al*, 2004) have provided compelling evidence for a functional intracellular TLR/NF-κB signaling cascade. Although, the direct ligand for horseshoe crab TLR activation is unclear, it has been proposed that the activation of LPS-sensitive blood coagulation cascade converts coagulogen (a homologue of Spätzle) to coagulin, which may serve as a ligand of horseshoe crab TLR (Bergner *et al*, 1996; Osaki and Kawabata, 2004; Wang *et al*, 2003). Furthermore, we have isolated two cDNAs which are highly homologous to other components of the Rel/NF-κB pathway, including the TNF receptor-associated factor, CrTRAF and CrSlimb (Ding *et al*, 2005). The CrSlimb is a homologue of human β-TrCP and *Drosophila* Slimb which are involved in the degradation of IκB proteins (Spencer *et al*, 1999). Although the biological functions of these components remain to be elucidated further, their existence nonetheless provides additional evidence for a functional TLR/NF-κB cascade since several hundred million years ago, and the co-evolution of this signaling cascade. Our findings provide further support to the view that a signaling mechanism mediated via NF-κB family of proteins, which controls the expression of immune defense genes probably originated from a common ancestry and was already present in the *Urbilateria* (Hoffmann and Reichhart, 2002). Figure 4.1 illustrates a scheme for this conservation and co-evolution of the NF-κB signaling pathway (Wang *et al*, 2006b).

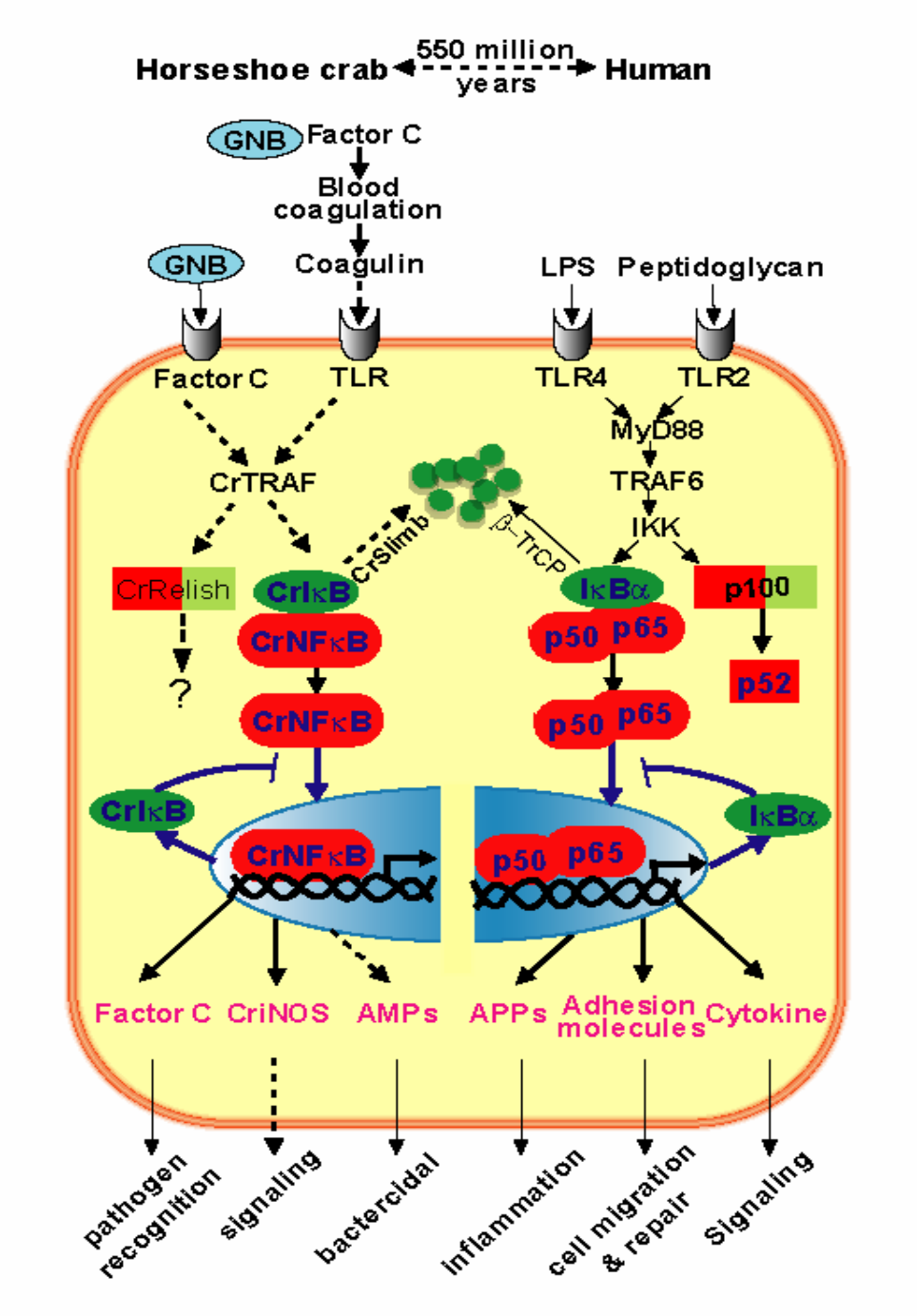
Horseshoe crab
550 million years
Human
GNB
Factor C
Blood coagulation
GNB
Coagulin
LPS
Peptidoglycan
Factor C
TLR
TLR4
TLR2
MyD88
CrTRAF
TRAF6
IKK
CrSlimb
β-TrCP
CrRelish
CrIκB
IκBα
p100
p50
p65
CrNFκB
p52
?
CrIκB
IκBα
CrNFκB
p50
p65
Factor C
CriNOS
AMPs
APPs
Adhesion molecules
Cytokine
pathogen recognition
signaling
bactericidal
inflammation
cell migration & repair
Signaling

4.2 The horseshoe crab Imd/Relish pathway

In *Drosophila,* the Toll pathway mainly mediates immune defense against Gram-positive bacteria and fungi. The Imd pathway confers protection against Gram-negative bacterial infection. In mosquito (*Aedes aegypti*), researches have shown that the Relish homologue is responsible for the regulation of the immune response to bacterial challenge; and REL1, a homologue of *Drosophila* Dorsal, regulates the antifungal immune pathway (Shin *et al*, 2005; Shin *et al*, 2003).

In this project, we also isolated two NF-κB transcription factors, CrNFκB (a homologue of *Drosophila* Dorsal and mammalian p65) and CrRelish (a homologue of *Drosophila* Relish and mammalian p100). The Gram-negative bacterial infection significantly enhanced the κB binding activity in the horseshoe crab hemocytes suggesting that Gram-negative bacterial infection could activate the horseshoe crab NF-κB signaling pathway *in vivo*. Addition of specific antibodies against CrNFκB only caused a partial supershift of the κB-binding complex. The majority of the κB-binding complex could not be supershifted by the anti-CrNFκB antibody, which suggests the presence of κB motif-binding proteins other than CrNFκB in the horseshoe crab hemocyte. Previous study has shown that amongst the three *Drosophila* NF-κB homologues (Dorsal, Dif and Relish), Relish has relatively higher and broader binding activity to κB motifs (Han and Ip, 1999). A similar mechanism is probably operational in the horseshoe crab as well and CrRelish may play a major role in forming the κB complex and in mediating the protection against Gram-negative bacterial infection. However, at this stage, whether the horseshoe crab CrNFκB and CrRelish play similar

roles as their corresponding homologues in the *Drosophila* and mosquito remains unknown. The functional relevance of CrRelish and CrNFκB in mediating anti-bacterial activities against Gram-positive and against Gram-negative bacteria is the subject for further studies. Nevertheless, the partial supershift with anti-CrNFκB antibody suggests that the DNA–protein complex formed with κB motif at least involves the presence of CrNFκB (Figure 3.17A). Furthermore, although the exact identity of the unshifted complexes is unknown at this juncture, the data in Figure 3.16 nevertheless provide adequate evidence to show that the complexes are formed by κB motif binding proteins.

4.3 The activation of NF-κB signaling pathway in horseshoe crab

It has been observed that the activation of Toll in *Drosophila* and the activation of TLR in mammals are clearly different with regards to the detection of microorganisms (Hoffmann and Reichhart, 2002). In the *Drosophila*, fungi and Gram-positive bacteria are recognized by circulating PRRs which then lead to the activation of a serine protease cascade and the proteolytically processed product of this cascade, Spätzle, is believed to be the ligand for Toll activation (Wang *et al*, 2003). However, in mammals, the TLRs on the cell membrane interact directly with the PAMPs and activate the downstream NF-κB signaling pathway. So far, only one Toll receptor in *Drosophila* is known to be strictly required for immune defense, although fruit flies express nine distinct Toll receptors (Tauszig *et al*, 2000). This is distinct from the extensive roles played by the various mammalian TLRs which can recognize various PAMPs such as peptidoglycan,

lipoproteins, LPS, flagellin, DNA and RNA (Akira and Takeda, 2004). It has been suggested that a significant number of circulating recognition proteins (such as the peptidoglycan recognition protein, PGRP) in the *Drosophila* may reflect the recognition of a broad spectrum of microbial patterns by the mammalian TLR family (Hoffmann and Reichhart, 2002).

The exact mechanism of how horseshoe crab NF-κB is switched on upon pathogen infection is still uncertain. However, like *Drosophila*, the horseshoe crab contains a plethora of proteins that have been shown to function as pathogen recognition proteins, such as Factor C, Factor G and C-reactive proteins (Iwanaga, 2002). So far, only one type of TLR has been cloned from the horseshoe crab (Inamori *et al*, 2004). Therefore it is reasonable to postulate that similar to *Drosophila*, horseshoe crab probably utilizes a plethora of circulating pathogen recognition proteins in the blood, not a family of TLRs on the cell membrane, to detect the presence of intruding pathogens.

Interestingly, it was recently reported that the Factor C of the Japanese horseshoe crab, like the mammalian TLR4 but not *Drosophila* Toll (Wasserman, 2000), could function as a pattern-recognition protein for LPS on the hemocyte surface. In this regard, the proteolytic activity of Factor C on the hemocytes was found to trigger a G protein-mediated exocytosis for innate immune response (Ariki *et al*, 2004). It will be interesting to investigate whether the membrane-localized Factor C could function as a receptor to activate the downstream signaling pathway that regulates the innate immune response. Indeed, previous studies also suggested that the exocytosis is mediated by a heterotrimeric GTP-binding protein that stimulates the inositol-1,4,5,-triphosphate (IP_3)-signaling pathway which leads to the increase of intracellular Mg^{2+} and Ca^{2+} (Solon *et al*,

1996). It has also been reported that NF-κB signaling pathway can be activated by G-protein coupled receptors via the IP_3-Ca^{2+} signaling (Ye, 2001). These observations corroborate the possibility that, like mammalian TLR (Hoffmann and Reichhart, 2002), Factor C may also function as a receptor on the membrane for the activation of NF-κB signaling pathway in the horseshoe crab (Wang *et al*, 2003).

It is widely believed that LPS is a strong inducer of Toll/NF-κB signaling pathway in mammals (Akira and Takeda, 2004), however the function of LPS in activating NF-κB signaling in invertebrates is still unclear. In 2003, Werner *et al* reported that both LPS and peptidoglycan could induce the expression of *Drosophila* antimicrobial peptides that is mediated by peptidoglycan recognition protein, PGRP-LC. They found that PGRP-LCx is the only isoform required to mediate signals from Gram-positive bacterial peptidoglycan. In contrast, the recognition of Gram-negative bacteria and bacterial LPS requires both PGRP-LCa and LCx (Werner *et al*, 2003). They also postulated that the simultaneous requirement of two splice forms for the response to LPS suggests that the PGRPs may act as heterodimers or perhaps as higher multimers (Werner *et al*, 2003). However, in the same year, Leulier *et al.* reported in *Drosophila*, that the Toll pathway is predominantly activated by Gram-positive lysine-type peptidoglycan, and that Gram-negative diaminopimelic acid-type peptidoglycan is the most potent inducer for the Imd pathway. This observation suggests that the ability of *Drosophila* to discriminate between Gram-positive and Gram-negative bacteria relies on the recognition of specific forms of peptidoglycan but not LPS. Indeed, they clarified that LPS is not the main determinant for Gram-negative bacterial recognition in *Drosophila*, which is in contrast to vertebrates (Leulier *et al*, 2003). Because peptidoglycans from Gram-negative

bacteria are crosslinked with a peptide containing a diaminopimelic acid (DAP) residue, whereas a lysine is found in the same position of Gram-positive bacteria (Figure 4.2), they suggested that this variation probably results in distinct conformational difference, allowing discriminatory recognition (Leulier *et al*, 2003).

In our studies, we observed that the Gram-negative bacteria could strongly induce the degradation of CrIκB and activate the NF-κB signaling pathway. However, it is still unknown whether LPS or the Gram-negative peptidoglycan triggered the NF-κB signaling pathway. Also, in horseshoe crabs, LPS has been shown to trigger the coagulation cascade that involves three serine protease zymogens: Factor C, Factor B and proclotting enzyme (Ding *et al*, 1993). Factor C responds to picomolar of LPS and autocatalytically converts to its active form, which in turn transforms Factor B. The activated Factor B converts the proclotting enzyme to clotting enzyme which converts coagulogen to an insoluble coagulin gel (Ding *et al*, 2004). Therefore, it will be interesting to determine whether the ligands for the NF-κB signaling pathway are similar to that of the coagulation cascade, as well as to study the relationship between NF-κB signaling pathway and the coagulation cascade.

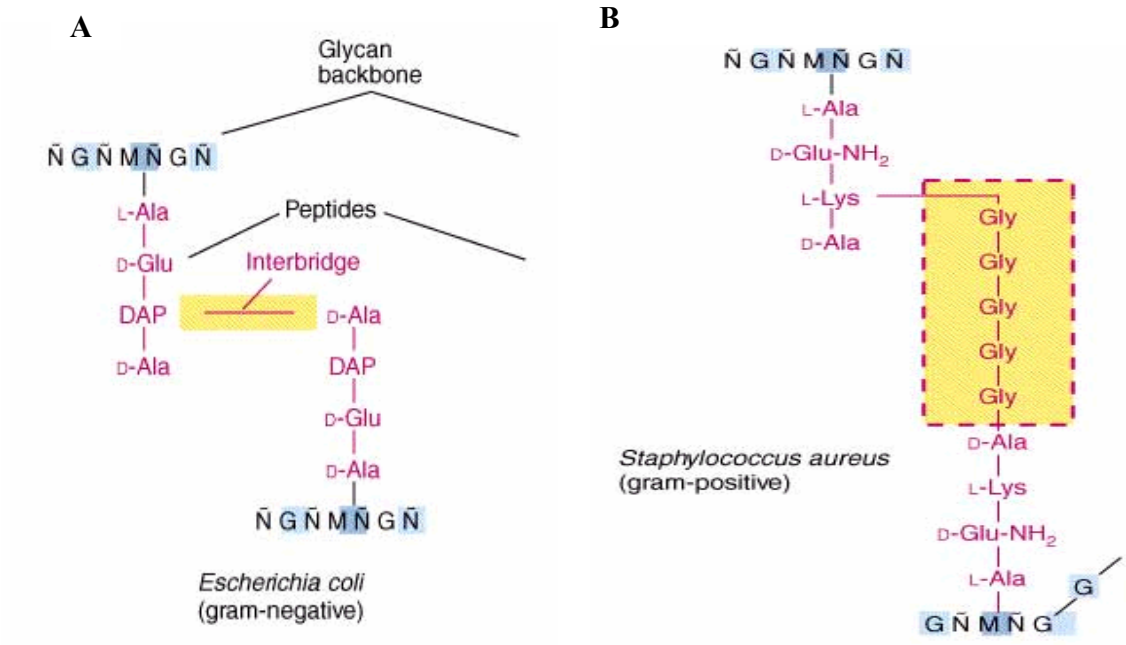

Figure 4.2: The structural comparison of Gram-negative and Gram-positive peptidoglycan. Peptidoglycan is a vast polymer consisting of interlocking chains of identical peptidoglycan monomers. A peptidoglycan monomer consists of two joined amino sugars, N-acetylglucosamine (NG) and N-acetylmuramic acid (NM), with a pentapeptide. The long sugar chains are joined to one another by means of peptide cross-links between the peptides. The major difference between the Gram-negative and Gram-positive peptidoglycan is the third amino acid in the peptide chain. The third amino acid in the peptide chain of the Gram-negative bacterial peptidoglycan is diaminopimelic acid (DAP) **(A)**. However, the third amino acid in the peptide chain of the Gram-positive bacterial peptidoglycan is lysine **(B)**. Furthermore, the peptidoglycan of Gram-negative bacteria is cross-linked by bond formation between the DAP molecule extending from one sugar backbone and the terminal Alanine of another **(A)**. However, the Gram-positive peptidoglycan is linked by a 5 amino acids interbridge between the Lysine of one sugar backbone to the Alanine of the second **(B)**. This figure is adapted from this website: http://www.arches.uga.edu/~emilyd/mibo3510/theory.html.

4.4 The exocytosis and NF-κB signaling

It is well known that the LPS-induced exocytosis of granular hemocytes is a key component of innate immunity in horseshoe crab. In response to stimulation by LPS, the antimicrobial elicitors stored in the hemocyte granules are immediately secreted by

exocytosis (Solon *et al*, 1996). However, how these intra-granular molecules are replenished remains a mystery. Our finding suggests that the expression of CrFC, which is an important defense molecule in the large granules, is under the control of NF-κB signaling pathway. It is well known that the expression of a plethora of antimicrobial peptides in the *Drosophila* and mosquito is under the control of NF-κB signaling pathway (De Gregorio *et al*, 2002; Osta *et al*, 2004). Hence, it is conceivable that the expression of horseshoe crab antimicrobial peptides is under similar transcriptional regulation. This phenomenon indicates that upon infection, the NF-κB signaling pathway-controlled transcription activation is a possible mechanism for replenishing the store of CrFC and antimicrobial peptides after exocytosis of the hemocyte granules. This requires the sacrificial degranulation of the hemocyte (Iwanaga, 2002).

In conclusion, although absent in *C. elegans*, the NF-κB/IκB signaling pathway has co-evolved and remained well-conserved from horseshoe crab to human, playing an archaic but crucial and fundamental role in innate immune response to regulate the expression of critical immune defense molecules. We believe that the accumulation of data on NF-κB signal pathway from different invertebrates other than *Drosophila* should provide further insights into the invertebrate immunity.

4.5 A novel form of TRX which regulates NF-κB activity

TRX is generally a low-molecular weight 12 kDa cellular redox protein that is involved in numerous biological functions. TRX is generally characterized by an amino acid sequence motif containing an active site, CGPC. The two cysteine residues can be reversibly oxidized to form a disulfide bridge. TRX has been reported to function as a reductive factor through its dithiol group and has multiple biological activities via the regulation of intracellular redox status (Hirota *et al*, 2002). A majority of the TRX that have been reported to date from eukaryotic and prokaryotic organisms are initially translated as a 12 kDa protein (Powis and Montfort, 2001). In this thesis, we describe the identification and characterization of a novel 16 kDa TRX which contains a WCPPC active motif in the horseshoe crab *Carcinoscorpius rotundicauda* (Cr-TRX1). Despite notable differences in the mass and sequence of the catalytic site, the Cr-TRX1 appears to be functionally similar to the 12 kDa TRXs.

4.5.1 The 16 kDa Cr-TRX1 is functionally similar to the 12 kDa TRX

The Cr-TRX1 was cloned from a hemocyte subtractive library. Sequence analysis revealed that the Cr-TRX1 is larger than the known classical 12 kDa counterpart and contains an atypical WCPPC catalytic motif. Although Cr-TRX1 contains three Cys, only two in its active motif are exposed and redox sensitive. The extra Cys residue at the N-terminus may be involved in homodimer formation. To evaluate the TRX activity of Cr-TRX1, insulin reduction assay was performed according to the classical method described by Holmgren (1985). The results suggest that the Cr-TRX1 is not only

functional, but it appears more efficacious than the *E. coli* counterpart. To test the cross-species (cross-phylum in this case) functionality of Cr-TRX1, we examined whether oxidized Cr-TRX1 can be reduced by rat TRXR in the presence of NADPH, by monitoring NADPH oxidation at 340 nm. The results indicate that Cr-TRX1 could undergo cross-phylum reduction by mammalian thioredoxin reductase. To confirm that Cr-TRX1 can function by itself as an antioxidant and protect DNA, we performed the DNA nicking assay. The results indicate that Cr-TRX1 can protect DNA from reactive oxygen species-mediated nicking. All of these results suggest that despite notable differences in its molecular mass and the active site sequence, the Cr-TRX1 is functionally similar to the 12 kDa TRX.

4.5.2 The 16 kDa TRX is conserved from *C. elegans* to human

The TRXs that have been characterized to date are nearly uniformly 12 kDa proteins with an active motif of WCGPC. More recently, a 16 kDa class of TRX with an active motif of WCPPC (see Figure 3.23) was identified in the parasitic protozoa, trypanosomes (Ludemann *et al*, 1998). All of these parasitic protozoa lack of the ubiquitous glutathione/glutathione reductase system and are very sensitive towards oxidative stress (Reckenfelderbaumer and Krauth-Siegel, 2002). Since then, the 16 kDa TRX is believed to exist only in this protozoan and; therefore, it has been used as an attractive target for the development of new anti-parasitic drugs (Krauth-Siegel and Coombs, 1999).

Here, we report the identification of a 16 kDa TRX, with an active motif of WCPPC, in the horseshoe crab (an ancient arthropod) and demonstrate that the 16 kDa

TRXs are evolutionarily conserved from *C. elegans* to human. Sequence alignment of these homologous proteins revealed that the catalytic WCPPC motif was largely conserved, indicating the potential importance of this motif in the 16 kDa TRX function. Although the active motifs of the 16 kDa TRXs in mammals have undergone marked changes, several other regions remained well conserved amongst the 16 kDa TRXs compared with the 12 kDa TRXs. This observation suggests that the members of the 16 kDa TRX has evolutionarily diverged from the 12 kDa TRXs at an early stage. The predicted three-dimensional structure of 16 kDa revealed a folding very similar to that of parasitic protozoa 16 kDa TRX with five-stranded β-sheet surrounded by four α-helices (see Figure 1.6) (Alphey *et al*, 1999). In particular, the active site motif CPPC is in a position homologous to that of the corresponding motif in parasitic protozoa 16 kDa TRX. Interestingly, although the 16 kDa TRX is present in many species, from *C. elegans* to human, it is absent in several insect species such as *Drosophila* and mosquito which, like horseshoe crab, also belong to arthropods. It has been demonstrated that the antioxidant system in *Drosophila*, and probably in related insects, differs fundamentally from that in other organisms. It lacks the glutathione reductase and the thioredoxin system supports GSSG reduction (Kanzok *et al*, 2001). Our observation provides further support to the notion that antioxidant defense in insects is unusual compared to that in other organisms (Kanzok *et al*, 2001). Our findings of the functional Cr-TRX1 (this work) and a full repertoire of GSTs (Ding *et al*, 2005) in the horseshoe crab suggest that although this species belongs to the arthropods, shared by insects, its oxidoreductase systems must have undergone substantial divergence from the insects.

4.6 The catalytic sequences of TRX families

All organisms from bacteria to mammals contain multiple TRX isoforms. Although the amino acid sequences of TRX proteins from different species are not highly conserved, they all contain the conserved catalytic sequence, CXXC. The sequence of the catalytic site from the 12 kDa class of TRX is highly conserved. However, members of the TRX protein family that are larger than 12 kDa have variable residues associated with the active-site motif (Kunchithapautham *et al*, 2003). For example, a human 32 kDa transmembrane protein, TMX, was found to contain the active site sequence WCPAC (Matsuo *et al*, 2001), a human 45 kDa TRX-related protein (PC-TRP) with the active site sequence of WCGHC (Wrammert *et al*, 2004), and a human 14 kDa TRX (TRP14) with the active site sequence WCPDC (Jeong *et al*, 2004b). Similarly, the 16 kDa horseshoe crab TRX also contains an unusual WCPPC active-site motif. Except for the diversity in the active site sequences, the enzymatic activity of various TRX isoforms is also different. For example, the 14 kDa human TRX (TRP14), with an active motif of WCPDC, exhibits markedly different substrate specificity compared to the 12 kDa TRXs. Although TRP14 could reduce small disulfide-containing peptides, it did not reduce the disulfides of known human TRX1 substrates, ribonucleotide reductase and peroxiredoxin (Jeong *et al*, 2004b). In contrast, despite notable differences in the amino acid sequence of the catalytic site, the 16 kDa Cr-TRX1 appeared to be functionally similar to the classical 12 kDa TRXs. This is consistent with the reports that the same variant active site (WCPPC) of TRXs in trypanosomes, *Arabidopsis thaliana* and human nucleoredoxin displayed comparable activity (Kurooka *et al*, 1997; Ludemann *et al*, 1998). Therefore, it appears

that there is considerable flexibility in the two residues between the conserved Cys residues in the active site, and that the different catalytic sequences might confer diverse enzymatic activity and substrate specificity, indicating the functional diversity of the TRX system.

Interestingly, like the other 16 kDa thioredoxin, the Cr-TRX1 also lacks the highly conserved Asp^{26}, which is present in the *E. coli* TRX, and has been shown to play a crucial role for catalytic activity. It is the only acidic residue not localized on the surface of the protein and mutation to an Ala increased the *K*m value for thioredoxin reductase by a factor for 10 (Katti *et al*, 1990). In addition, the mutant *E. coli* thioredoxin protein had a drastically lowered ability to serve as a hydrogen donor for ribonucleotide reductase (Reckenfelderbaumer *et al*, 2000). Our results clearly showed that the Cr-TRX1 is an excellent substrate of mammalian thioredoxin reductase and is able to reduce insulin effectively. These findings indicate that unlike the classical 12 kDa TRX, an acidic residue at this position is not essential for the catalytic activity of Cr-TRX1.

4.7 The N-terminal extra cysteine residue of Cr-TRX1

Based on the study on the human TRX1, it has been shown that the mammalian 12 kDa TRXs have three conserved cysteine residues at positions 62, 69 and 73, besides the two conserved cysteines in the active motif. Those Cys residues may impart unique biological properties to the mammalian 12 kDa TRXs (Holmgren, 1985). The crystal structure also revealed that human TRX1 can form a dimer via Cys^{73}, and the active site residues are buried in the dimer interface (Weichsel *et al*, 1996). Surprisingly, although most of the 16 kDa TRXs, like the bacterial 12 kDa TRX, do not contain an extra Cys

residue besides the ones in the active site, the Cr-TRX1 possesses an extra Cys residue at the N-terminus (Figure 3.23). Interestingly, while the Cr-TRX1 lacks the C-terminal extra Cys residue, it could form a dimer with a molecular mass of 32 kDa (Figure 3.31). It is possible the Cr-TRX1 can form a dimer via the N-terminal Cys^{15}. However, at this stage, it is still unclear if such dimer also exists under physiological conditions, and therefore, the role of the extra N-terminal Cys in the dimer formation needs further examination. Nevertheless, the mass spectrometric analysis of the Cr-TRX1 demonstrated that only the two conserved Cys residues in the active site were redox active indicating that, similar to the human TRX1, the Cr-TRX1 dimer may represent a naturally occurring form of protein (Weichsel *et al*, 1996). Further mutation and structure studies would be useful to define the function of the extra N-terminal Cys^{15} residue in Cr-TRX1.

4.8 The origin of the vertebrate 24 kDa TRXs

In the vertebrates, there are two families of TRXs with high homology to the 16 kDa TRX; one is 16 kDa and another one is 24 kDa (TRX6) (Figure 3.43). However the invertebrates only possess the 16 kDa TRXs and the bacteria are devoid of these homologues. This observation suggests that the 16 kDa TRXs have evolutionarily diverged from the 12 kDa TRXs at an early stage and the 16 kDa TRXs probably underwent gene duplication and divergence in the vertebrates and gave rise to the 24 kDa TRXs (Zhang, 2003) (Figure 3.43). Interestingly, unlike the invariable WCPPC catalytic motif in the 16 kDa TRXs of invertebrates, the active sites of the 16 kDa and 24 kDa TRXs of vertebrates have undergone marked changes (Figure 3.44). For human 16 kDa

TRX and zebrafish 24 kDa TRX, even the most conserved Cys residues has been replaced with Ser residues. It is therefore reasonable to postulate that the duplication and further evolution of the gene encoding the 16 kDa TRX in the vertebrates have probably relaxed the selection pressures and accelerated the evolution of novel catalytic motifs and functions (Force *et al*, 1999; Zhang, 2003). Therefore, it will be interesting to investigate if the 16 kDa and 24 kDa TRXs in mammals still conserve and exhibit the basic enzymatic functions of the invertebrate 16 kDa counterparts. Simultaneously, it would be pertinent to explore the functional similarities /differences between the 16 kDa and 24 kDa TRXs in the vertebrates. This begs the following question: is it possible that each of these very similar TRX proteins will fulfill specific and important roles in the cell in addition to their ability to backup one another under some stress or inflammatory conditions? The differing specificities may be due to their different amino acid sequences in the active motif that permit interactions with particular substrate proteins (Aslund and Beckwith, 1999). Alternatively, there might be an adaptor molecule that connects the various TRXs and links TRXs to their respective substrates.

4.9 Cr-TRX1 regulates NF-κB signaling pathway

Human TRX1 has been shown to regulate the NF-κB activity distinctly in the cytoplasm and in the nucleus. In the nucleus, TRX1 enhances NF-κB transactivation activity; however in the cytoplasm, TRX1 inhibits the degradation of IκB and prevents the activation of NF-κB (Hirota *et al*, 1999). Studies by Matthews *et al.* (1992) and Meyer *et al*. (1993) showed the DNA-binding activity of NF-κB to be under redox regulation through the modulation of Cys residues, and that the NF-κB components, p50

and p65, contain well-conserved cysteine residues in their DNA-binding loops (Ghosh *et al*, 1995). This implies that to activate NF-κB, an oxidative process that is antagonized by TRX must first facilitate IκB degradation, then translocated NF-κB in the nucleus must be reduced by TRX for effective DNA binding and transactivation (Flohe *et al*, 1997).

Our transient transfection studies showed that the 16 kDa Cr-TRX1 could positively regulate the TNFα-induced NF-κB activation and the enhancement of NF-κB-dependent gene expression was not due to the expression level and subcellular localization of NF-κB proteins (Figure 3.39). This regulation of NF-κB activity could be due to the redox regulation through the modulation of cysteine residues in Cr-TRX1, as observed from the complete loss of the augmentation of NF-κB activity when the HeLa cells were transfected with Cys-mutant Cr-TRX1 instead (Figure 3.38). This suggests that, like human TRX1, the activity of the Cr-TRX1 could be attributable to the two strategically located cysteine residues at its active site, and that its activation of NF-κB activity is via the redox regulation.

To determine whether the increase in NF-κB activity observed was indeed due to increase in its DNA-binding activity, gel shift assay utilizing biotin-labeled human NF-κB consensus sequence was performed. From Figure 3.40, it could be observed that under normal conditions, the DNA-binding activity of NF-κB was minimal. However, with TNFα stress alone, there was a dramatic increase in the DNA-binding activity of NF-κB, as observed from the increased intensity of the protein-DNA complex. With overexpression of Cr-TRX1 in the HeLa cells, the protein-DNA complex formation became more intense; but when mutant Cr-TRX1 was introduced instead, this complex

returned to the basal level (HeLa with TNFα stress only). Hence, the TNFα-mediated increase in NF-κB activity in association with the overexpression of Cr-TRX1 is specifically attributable to the increase in DNA-binding activity of NF-κB. Therefore, it is reasonable to postulate that similar to human TRX1 (Hirota *et al*, 1999; Matthews *et al*, 1992), the Cr-TRX1 could reduce the Cys residue in the CrNFκB DNA-binding motif to enhance its binding to κB site.

Interestingly, we found that the NF-κB-modulating activity is rather conserved in the human TRX6 as it could cross-enhance the horseshoe crab NF-κB DNA-binding activity as well (Figure 3.46), suggesting the functional conservation amongst the 16 kDa and 24 kDa TRXs. Although the exact mechanism underlying the regulation of the NF-κB activity by Cr-TRX1 and TRX6 is still unknown, our studies strongly suggest that the NF-κB regulatory activity might be a common characteristic of the 16 kDa TRXs. The mechanism of TRX6-mediated regulation of the human NF-κB signaling pathway upon various stress conditions is being investigated in this lab to further define the functions of TRX6.

Recently, Leveillard *et al*. (2004) demonstrated that a mouse homologue of the 24 kDa human TRX6, named rod-derived cone viability factor (RdCVF), could slow down the degeneration of cone cell in animal models. Thus, it offers a possible treatment for retinitis pigmentosa – an untreatable retinal disease. The disease initiates with the loss of night vision due to rod photoreceptor degeneration, followed by irreversible, progressive loss of cone photoreceptors (Kajiwara *et al*, 1994). As cones are essential for day and high-acuity vision, loss of the cones is responsible for the main visual handicap. Although the mechanism of how RdCVF protects the cone cells is still unknown, another

study by Krishnamoorthy (1999) found that preservation of NF-κB binding activity in the nucleus may be essential for mouse cone photoreceptor cells to survive photo-oxidative damage induced apoptosis.

In this study, we have found that the human TRX6 could enhance the DNA binding ability of the horseshoe crab NF-κB in electrophoretic mobility shift assay, thereby indicating cross-species functionality and the conservation of an important biological function of the TRX6. Therefore, we hypothesize that the human TRX6 might express a protective function similar to RdCVF, via modulating the NF-κB signaling pathway.

CHAPTER 5: CONCLUSIONS AND FUTURE PERSPECTIVES

5.1 Conclusions

5.1.1 NF-κB/IκB signaling cascade

In this thesis, we have reported the elucidation of similar homologues of NF-κB and IκB in a species of horseshoe crab, the *C. rotundicauda*, and showed that their activation mechanism and transactivation properties were functionally comparable to that of the *Drosophila* and mammals. We further demonstrated that the activated NF-κB can regulate the expression of immune-related genes in the hemocytes, including Factor C and iNOS. Our findings clearly demonstrate that although absent in the *C. elegans*, the NF-κB/IκB signaling pathway has co-evolved and remained well-conserved from horseshoe crab to human, playing an archaic but crucial and fundamental role in innate immune response to regulate the expression of critical immune defense molecules (Wang *et al*, 2006b). These observations reveal the earliest origin of a seminal signaling cascade and provide critical insights into the evolution of the NF-κB transcription factors. Our findings provide further support to the view that NF-κB proteins originated from a common ancestry and was already present in the *Urbilateria* (Hoffmann and Reichhart, 2002).

5.1.2 The novel 16 kDa Cr-TRX1 and its role in NF-κB signaling pathway

We also discovered a novel 16 kDa thioredoxin (Cr-TRX1) from the horseshoe crab which regulates the CrNFκB activity. Previously, this 16 kDa TRX was thought to only exist in the parasitic protozoa of trypanosomes, an etiological cause of severe tropical diseases. However we found that these 16 kDa TRXs also exist in higher eukaryotes and are evolutionary conserved from *C. elegans* to humans. Although the Cr-TRX1 is larger than the classical 12 kDa counterpart and contains an atypical catalytic motif, it possesses the classical thioredoxin activity. Cr-TRX1 activates the NF-κB activity by enhancing its DNA-binding activity, suggesting possible roles of the Cr-TRX1 in modulating NF-κB signaling pathway. Importantly, we found that the 16 kDa TRX probably underwent gene duplication in the mammals to give rise to a novel 24 kDa TRX. We also demonstrated, surprisingly, that the human 24 kDa TRX could exert a cross-phylum enhancement of the DNA-binding activity of the horseshoe crab NF-κB, suggesting the functional conservation amongst the 16 kDa and 24 kDa TRXs.

5.2 Future perspectives

Based on work done in this thesis, there are several interesting directions for future work in the areas of NF-κB signaling pathway and thioredoxin–mediated regulation of the NF-κB activity. The following questions may be posed and innovative experiments may be designed to elucidate:

1) What are the functional differences/ similarities between CrNFκB and CrRelish?

We have isolated two NF-κB homologues, CrNFκB and CrRelish. To better understand their roles in immune response, it will be necessary to examine the functional similarities/differences between the two NF-κB proteins. Challenging the horseshoe crabs with different pathogens and inspecting the resulting activation of CrNFκB and CrRelish may serve to give an indication on how these NF-κB homologues mediate pathogen specific immune reactions. Like its insect and mammalian homologues, the CrRelish is a mosaic protein which contains both RHD and inhibitory IκB domain. It will be important to determine whether CrRelish is proteolytically processed during bacterial challenge and the consequential subcellular localization of the full-length and the cleavaged CrNFκB proteins. Furthermore, the interactions between CrRelish and CrNFκB and the roles of different homo- and heterodimers on gene transcription may be investigated to better characterize their roles in innate immunity.

2) What are the receptors for horseshoe crab NF-κB pathway activation?

Further study is also needed to demonstrate which receptor is responsible for the activation of horseshoe crab NF-κB signaling pathway (Inamori *et al*, 2004). Recently, our lab has isolated a TLR homologue from the horseshoe crab (Loh *et al.* unpublished data). It is therefore pertinent for us to examine if the horseshoe crab TLR could activate the NF-κB signaling pathway. This can be achieved by overexpression of the horseshoe crab TLR and examining the activation of NF-κB pathway. It will be interesting to demonstrate the membrane localization of the horseshoe crab TLR by immunocytochemistry. Given that the horseshoe crab contains two NF-κB homologues,

further analysis may be required in order to understand the contribution of TLR to the activation of each of these NF-κB homologues upon pathogen infection.

Recently, it has been demonstrated that the horseshoe crab Factor C also exist on the hemocytes membrane as a receptor for invading pathogens (Ariki *et al*, 2004). It would be interesting to determine whether recognition of pathogen by the "Factor C receptor" would lead to the activation of NF-κB signaling pathway in horseshoe crab.

3) What are the functions of horseshoe crab iNOS in immune response and its transcription regulation

An iNOS homologue named CriNOS has been cloned from the horseshoe crab in our lab (unpublished data). iNOS plays an important role in immune response in the *Drosophila* and mammals (Foley and O'Farrell, 2003). Surprisingly, the *C. elegans* genome does not encode the NF-κB and iNOS gene. It suggests that the CriNOS is probably the most ancient iNOS gene. It also indicates that the NF-κB transcription factor and iNOS probably originated at the same time and have co-evolved**.** Therefore, it will be interesting to investigate the function of CriNOS in the immune defense of horseshoe crab. Several experiments can be carried out to characterize the functions of CriNOS: i) analysis of the mRNA expression of iNOS and the level of NO in horseshoe crab hemocytes with or without bacterial challenge; ii) whether the recombinant iNOS can produce NO.

Furthermore, our RT-PCR experiments already showed that bacterial infection can significantly induce the expression of iNOS and horseshoe crab NF-κB signaling pathway probably controls the up-regulation of CriNOS in the hemocytes (Figure 3.21).

The observation is very interesting because no such evidence has been forthcoming in any invertebrate. In order to understand the mechanism of transcription regulation of CriNOS, the promoter of CriNOS could be isolated and characterized. We expect the existence of potential κB site(s) on the promoter of CriNOS. Then gel shift using iNOS promoter κB binding site(s) as probe may be performed to examine the binding characteristic of the CriNOS κB motif(s) with the NF-κB proteins. Cotransfection of CrNFκB and iNOS promoter reporter can be performed as well to elucidate/delineate the promoter activity and active site(s) of CriNOS promoter.

4) What are the roles of the human 16 kDa TRX homologue (TRX6) in regulating NF-κB signaling pathway?

We have found that the 16 kDa Cr-TRX1 in the horseshoe crab could regulate the NF-κB signaling pathway. Its human counterpart, TRX6, could enhance the horseshoe crab NF-κB DNA-binding activity as well. It is thus imperative to seek translational insights from the horseshoe crab innate immune system to the human innate immune system. To this end, it would be logical to test the ability of human TRX6 in regulating the human NF-κB signaling pathway.

To achieve this, TRX6 will be overexpressed in different human cell lines and examined for its functions upon pathogen challenge and stress conditions. We expect the TRX6 to synergistically up-regulate NF-κB activity upon challenge. To gain further insights into the mechanisms of action, real-time bioimaging may be exployed to examine whether TRX6 translocates into nucleus and colocalize with NF-κB using.

Furthermore, the role of TRX6 in regulating NF-κB signaling will be examined in NF-κB knockout mice.

We envisage that research on the horseshoe crab innate immunity will establish fundamental understanding of the signaling pathway, which regulates the immune defense against the microbial infection. Being devoid of adaptive immune response, our study on the horseshoe crab NF-κB signaling pathway and its regulation is unperturbed by potential interference of the adaptive immune response and serves as a prelude to the ultimate understanding of innate immune defense mechanisms in the vertebrate including the human.

Bibliography

Aaronson JS, Eckman B, Blevins RA, Borkowski JA, Myerson J, Imran S, Elliston KO (1996) Toward the development of a gene index to the human genome: an assessment of the nature of high-throughput EST sequence data. *Genome Res* **6:** 829-845

Aderem A, Ulevitch RJ (2000) Toll-like receptors in the induction of the innate immune response. *Nature* **406:** 782-787

Agaisse H, Perrimon N (2004) The roles of JAK/STAT signaling in *Drosophila* immune responses. *Immunol Rev* **198:** 72-82

Akira S, Takeda K (2004) Toll-like receptor signaling. *Nat Rev Immunol* **4:** 499-511

Alberts B, Johnson A, Lewis J, Raff M, Roberts K, Walter P. (2002) *Molecular Biology of the Cell - Fourth Edition*.

Alphey MS, Leonard GA, Gourley DG, Tetaud E, Fairlamb AH, Hunter WN (1999) The high resolution crystal structure of recombinant *Crithidia fasciculata* tryparedoxin-I. *J Biol Chem* **274:** 25613-25622

Ariki S, Koori K, Osaki T, Motoyama K, Inamori K, Kawabata S (2004) A serine protease zymogen functions as a pattern-recognition receptor for lipopolysaccharides. *Proc Natl Acad Sci USA* **101:** 953-958

Arner ES, Holmgren A (2000) Physiological functions of thioredoxin and thioredoxin reductase. *Eur J Biochem* **267:** 6102-6109

Aslund F, Beckwith J (1999) The thioredoxin superfamily: redundancy, specificity, and gray-area genomics. *J Bacteriol* **181:** 1375-1379

Baeuerle PA, Baltimore D (1996) NF-κB: ten years after. *Cell* **87:** 13-20

Barillas-Mury C, Charlesworth A, Gross I, Richman A, Hoffmann JA, Kafatos FC (1996) Immune factor Gambif1, a new rel family member from the human malaria vector, *Anopheles gambiae*. *EMBO J* **15:** 4691-4701

Bauer H, Kanzok SM, Schirmer RH (2002) Thioredoxin-2 but not thioredoxin-1 is a substrate of thioredoxin peroxidase-1 from *Drosophila melanogaster*: isolation and characterization of a second thioredoxin in *D. Melanogaster* and evidence for distinct biological functions of Trx-1 and Trx-2. *J Biol Chem* **277:** 17457-17463

Belvin MP, Anderson KV (1996) A conserved signaling pathway: the Drosophila toll-dorsal pathway. *Annu Rev Cell Dev Biol* **12:** 393-416

Bergner A, Oganessyan V, Muta T, Iwanaga S, Typke D, Huber R, Bode W (1996) Crystal structure of a coagulogen, the clotting protein from horseshoe crab: a structural homologue of nerve growth factor. *EMBO J* **15:** 6789-6797

Bogdan C (2001) Nitric oxide and the immune response. *Nat Immunol* **2:** 907-916

Bonizzi G, Karin M (2004) The two NF-κB activation pathways and their role in innate and adaptive immunity. *Trends Immunol* **25:** 280-288

Boutros M, Agaisse H, Perrimon N (2002) Sequential activation of signaling pathways during innate immune responses in *Drosophila*. *Dev Cell* **3:** 711-722

Bradford MM (1976) A rapid and sensitive method for the quantitation of microgram quantities of protein utilizing the principle of protein-dye binding. *Anal Biochem* **72:** 248-254

Caamano J, Hunter CA (2002) NF-kappaB family of transcription factors: central regulators of innate and adaptive immune functions. *Clin Microbiol Rev* **15:** 414-429

Chang TS, Cho CS, Park S, Yu S, Kang SW, Rhee SG (2004) Peroxiredoxin III, a mitochondrion-specific peroxidase, regulates apoptotic signaling by mitochondria. *J Biol Chem* **279:** 41975-41984

Chen LF, Greene WC (2004) Shaping the nuclear action of NF-κB. *Nat Rev Mol Cell Biol* **5:** 392-401

Choe KM, Werner T, Stoven S, Hultmark D, Anderson KV (2002) Requirement for a peptidoglycan recognition protein (PGRP) in Relish activation and antibacterial immune responses in *Drosophila*. *Science* **296:** 359-362

Christophides GK, Zdobnov E, Barillas-Mury C, Birney E, Blandin S, Blass C, Brey PT, Collins FH, Danielli A, Dimopoulos G, Hetru C, Hoa NT, Hoffmann JA, Kanzok SM, Letunic I, Levashina EA, Loukeris TG, Lycett G, Meister S, Michel K, Moita LF, Muller HM, Osta MA, Paskewitz SM, Reichhart JM, Rzhetsky A, Troxler L, Vernick KD, Vlachou D, Volz J, von Mering C, Xu J, Zheng L, Bork P, Kafatos FC (2002) Immunity-related genes and gene families in *Anopheles gambiae*. *Science* **298:** 159-165

Correa RG, Tergaonkar V, Ng JK, Dubova I, Izpisua-Belmonte JC, Verma IM (2004) Characterization of NF-kappa B/I kappa B proteins in zebra fish and their involvement in notochord development. *Mol Cell Biol* **24:** 5257-5268

De Gregorio E, Spellman PT, Tzou P, Rubin GM, Lemaitre B (2002) The Toll and Imd pathways are the major regulators of the immune response in *Drosophila*. *EMBO J* **21:** 2568-2579

Ding JL, Navas MA, 3rd, Ho B (1993) Two forms of factor C from the amoebocytes of *Carcinoscorpius rotundicauda*: purification and characterisation. *Biochim Biophys Acta* **1202:** 149-156

Ding JL, Tan KC, Thangamani S, Kusuma N, Seow WK, Bui TH, Wang J, Ho B (2005) Spatial and temporal coordination of expression of immune response genes during Pseudomonas infection of horseshoe crab, *Carcinoscorpius rotundicauda*. *Genes Immun* **6:** 557-574

Ding JL, Wang LH, Ho B (2004) Current genome-wide analysis on serine proteases in innate immunity. *Current Genomics* **5:** 147-155

Dixit V, Mak TW (2002) NF-κB signaling. Many roads lead to madrid. *Cell* **111:** 615-619

Dushay MS, Asling B, Hultmark D (1996) Origins of immunity: Relish, a compound Rel-like gene in the antibacterial defense of *Drosophila*. *Proc Natl Acad Sci USA* **93:** 10343-10347

Ernst MK, Dunn LL, Rice NR (1995) The PEST-like sequence of IκBα is responsible for inhibition of DNA binding but not for cytoplasmic retention of c-Rel or RelA homodimers. *Mol. Cell. Biol.* **15:** 872-882

Flohe L, Brigelius-Flohe R, Saliou C, Traber MG, Packer L (1997) Redox regulation of NF-kappa B activation. *Free Radic Biol Med* **22:** 1115-1126

Foley E, O'Farrell PH (2003) Nitric oxide contributes to induction of innate immune responses to gram-negative bacteria in *Drosophila*. *Genes Dev* **17:** 115-125

Force A, Lynch M, Pickett FB, Amores A, Yan YL, Postlethwait J (1999) Preservation of duplicate genes by complementary, degenerative mutations. *Genetics* **151:** 1531-1545

Friemann R, Schmidt H, Ramaswamy S, Forstner M, Krauth-Siegel RL, Eklund H (2003) Structure of thioredoxin from *Trypanosoma brucei brucei*. *FEBS Lett* **554:** 301-305

Gao Y, Lecker S, Post MJ, Hietaranta AJ, Li J, Volk R, Li M, Sato K, Saluja AK, Steer ML, Goldberg AL, Simons M (2000) Inhibition of ubiquitin-proteasome pathway-mediated I kappa B alpha degradation by a naturally occurring antibacterial peptide. *J Clin Invest* **106:** 439-448

Gay NJ, Keith FJ (1992) Regulation of translation and proteolysis during the development of embryonic dorso-ventral polarity in *Drosophila*. Homology of easter proteinase with *Limulus* proclotting enzyme and translational activation of Toll receptor synthesis. *Biochim Biophys Acta* **1132:** 290-296

Geisler R, Bergmann A, Hiromi Y, Nusslein-Volhard C (1992) Cactus, a gene involved in dorsoventral pattern formation of *Drosophila*, is related to the I kappa B gene family of vertebrates. *Cell* **71:** 613-621

Ghosh G, van Duyne G, Ghosh S, Sigler PB (1995) Structure of NF-kappa B p50 homodimer bound to a kappa B site. *Nature* **373:** 303-310

Ghosh S, May MJ, Kopp EB (1998) NF-κB and Rel proteins: evolutionarily conserved mediators of immune responses. *Annu Rev Immunol* **16:** 225-260

Gilmore TD (1999) The Rel/NF-κB signal transduction pathway: introduction. *Oncogene* **18:** 6842-6844

Gommel DU, Nogoceke E, Morr M, Kiess M, Kalisz HM, Flohe L (1997) Catalytic characteristics of tryparedoxin. *Eur J Biochem* **248:** 913-918

Han ZS, Ip YT (1999) Interaction and specificity of Rel-related proteins in regulating *Drosophila* immunity gene expression. *J Biol Chem* **274:** 21355-21361

Hatada EN, Nieters A, Wulczyn FG, Naumann M, Meyer R, Nucifora G, McKeithan TW, Scheidereit C (1992) The ankyrin repeat domains of the NF-kappa B precursor p105 and the protooncogene bcl-3 act as specific inhibitors of NF-kappa B DNA binding. *Proc Natl Acad Sci U S A* **89:** 2489-2493

Hayashi T, Ueno Y, Okamoto T (1993) Oxidoreductive regulation of nuclear factor kappa B. Involvement of a cellular reducing catalyst thioredoxin. *J Biol Chem* **268:** 11380-11388

Hayden MS, Ghosh S (2004) Signaling to NF-κB. *Genes Dev* **18:** 2195-2224

Hedengren M, Asling B, Dushay MS, Ando I, Ekengren S, Wihlborg M, Hultmark D (1999) Relish, a central factor in the control of humoral but not cellular immunity in *Drosophila*. *Mol Cell* **4:** 827-837

Hirota K, Murata M, Sachi Y, Nakamura H, Takeuchi J, Mori K, Yodoi J (1999) Distinct roles of thioredoxin in the cytoplasm and in the nucleus. A two-step mechanism of redox regulation of transcription factor NF-kappaB. *J Biol Chem* **274:** 27891-27897

Hirota K, Nakamura H, Masutani H, Yodoi J (2002) Thioredoxin superfamily and thioredoxin-inducing agents. *Ann N Y Acad Sci* **957:** 189-199

Hoffmann JA (2003) The immune response of *Drosophila*. *Nature* **426:** 33-38

Hoffmann JA, Kafatos FC, Janeway CA, Ezekowitz RA (1999) Phylogenetic perspectives in innate immunity. *Science* **284:** 1313-1318

Hoffmann JA, Reichhart JM (2002) *Drosophila* innate immunity: an evolutionary perspective. *Nat Immunol* **3:** 121-126

Holmgren A (1985) Thioredoxin. *Annu Rev Biochem* **54:** 237-271

Huang TT, Kudo N, Yoshida M, Miyamoto S (2000) A nuclear export signal in the N-terminal regulatory domain of IκBα controls cytoplasmic localization of inactive NF-κB/IκBα complexes. *Proc Natl Acad Sci USA* **97:** 1014-1019

Imler JL, Bulet P (2005) Antimicrobial peptides in Drosophila: structures, activities and gene regulation. *Chem Immunol Allergy* **86:** 1-21

Inamori K, Ariki S, Kawabata S (2004) A Toll-like receptor in horseshoe crabs. *Immunol Rev* **198:** 106-115

Iwanaga S (2002) The molecular basis of innate immunity in the horseshoe crab. *Curr Opin Immunol* **14:** 87-95

Iwanaga S, Kawabata S (1998) Evolution and phylogeny of defense molecules associated with innate immunity in horseshoe crab. *Front Biosci* **3:** D973-984

Iwanaga S, Kawabata S, Muta T (1998) New types of clotting factors and defense molecules found in horseshoe crab hemolymph: their structures and functions. *J Biochem (Tokyo)* **123:** 1-15

Iwanaga S, Lee BL (2005) Recent advances in the innate immunity of invertebrate animals. *J Biochem Mol Biol* **38:** 128-150

Janeway CA, Jr., Medzhitov R (2002) Innate immune recognition. *Annu Rev Immunol* **20:** 197-216

Jeong W, Chang TS, Boja ES, Fales HM, Rhee SG (2004a) Roles of TRP14, a thioredoxin-related protein in tumor necrosis factor-alpha signaling pathways. *J Biol Chem* **279:** 3151-3159

Jeong W, Yoon HW, Lee SR, Rhee SG (2004b) Identification and characterization of TRP14, a thioredoxin-related protein of 14 kDa. New insights into the specificity of thioredoxin function. *J Biol Chem* **279:** 3142-3150

Kajiwara K, Berson EL, Dryja TP (1994) Digenic retinitis pigmentosa due to mutations at the unlinked peripherin/RDS and ROM1 loci. *Science* **264:** 1604-1608

Kanzok SM, Fechner A, Bauer H, Ulschmid JK, Muller HM, Botella-Munoz J, Schneuwly S, Schirmer R, Becker K (2001) Substitution of the thioredoxin system for glutathione reductase in *Drosophila melanogaster*. *Science* **291:** 643-646

Karin M, Ben-Neriah Y (2000) Phosphorylation meets ubiquitination: the control of NF-κB activity. *Annu Rev Immunol* **18:** 621-663

Katti SK, LeMaster DM, Eklund H (1990) Crystal structure of thioredoxin from *Escherichia coli* at 1.68 A resolution. *J Mol Biol* **212:** 167-184

Kim DH, Ausubel FM (2005) Evolutionary perspectives on innate immunity from the study of *Caenorhabditis elegans*. *Curr Opin Immunol* **17:** 4-10

Krauth-Siegel RL, Coombs GH (1999) Enzymes of parasite thiol metabolism as drug targets. *Parasitol Today* **15:** 404-409

Krishnamoorthy RR, Crawford MJ, Chaturvedi MM, Jain SK, Aggarwal BB, Al-Ubaidi MR, Agarwal N (1999) Photo-oxidative stress down-modulates the activity of nuclear factor-kappaB via involvement of caspase-1, leading to apoptosis of photoreceptor cells. *J Biol Chem* **274:** 3734-3743

Kunchithapautham K, Padmavathi B, Narayanan RB, Kaliraj P, Scott AL (2003) Thioredoxin from *Brugia malayi*: defining a 16-kilodalton class of thioredoxins from nematodes. *Infect Immun* **71:** 4119-4126

Kurooka H, Kato K, Minoguchi S, Takahashi Y, Ikeda J, Habu S, Osawa N, Buchberg AM, Moriwaki K, Shisa H, Honjo T (1997) Cloning and characterization of the nucleoredoxin gene that encodes a novel nuclear protein related to thioredoxin. *Genomics* **39:** 331-339

Kurz CL, Ewbank JJ (2003) *Caenorhabditis elegans*: an emerging genetic model for the study of innate immunity. *Nat Rev Genet* **4:** 380-390

Lee KK, Murakawa M, Takahashi S, Tsubuki S, Kawashima S, Sakamaki K, Yonehara S (1998) Purification, molecular cloning, and characterization of TRP32, a novel thioredoxin-related mammalian protein of 32 kDa. *J Biol Chem* **273:** 19160-19166

Lehrer RI, Ganz T (1999) Antimicrobial peptides in mammalian and insect host defence. *Curr Opin Immunol* **11:** 23-27

Lemaitre B, Nicolas E, Michaut L, Reichhart JM, Hoffmann JA (1996) The dorsoventral regulatory gene cassette spatzle/Toll/cactus controls the potent antifungal response in *Drosophila* adults. *Cell* **86:** 973-983

Leulier F, Parquet C, Pili-Floury S, Ryu JH, Caroff M, Lee WJ, Mengin-Lecreulx D, Lemaitre B (2003) The *Drosophila* immune system detects bacteria through specific peptidoglycan recognition. *Nat Immunol* **4:** 478-484

Leveillard T, Mohand-Said S, Lorentz O, Hicks D, Fintz AC, Clerin E, Simonutti M, Forster V, Cavusoglu N, Chalmel F, Dolle P, Poch O, Lambrou G, Sahel JA

(2004) Identification and characterization of rod-derived cone viability factor. *Nat Genet* **36:** 755-759

Li P, Wohland T, Ho B, Ding JL (2004) Perturbation of Lipopolysaccharide (LPS) Micelles by Sushi 3 (S3) antimicrobial peptide. The importance of an intermolecular disulfide bond in S3 dimer for binding, disruption, and neutralization of LPS. *J Biol Chem* **279:** 50150-50156

Lin AW, Chang CC, McCormick CC (1996) Molecular cloning and expression of an avian macrophage nitric-oxide synthase cDNA and the analysis of the genomic 5'-flanking region. *J Biol Chem* **271:** 11911-11919

Lin CC, Chou CM, Hsu YL, Lien JC, Wang YM, Chen ST, Tsai SC, Hsiao PW, Huang CJ (2004) Characterization of two mosquito STATs, AaSTAT and CtSTAT. Differential regulation of tyrosine phosphorylation and DNA binding activity by lipopolysaccharide treatment and by Japanese encephalitis virus infection. *J Biol Chem* **279:** 3308-3317

Little TJ, Hultmark D, Read AF (2005) Invertebrate immunity and the limits of mechanistic immunology. *Nat Immunol* **6:** 651-654

Liu ZP, Galindo RL, Wasserman SA (1997) A role for CKII phosphorylation of the cactus PEST domain in dorsoventral patterning of the *Drosophila* embryo. *Genes Dev* **11:** 3413-3422

Lu S, Saydak M, Gentile V, Stein JP, Davies PJ (1995) Isolation and characterization of the human tissue transglutaminase gene promoter. *J Biol Chem* **270:** 9748-9756

Ludemann H, Dormeyer M, Sticherling C, Stallmann D, Follmann H, Krauth-Siegel RL (1998) *Trypanosoma brucei* tryparedoxin, a thioredoxin-like protein in African *trypanosomes*. *FEBS Lett* **431:** 381-385

Lyss G, Knorre A, Schmidt TJ, Pahl HL, Merfort I (1998) The anti-inflammatory sesquiterpene lactone helenalin inhibits the transcription factor NF-κB by directly targeting p65. *J Biol Chem* **273:** 33508-33516

Martin JL (1995) Thioredoxin--a fold for all reasons. *Structure* **3:** 245-250

Matsuo Y, Akiyama N, Nakamura H, Yodoi J, Noda M, Kizaka-Kondoh S (2001) Identification of a novel thioredoxin-related transmembrane protein. *J Biol Chem* **276:** 10032-10038

Matthews JR, Wakasugi N, Virelizier JL, Yodoi J, Hay RT (1992) Thioredoxin regulates the DNA binding activity of NF-kappa B by reduction of a disulphide bond involving cysteine 62. *Nucleic Acids Res* **20:** 3821-3830

May MJ, Ghosh S (1997) Rel/NF-kappa B and I kappa B proteins: an overview. *Semin Cancer Biol* **8:** 63-73

Medvedev A, Saunders NA, Matsuura H, Chistokhina A, Jetten AM (1999) Regulation of the transglutaminase I gene. Identification of DNA elements involved in its transcriptional control in tracheobronchial epithelial cells. *J Biol Chem* **274:** 3887-3896

Medzhitov R, Janeway C, Jr. (2000) Innate immunity. *N Engl J Med* **343:** 338-344

Medzhitov R, Janeway CA, Jr. (1998) Innate immune recognition and control of adaptive immune responses. *Semin Immunol* **10:** 351-353

Meyer M, Schreck R, Baeuerle PA (1993) H2O2 and antioxidants have opposite effects on activation of NF-kappa B and AP-1 in intact cells: AP-1 as secondary antioxidant-responsive factor. *EMBO J* **12:** 2005-2015

Miranda-Vizuete A, Damdimopoulos AE, Spyrou G (2000) The mitochondrial thioredoxin system. *Antioxid Redox Signal* **2:** 801-810

Montagnani C, Kappler C, Reichhart JM, Escoubas JM (2004) *Cg*-Rel, the first Rel/NF-κB homolog characterized in a mollusk, the Pacific oyster *Crassostrea gigas*. *FEBS Lett* **561:** 75-82

Nakamura H, Nakamura K, Yodoi J (1997) Redox regulation of cellular activation. *Annu Rev Immunol* **15:** 351-369

Nakano H, Nakajima A, Sakon-Komazawa S, Piao JH, Xue X, Okumura K (2006) Reactive oxygen species mediate crosstalk between NF-kappaB and JNK. *Cell Death Differ* **13:** 730-737

Ng PM, Jin Z, Tan SS, Ho B, Ding JL (2004) C-reactive protein: a predominant LPS-binding acute phase protein responsive to *Pseudomonas* infection. *J Endotoxin Res* **10:** 163-174

Osaki T, Kawabata S (2004) Structure and function of coagulogen, a clottable protein in horseshoe crabs. *Cell Mol Life Sci* **61:** 1257-1265

Osta MA, Christophides GK, Vlachou D, Kafatos FC (2004) Innate immunity in the malaria vector *Anopheles gambiae*: comparative and functional genomics. *J Exp Biol* **207:** 2551-2563

Powis G, Montfort WR (2001) Properties and biological activities of thioredoxins. *Annu Rev Biophys Biomol Struct* **30:** 421-455

Pujol N, Link EM, Liu LX, Kurz CL, Alloing G, Tan MW, Ray KP, Solari R, Johnson CD, Ewbank JJ (2001) A reverse genetic analysis of components of the Toll signaling pathway in *Caenorhabditis elegans*. *Curr Biol* **11:** 809-821

Radomski MW, Martin JF, Moncada S (1991) Synthesis of nitric oxide by the haemocytes of the American horseshoe crab (*Limulus polyphemus*). *Philos Trans R Soc London Ser B* **334:** 129-133

Reckenfelderbaumer N, Krauth-Siegel RL (2002) Catalytic properties, thiol pK value, and redox potential of *Trypanosoma brucei* tryparedoxin. *J Biol Chem* **277:** 17548-17555

Reckenfelderbaumer N, Ludemann H, Schmidt H, Steverding D, Krauth-Siegel RL (2000) Identification and functional characterization of thioredoxin from *Trypanosoma brucei brucei*. *J Biol Chem* **275:** 7547-7552

Royet J (2004) Infectious non-self recognition in invertebrates: lessons from *Drosophila* and other insect models. *Mol Immunol* **41:** 1063-1075

Royet J, Reichhart JM, Hoffmann JA (2005) Sensing and signaling during infection in *Drosophila*. *Curr Opin Immunol* **17:** 11-17

Rutschmann S, Jung AC, Hetru C, Reichhart JM, Hoffmann JA, Ferrandon D (2000) The Rel protein DIF mediates the antifungal but not the antibacterial host defense in *Drosophila*. *Immunity* **12:** 569-580

Sadek CM, Damdimopoulos AE, Pelto-Huikko M, Gustafsson JA, Spyrou G, Miranda-Vizuete A (2001) Sptrx-2, a fusion protein composed of one thioredoxin and three tandemly repeated NDP-kinase domains is expressed in human testis germ cells. *Genes Cells* **6:** 1077-1090

Sadek CM, Jimenez A, Damdimopoulos AE, Kieselbach T, Nord M, Gustafsson JA, Spyrou G, Davis EC, Oko R, van der Hoorn FA, Miranda-Vizuete A (2003) Characterization of human thioredoxin-like 2. A novel microtubule-binding thioredoxin expressed predominantly in the cilia of lung airway epithelium and spermatid manchette and axoneme. *J Biol Chem* **278:** 13133-13142

Sagisaka A, Tanaka H, Furukawa S, Yamakawa M (2004) Characterization of a homologue of the Rel/NF-kappaB transcription factor from a beetle, *Allomyrina dichotoma*. *Biochim Biophys Acta* **1678:** 85-93

Sambrook J, Fritsch, E.F. and Maniatis, T. (1988) *Molecular cloning: A laboratory manual, 2 nd edition*. Cold Spring Harbour laboratory, New York.

Schenk H, Klein M, Erdbrugger W, Droge W, Schulze-Osthoff K (1994) Distinct effects of thioredoxin and antioxidants on the activation of transcription factors NF-kappa B and AP-1. *Proc Natl Acad Sci USA* **91:** 1672-1676

Schneider DS, Jin Y, Morisato D, Anderson KV (1994) A processed form of the Spatzle protein defines dorsal-ventral polarity in the *Drosophila* embryo. *Development* **120:** 1243-1250

Schreck R, Rieber P, Baeuerle PA (1991) Reactive oxygen intermediates as apparently widely used messengers in the activation of the NF-kappa B transcription factor and HIV-1. *EMBO J* **10:** 2247-2258

Segal AW (2005) How neutrophils kill microbes. *Annu Rev Immunol* **23:** 197-223

Sen R, Baltimore D (1986) Multiple nuclear factors interact with the immunoglobulin enhancer sequences. *Cell* **46:** 705-716

Senftleben U, Cao Y, Xiao G, Greten FR, Krahn G, Bonizzi G, Chen Y, Hu Y, Fong A, Sun SC, Karin M (2001) Activation by IKKalpha of a second, evolutionary conserved, NF-kappa B signaling pathway. *Science* **293:** 1495-1499

Shevchenko A, Wilm M, Mann M (1997) Peptide sequencing by mass spectrometry for homology searches and cloning of genes. *J Protein Chem* **16:** 481-490

Shin SW, Kokoza V, Ahmed A, Raikhel AS (2002) Characterization of three alternatively spliced isoforms of the Rel/NF-κB transcription factor Relish from the mosquito *Aedes aegypti*. *Proc Natl Acad Sci USA* **99:** 9978-9983

Shin SW, Kokoza V, Bian G, Cheon HM, Kim YJ, Raikhel AS (2005) REL1, a Homologue of *Drosophila* Dorsal, Regulates Toll Antifungal Immune Pathway in the Female Mosquito *Aedes aegypti*. *J Biol Chem* **280:** 16499-16507

Shin SW, Kokoza V, Lobkov I, Raikhel AS (2003) Relish-mediated immune deficiency in the transgenic mosquito *Aedes aegypti*. *Proc Natl Acad Sci USA* **100:** 2616-2621

Silverman N, Maniatis T (2001) NF-kappaB signaling pathways in mammalian and insect innate immunity. *Genes Dev* **15:** 2321-2342

Silverman N, Zhou R, Stoven S, Pandey N, Hultmark D, Maniatis T (2000) A *Drosophila* IkappaB kinase complex required for Relish cleavage and antibacterial immunity. *Genes Dev* **14:** 2461-2471

Simeonidis S, Castagliuolo I, Pan A, Liu J, Wang CC, Mykoniatis A, Pasha A, Valenick L, Sougioultzis S, Zhao D, Pothoulakis C (2003) Regulation of the NK-1 receptor gene expression in human macrophage cells via an NF-kappa B site on its promoter. *Proc Natl Acad Sci USA* **100:** 2957-2962

Smith CL, DeLotto R (1992) A common domain within the proenzyme regions of the *Drosophila* snake and easter proteins and *Tachypleus* proclotting enzyme defines a new subfamily of serine proteases. *Protein Sci* **1:** 1225-1226

Solon E, Gupta AP, Gaugler R (1996) Signal transduction during exocytosis in *Limulus polyphemus* granulocytes. *Dev Comp Immunol* **20:** 307-321

Spencer E, Jiang J, Chen ZJ (1999) Signal-induced ubiquitination of IκBα by the F-box protein Slimb/β-TrCP. *Genes Dev* **13:** 284-294

Spyrou G, Enmark E, Miranda-Vizuete A, Gustafsson J (1997) Cloning and expression of a novel mammalian thioredoxin. *J Biol Chem* **272:** 2936-2941

Stieritz DD, Holder IA (1975) Experimental studies of the pathogenesis of infections due to *Pseudomonas aeruginosa*: description of a burned mouse model. *J Infect Dis* **131:** 688-691

Størmer L (1952) Phylogeny and taxonomy of fossil horseshoe crabs. *J Paleontol* **26:** 630-639

Swain SD, Rohn TT, Quinn MT (2002) Neutrophil priming in host defense: role of oxidants as priming agents. *Antioxid Redox Signal* **4:** 69-83

Tauszig S, Jouanguy E, Hoffmann JA, Imler JL (2000) Toll-related receptors and the control of antimicrobial peptide expression in *Drosophila*. *Proc Natl Acad Sci USA* **97:** 10520-10525

Tran K, Merika M, Thanos D (1997) Distinct functional properties of IκBα and IκBβ. *Mol Cell Biol* **17:** 5386-5399

Wahl MC, Irmler A, Hecker B, Schirmer RH, Becker K (2005) Comparative structural analysis of oxidized and reduced thioredoxin from *Drosophila melanogaster*. *J Mol Biol* **345:** 1119-1130

Wang L, Weber AN, Atilano ML, Filipe SR, Gay NJ, Ligoxygakis P (2006a) Sensing of Gram-positive bacteria in Drosophila: GNBP1 is needed to process and present peptidoglycan to PGRP-SA. *EMBO J* **25:** 5005-5014

Wang LH, Ho B, Ding JL (2003) Transcriptional regulation of *Limulus* factor C: repression of an NF-κB motif modulates its responsiveness to bacterial lipopolysaccharide. *J Biol Chem* **278:** 49428-49437

Wang XW, Liou YC, Ho B, Ding JL (2007) An evolutionarily conserved 16-kDa thioredoxin-related protein is an antioxidant which regulates the NF-kappaB signaling pathway. *Free Radic Biol Med* **42:** 247-259

Wang XW, Tan NS, Ho B, Ding JL (2006b) Evidence for the ancient origin of the NF-κB/IκB cascade: Its archaic role in pathogen infection and immunity. *Proc Natl Acad Sci USA* **103:** 4204-4209

Wasserman SA (2000) Toll signaling: the enigma variations. *Curr Opin Genet Dev* **10:** 497-502

Weichsel A, Gasdaska JR, Powis G, Montfort WR (1996) Crystal structures of reduced, oxidized, and mutated human thioredoxins: evidence for a regulatory homodimer. *Structure* **4:** 735-751

Werner T, Borge-Renberg K, Mellroth P, Steiner H, Hultmark D (2003) Functional diversity of the *Drosophila* PGRP-LC gene cluster in the response to lipopolysaccharide and peptidoglycan. *J Biol Chem* **278:** 26319-26322

Windle HJ, Fox A, Ni Eidhin D, Kelleher D (2000) The thioredoxin system of *Helicobacter pylori*. *J Biol Chem* **275:** 5081-5089

Witte S, Villalba M, Bi K, Liu Y, Isakov N, Altman A (2000) Inhibition of the c-Jun N-terminal kinase/AP-1 and NF-kappaB pathways by PICOT, a novel protein kinase C-interacting protein with a thioredoxin homology domain. *J Biol Chem* **275:** 1902-1909

Wrammert J, Kallberg E, Leanderson T (2004) Identification of a novel thioredoxin-related protein, PC-TRP, which is preferentially expressed in plasma cells. *Eur J Immunol* **34:** 137-146

Ye RD (2001) Regulation of nuclear factor κB activation by G-protein-coupled receptors. *J Leukoc Biol* **70:** 839-848

Zhang J (2003) Evolution by gene duplication: an update. *Trends in Ecology & Evolution* **18:** 292-298

Zhu Y, Thangamani S, Ho B, Ding JL (2005) The ancient origin of the complement system. *EMBO J*. **24:** 382-394